INFORMATION TO USERS

This manuscript has been reproduced from the microfilm master. UMI films the text directly from the original or copy submitted. Thus, some thesis and dissertation copies are in typewriter face, while others may be from any type of computer printer.

The quality of this reproduction is dependent upon the quality of the copy submitted. Broken or indistinct print, colored or poor quality illustrations and photographs, print bleedthrough, substandard margins, and improper alignment can adversely affect reproduction.

In the unlikely event that the author did not send UMI a complete manuscript and there are missing pages, these will be noted. Also, if unauthorized copyright material had to be removed, a note will indicate the deletion.

Oversize materials (e.g., maps, drawings, charts) are reproduced by sectioning the original, beginning at the upper left-hand corner and continuing from left to right in equal sections with small overlaps.

Photographs included in the original manuscript have been reproduced xerographically in this copy. Higher quality 6" x 9" black and white photographic prints are available for any photographs or illustrations appearing in this copy for an additional charge. Contact UMI directly to order.

Bell & Howell Information and Learning
300 North Zeeb Road, Ann Arbor, MI 48106-1346 USA
800-521-0600

Université d'Ottawa • University of Ottawa

A MULTI-TRACER ESTIMATION OF GROUNDWATER RECHARGE IN A GLACIOFLUVIAL AQUIFER IN SOUTHEASTERN MANITOBA

by

Andrea J. Cherry

A thesis submitted to the School of Graduate Studies and Research

in partial fulfillment of the requirements

for the degree of M.Sc in Earth Sciences

OTTAWA-CARLETON GEOSCIENCE CENTRE

AND

UNIVERSITY OF OTTAWA

OTTAWA, CANADA

Acknowledgements

I would like to thank my supervisor, Dr. Ian D. Clark, for his insightful scientific discussions and most importantly his support, enthusiasm, and sense of humour, without which I would not have enjoyed this experience nearly as much.

I would also like to thank Dr. Marc Hinton for his guidance, encouragement, and helpful comments both during field work and while working on this thesis. Thanks also to Dr. Tom Kotzer for helping me with analyses, for always taking the time to explain things to me and for his positive outlook throughout the many different stages of this thesis.

A special thanks to Frank Render for supplying me with invaluable information on the Sandilands, answering endless questions about the area, and for the opportunity to be involved in the drilling in the fall of 1998. Your support was very much appreciated. Thanks also to Robert Betcher for putting together lots of useful information and for helping us with the project.

I would like to express my gratitude to Stefan Roser and Stephanie Blandin for helping me with my field work, Dr. K. Solomon for answering many questions about CFCs and Y. Sun and L. Seybol for providing me with helpful advice on sampling techniques.

Thanks to my fellow grad students who helped make the last two years ones to remember. Thanks to Nic Alvarado-Quiroz, Julie Brown, Kelli Powis, Brad Sim, Paula Piilonen, Brian Luinstra, Sean McClenaghan, Alice Deschamps, Lori Henderson, Jean Ropchan and Francois Richard for their advice and encouragement, much of which was received on Friday afternoons at the Oak. Extra thanks to Simone Dumas for taking the time to translate my abstract into French, your help was very much appreciated.

Special thanks to my family who continually cheered me on. Thanks to my mom, Joan Cherry, for her support and words of wisdom, to my dad, John Cherry, for his advice and encouraging phone calls and to my grandma, Jean Getty, who is a constant source of inspiration to me. Very big thanks also to Dave '409' Cherry and Bridget 'the Chief' Mallon for their support, for letting me talk shop, and for making all the time I wasn't working on my thesis so much fun.

A final extra special thanks to John "Newfie" Buckle who helped me do three weeks of field work, was my personal GIS expert, and most importantly for supporting me in everything I do and for keeping me smiling while I do it. I couldn't imagine my life without you in it.

Abstract

Southeastern Manitoba relies predominantly on groundwater to supply municipal, industrial, rural residential and agricultural uses. As industry and agriculture continues to expand in the region it has become increasingly important to improve the understanding of groundwater resources and in particular to assess the extent of modern groundwater recharge to both the surficial and bedrock aquifers. The Sandilands glaciofluvial complex is believed to be a region of significant groundwater recharge in southeastern Manitoba.

Chlorofluorocarbon (CFC-11, CFC-12, and CFC-113), tritium (^3H) and tritium/helium ($^3H/^3He$) groundwater age dating methods were used to estimate and characterize groundwater recharge in the surficial aquifer in the Sandilands. The multi-tracer technique was used to provide comparison between groundwater age estimates and to evaluate if subsurface processes affected groundwater ages. Five sites within the Sandilands were instrumented with shallow nests (11-28 m total depth) of three piezometers with vertical spacings of 2-7 meters to determine groundwater age profiles and to estimate vertical groundwater velocities and recharge rates. Groundwater recharge was estimated at different locations in the study area to assess the spatial variability of recharge rates and to identify possible controlling factors. Piezometric and geochemical data (major ions, $\delta^{18}O$, $\delta^{13}C_{DIC}$) were also collected to aid in the interpretation of groundwater ages.

Comparison of groundwater ages estimated using each tracer indicated that sampling methods and trace CFC-113 contamination were the limiting factors on the dating techniques and typical non-conservative processes such as anaerobic degradation did not affect the CFC age estimates. CFC, ^3H and $^3H/^3He$ groundwater ages were comparable within 22 % suggesting that the groundwater age estimates were reasonably reliable and may have been affected only slightly by subsurface processes.

Average recharge rates were estimated using CFC and $^3H/^3He$ dating methods at three sites in the study area and were found to range between 43 ± 26 mm/yr and 174 ± 36 mm/yr and comprised between 8 and 30 % of the average annual precipitation. These rates were comparable with water balance and Darcy's Law estimates. Recharge rates were found to vary spatially within the Sandilands and were strongly correlated with variations in sediment type. Groundwater recharge was highest (174 ± 36 mm/yr) where sediments are dominated by coarse sands and lowest (43 ± 26 mm/yr) through clayey till sediments. Recharge in the surficial aquifer is likely highest in the central and western portions of the study area where near surface sediments are predominantly sands that extend to depths of over 40 meters Groundwater recharge from the surficial aquifers in the Sandilands to the bedrock aquifers in southeastern Manitoba may be strongly controlled by the distribution of sediment types and in particular by the distribution of thick clayey tills overlying the bedrock.

The understanding of groundwater recharge in the surficial aquifer in the Sandilands was significantly improved by recharge rate estimates obtained using a multi-tracer groundwater age dating technique. Application of these recharge rates to regional groundwater flow models and to direct future research in the Sandilands region will allow for better groundwater resource management in southeastern Manitoba.

Résumé

Le sud-est du Manitoba dépend fortement de ses ressources en eaux souterraines pour alimenter les municipalités, les industries, les résidences rurales et les agriculteurs. Étant donné l'expansion constante de l'industrie et et de l'agriculture dans cette région, il devient important de mieux comprendre les ressources en eaux souterraines et, en particulier, d'évaluer l'étendue de la recharge des aquifères de surface et du socle rocheux. Le complexe glacio-fluvial de Sandilands serait une importante région de recharge en eaux souterraines du sud-est Manitobain.

Les méthodes de datation aux chlorofluorocarbones (CFC-11, CFC-12, et CFC-113), tritium (^3H) et tritium/hélium ($^3H/^3He$) ont eté utilisées afin d'estimer et de caractériser la recharge en eaux souterraines des aquifères de surface du complexe Sandilands. La technique de traceurs multiples a été utilisée pour comparer les estimés de l'âge des eaux souterraines et pour évaluer de l'influence des processus souterrains sur l'âge des eaux souterraines. Afin de déterminer les profils d'âges et d'estimer les vitesses et les taux de recharge en eaux souterraines, cinq sites du complexe Sandilands ont été munis de groupes de trois piézomètres. Chacun des piézomètres d'un groupe étaient disposés sur un même axe vertical avec un espacement variant de 2 à 7 mètres (profondeur totale de 11 à 28 m). La recharge en eaux souterraines fut estimée à différents endroits dans la région d'étude afin d'évaluer la variabilité spatiale de celle-ci et les facteurs l'influençant. Des données piézometriques et géochimiques (ions majeurs, $\delta^{18}O$, $\delta^{13}C_{DIC}$) furent aussi amassées afin d'aider à l'interprétation de l'âge des eaux souterraines.

La comparaison des âges des eaux souterraines, estimés à l'aide de chacun des traceurs, a indiqué que les méthodes d'échantillonnage et la contamination du traceur CFC-113 étaient les principaux facteurs limitant les techniques de datation. De plus, les processus tels la dégradation anaérobique, n'ont pas affecté les estimés d'âges. Les estimations d'âge des eaux souterraines par CFC, ^3H et $^3H/^3He$ différaient d'au plus 22% ce qui porte à croire que les valeurs obtenues sont relativement fiables et peu influencées par les processus souterrains.

Pour trois des sites, les taux de recharge moyens ont été estimés grâce aux méthodes de datation faisant appel au CFC et $^3H/^3He$, variant entre 43 ± 26 mm/an et 174 ± 36 mm/an. Ces taux peuvent être comparés aux taux obtenus par le bilan de masse et par la loi de Darcy. La recharge en eaux souterraines équivaut à 8 à 30 % des précipitations precipitations annuelles dans la région. Les taux de recharge varient à l'intérieur du complexe Sandilands et ces variations semblent étroitement liées aux types de sédiments. Les taux les plus élevés (174 ± 36 mm/an) ont été observés dans les sables grossiers et les plus faibles (43 ± 26 mm/an) dans les tills argilleux. Les taux de recharge des aquifères superficiels les plus élevés devraient se retrouver dans les portions centrale et occidentale de la région d'étude, puisqu'elles sont dominées par des sables d'une épaisseur de 40 m. Il est possible que la recharge en eaux des aquifères du socle rocheux via les aquifères de surface dans la région du complexe Sandilands soit en grande partie controlée par la distribution des différents sédiments et plus particulièrement par la distribution des tills argilleux recouvrant le socle rocheux.

L'utilisation de traceurs mutliples afin d'estimer les taux de recharge a contribué de façon significative à l'avancement des connaissances sur la recharge des eaux souterraines des aquifères de surface du complexe Sandilands. L'utilisation de ces taux de recharge dans un contexte de modèle régional d'écoulement des eaux souterraines et comme guide pour de recherches futures dans le complexe Sandilands permettra une meilleure gestion des ressources en eaux dans le sud-est Manitobain.

Table of Contents

List of Figures

List of Tables

List of Equations

1.0 Introduction

Southeastern Manitoba relies heavily on groundwater to supply municipal, industrial, rural residential and agricultural uses. Much of this groundwater supply is drawn from the bedrock aquifers of the region and to a lesser degree from the surficial aquifers. Groundwater use from the bedrock aquifers is limited by the presence of brackish to saline water in the Winnipeg area, southwestern and south central Manitoba. Most of the municipalities overlying the freshwater portion of the bedrock aquifers in southeastern Manitoba rely almost entirely on it for their water supplies. Similarly, rural communities and farms in the southeast use groundwater from the surficial aquifers to meet their water supply needs (Betcher at al., 1995). As industry and agriculture continues to expand and intensify in southeastern Manitoba it has become increasingly important to improve the understanding of groundwater resources in the region and more specifically to assess the extent of modern groundwater recharge to both the surficial and bedrock aquifers.

The surficial deposits of the Sandilands glaciofluvial complex in southeastern Manitoba are believed to be an important source of modern groundwater recharge to the surficial and bedrock aquifers (Render, 1970; Fritz et al., 1974; Betcher, 1995). The Sandilands region is located 80 km southeast of the City of Winnipeg and forms the topographic high in southeastern Manitoba (Figure 1). The area is characterized by a thick sequence of glacial deposits, ranging from coarse sands and gravels to clayey tills, which overlie the major regional bedrock aquifers in southeastern Manitoba.

Previous work done in southeastern Manitoba includes a general groundwater study of southeastern Manitoba that presents hydrogeological data in the form of maps and tables

illustrating piezometric data, stratigraphy of the sediments and groundwater geochemistry (Little, 1980). Data presented in this report from the Sandilands were limited and provided a broad understanding of groundwater in the area. Current research conducted by the Manitoba Water Resources Branch in the Sandilands includes regional monitoring of groundwater levels in viable sand and gravel aquifers, compilation of geological information from test hole drilling and groundwater quality testing in agricultural areas (Render and Betcher, personal communication, 1998). To date, however, there has been no detailed groundwater study and more specifically no evaluation of groundwater recharge in the Sandilands.

Recent advances in the use of environmental tracers such as tritium/helium ($^3H/^3He$) and chlorofluorocarbons (CFCs) to estimate groundwater ages offers an alternative method to water balance and Darcian approaches for estimating groundwater recharge. Previous studies have found that groundwater age dating is an effective method to estimate groundwater flow velocities and recharge rates and generally with a greater degree of certainty than with traditional methods. In particular, the use of multiple tracers to estimate groundwater ages can eliminate some of the uncertainties associated with the groundwater age dating technique (Lerner et al., 1990; Solomon and Sudicky, 1991; Ekwurzel et al., 1994; Szabo et al., 1996).

The objective of this study was to estimate and characterize groundwater recharge in the surficial aquifer in the Sandilands using chlorofluorocarbon (CFC-11, CFC-12, and CFC-113), tritium (^3H) and tritium/helium ($^3H/^3He$) groundwater age dating methods. The study was initiated with the instrumentation of five sites with shallow piezometer nests (11-28 m total depth) each consisting of three piezometers with vertical spacings of 2-7 meters and one

site with a single shallow piezometer distributed over a 50 km^2 area around the highest topographic elevation in the Sandilands.

The multi-tracer technique was used to provide comparison between groundwater ages and to evaluate the use of the age dating techniques in the Sandilands hydrogeological setting. Groundwater ages estimated using each CFC compound, ^3H and $^3H/^3He$ were compared to determine if non-conservative processes or groundwater flow conditions were affecting groundwater age estimates. Groundwater age profiles were determined at five piezometer nests and one provincial well nest to provide insight into the groundwater flow system and estimate vertical groundwater velocities and recharge rates. The piezometer nests were distributed regionally within the Sandilands to evaluate the spatial variability of groundwater recharge and determine possible controlling factors.

To aid in the interpretation of groundwater ages, it was also part of this study to improve the understanding of the groundwater flow system and groundwater geochemistry of the region. Piezometric data were collected from the piezometer nests and existing provincial monitoring wells to determine water table elevations and groundwater flow directions $\delta^{18}O$ isotope analyses were done to assess the seasonal variations of groundwater recharge The piezometer nests, provincial wells and domestic wells in the region were sampled for major ion geochemistry and $\delta^{13}C_{DIC}$ to define the local and regional groundwater geochemistry

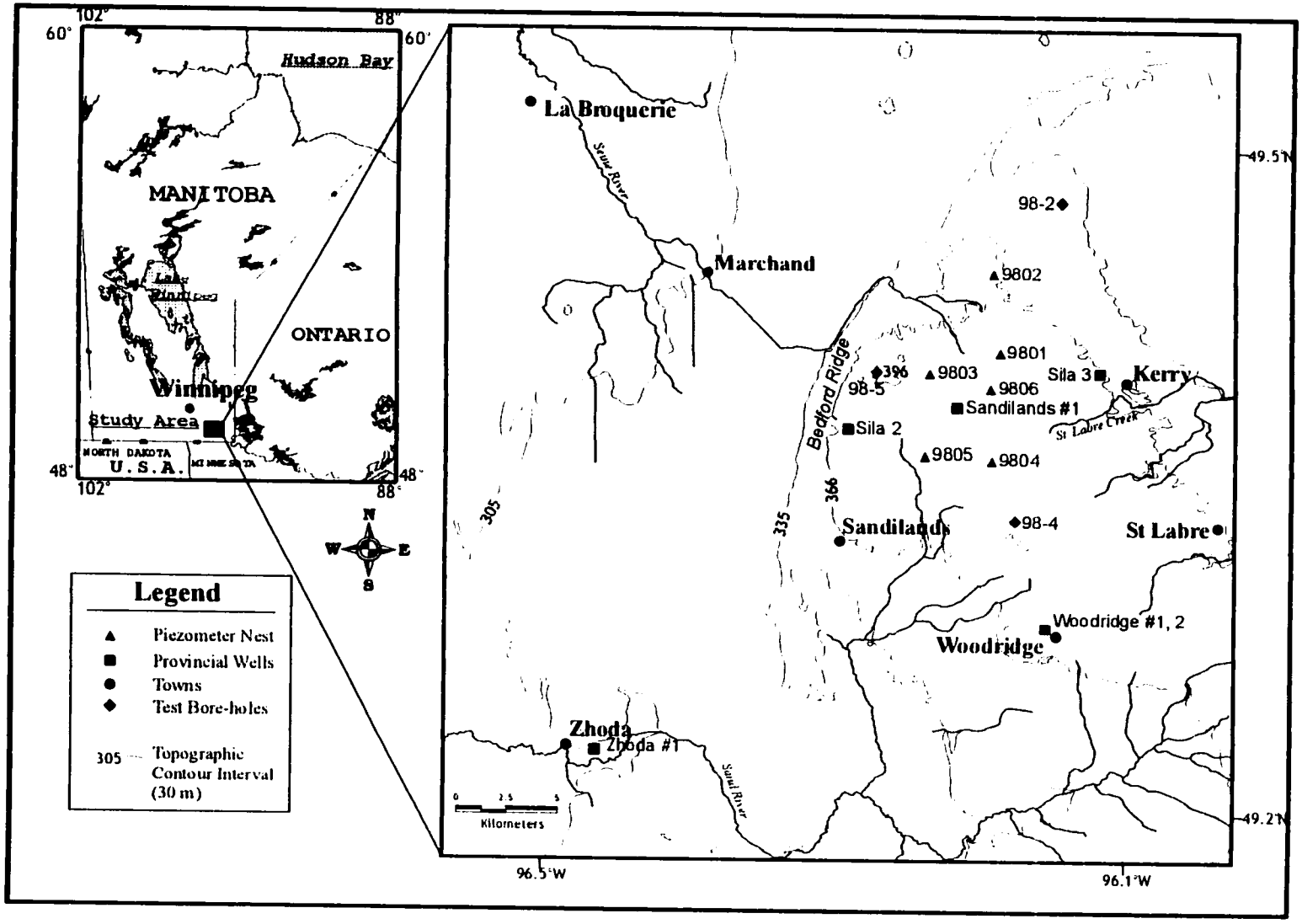

Figure 1. Map of the study area showing the topography of the Bedford Ridge and the location of the piezometer nests, provincial wells and towns where groundwater samples were collected. The Bedford Ridge is considered the western boundary of the Sandilands glaciofluvial complex (Teller and Fenton, 1980). Digital data used to construct this map was provided by the Geological Survey of Canada (personal communication, 1999).

2.0 Background

2.1 Chlorofluorocarbons (CFCs)

Atmospheric concentrations of chlorofluorocarbons (CFC-11, CFC-12, and CFC-113) have been steadily increasing over the past 50 years (Figure 2). CFCs were recognized for their use as environmental tracers in the 1970s and are now routinely used as tracers of oceanic circulation (Hammer et al., 1978; Gammon et al., 1982; Bullister and Weiss, 1983) and of groundwater flow (Thompson and Hayes, 1979; Busenberg and Plummer, 1992; Dunkle et al., 1993; Szabo et al., 1996; Johnston et al., 1998). Previous studies have found that CFCs can be effective dating tools for estimating groundwater ages between 0-50 years and have been successfully used to determine groundwater velocities and recharge rates (Ekwurzel et al., 1994; Reilly et al., 1994; Bohlke and Denver, 1995). CFCs can, however, be affected by non-conservative processes such as contamination, sorption, and anaerobic microbial degradation (Semprini et al, 1991; Kahil and Rasmussen, 1989; Lovely and Woodward, 1992). In general, the above processes affect CFC-11, CFC-12 and CFC-113 to varying degrees and a comparison of each compound can provide insight into the factors affecting subsurface CFC concentrations (Russell and Thompson, 1983; Cook et al., 1995; Plummer et al., 1998).

2.1.1 CFC Groundwater Age Dating Method

The principle of dating groundwater using CFCs is based on the equilibrium solubilities of CFCs in water according to their atmospheric concentration. CFCs enter the groundwater by partitioning between the unsaturated zone atmosphere and the infiltrating water at the water table. Groundwater ages are determined by measuring the dissolved

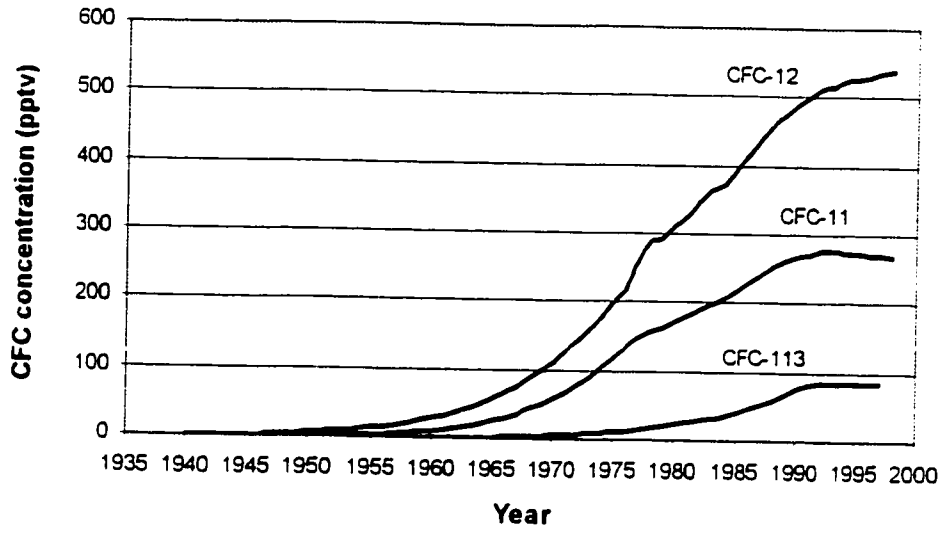

Figure 2. CFC-11, CFC-12 and CFC-113 atmospheric concentrations versus time. Pre-1975 CFC-12, CFC-11 and CFC-113 atmospheric curve data are estimates from production records and normalized to CFC values measured in the Pacific Northwest in 1977 (McCarthy et al., 1977; Busenberg and Plummer, 1991). From 1975-1976, CFC-12 and CFC-11 data are yearly averages of measurements made by Rasmussen and Kahil (1986) at the Pacific Northwest station in Oregon. All post 1976 CFC-12 and CFC-11 data are averages of monthly concentrations measured by NOAA at Niwot Ridge, Colorado. CFC-113 data from 1977-1990 are from W. Smethie (1998) and data from 1991-1997 are averages of monthly concentrations measured by NOAA at Niwot Ridge, Colorado.

concentration of CFC in groundwater, calculating the equilibrium partial pressure of the CFC and comparing it with the atmospheric growth curve to determine the year in which the groundwater was recharged. This method assumes that the soil air directly above the saturated zone is in equilibrium with the troposphere and that the recharge year is the time when the groundwater was isolated from the unsaturated zone. In practice, diffusion of CFCs through thick unsaturated zones to the water table can take several years and must be corrected for in the CFC groundwater ages. If there is a diffusive time lag of CFCs in the unsaturated zone that is not accounted for CFC groundwater ages can be overestimated.

Johnston et al. (1998) found that CFC-11 groundwater ages were between 6 and 10 years greater than $^{3}H/^{3}He$ groundwater ages due to a diffusional time lag through a 25 m thick unsaturated zone (Weeks et al., 1982; Cook and Solomon, 1995; Johnston et al., 1998).

CFC concentrations in groundwater can also be affected by dispersion. Previous studies have modeled CFC concentrations in groundwater under the influence of dispersion and found that CFCs are affected to a lesser degree by dispersion than other tracers, such as tritium and helium. This was attributed to the steady increase in atmospheric CFC concentrations which minimizes the effect that dispersion has on concentration profiles (Ekwurzel et al., 1994; Reilly et al., 1994). Ekwurzel and others (1994) showed that for dispersivities of 0.5 m or less, the difference between CFC age estimates and actual groundwater travel times was less than 3 years.

The process of calculating the equivalent partial pressure of the CFC at the time of recharge is based on Henry's Law:

$$C_i = K_i * P_i \qquad (1)$$

where C_i is the concentration of the *i*th CFC in water, K_i is the Henry's Law constant and P_i is the partial pressure of the *i*th CFC in the unsaturated zone atmosphere at the time of recharge. For total pressures close to 1 atm, the CFC partial pressure is then close to the CFC concentration in parts per trillion volume (pptv) in air. For a complete discussion of the relationship between atmospheric pressure in the Sandilands, calculated CFC partial pressures and groundwater ages refer to Appendix II. The Henry's Law constants for CFC-11, CFC-12 and CFC-113 are calculated from the solubility relationships determined by

Warner and Weiss (1985) and Bu and Warner (1995). The CFC solubility relationship is temperature and salinity dependent and for zero salinity is as follows:

$$\ln K = a_1 + a_2(100/T) + a_3 \ln(T/100) \quad (2)$$

where K is the Henry's Law constant, T is the recharge temperature in Kelvin, and a_1,a_2, and a_3 are the solubility constants for the calculation of K.

The Henry's Law constant for each CFC compound is then inserted into Equation 1 and the equilibrium CFC partial pressure is calculated and compared with the atmospheric CFC values to determine the year the groundwater was recharged. For a detailed discussion of the data used to produce the atmospheric curves used in this study refer to Appendix III. Calculated CFC partial pressures in parts per trillion volume (pptv) that fell between the yearly averages were estimated to the nearest month using linear interpolation.

2.2 Tritium/Helium (^{3}H/^{3}He)

Atmospheric concentrations of tritium (^{3}H), a radioactive isotope of hydrogen, increased dramatically due to the above ground testing of thermonuclear devices and has been extensively used as an environmental tracer in groundwater studies over the past 35 years (von Buttlar, 1959; Brown, 1961; Nir, 1964). More recently the radioactive decay product of ^{3}H, helium (^{3}He), has been used in groundwater investigations to determine the year of groundwater recharge (Cerling,et al., 1987; Poreda et al., 1988; Schlosser et al., 1988; Solomon et al., 1992; Solomon et al, 1993). The ^{3}H/^{3}He groundwater dating method has an advantage over the ^{3}H method as it is less sensitive to uncertainties in the tritium input function and groundwater velocities can be determined from a single point below the water

table. Modeling done by Solomon and Sudicky (1991) examined the variation in $^3H/^3He$ groundwater ages for different tritium input values and found that the ^3H distribution in the aquifer was highly sensitive to the input values. In contrast, the ratio of ^3H to ^3He in groundwater and hence, the groundwater age distribution, was relatively insensitive to the ^3H input function.

The use of the $^3H/^3He$ dating method to determine groundwater recharge rates has been validated by Solomon et al. (1993) at a well characterized study site in Sturgeon Falls, Ontario. Groundwater ages determined using the $^3H/^3He$ method were found to be very similar to those determined from the location of the mid-1960s ^3H peak. $^3H/^3He$ groundwater ages can be effected by dispersion and must be examined with respect to the groundwater flow system. Previous studies have found that in a one dimensional vertical groundwater flow system the longitudinal spreading over a short distance (<10 or 20 m) can often be represented by local scale dispersivities on the order of 0.1 m (Sudicky et al., 1993). In groundwater systems where the velocity is 0.5 m/yr or greater with dispersivities on the order of 0.1 m, the difference between $^3H/^3He$ groundwater ages and actual groundwater travel times are less than 10% (Solomon and Sudicky, 1991). Greater longitudinal dispersivities, on the order of 1 m, can result in differences between $^3H/^3He$ groundwater ages and actual groundwater travel times of up to 5 and 12 years above and below the mid 1960's bomb peak, respectively. Dissolved concentrations of helium in groundwater may also be affected by diffusive losses near the water table and sample collection may be influenced by air entrapment and gas stripping (Schlosser et al., 1989; Solomon et al., 1992; Ekwurzel et al., 1994).

2.2.1 $^3H/^3He$ Groundwater Age Dating Method

The long term record of ^3H in precipitation in Ottawa, Ontario shows that ^3H concentrations in precipitation increased dramatically in the mid-1960s (Figure 3). The measurement of ^3H in groundwater can be compared with the decayed values of tritium in precipitation to estimate a groundwater age and recharge rate (Allison and Hughes, 1975; Egboka et al., 1983; Robertson and Cherry, 1989).

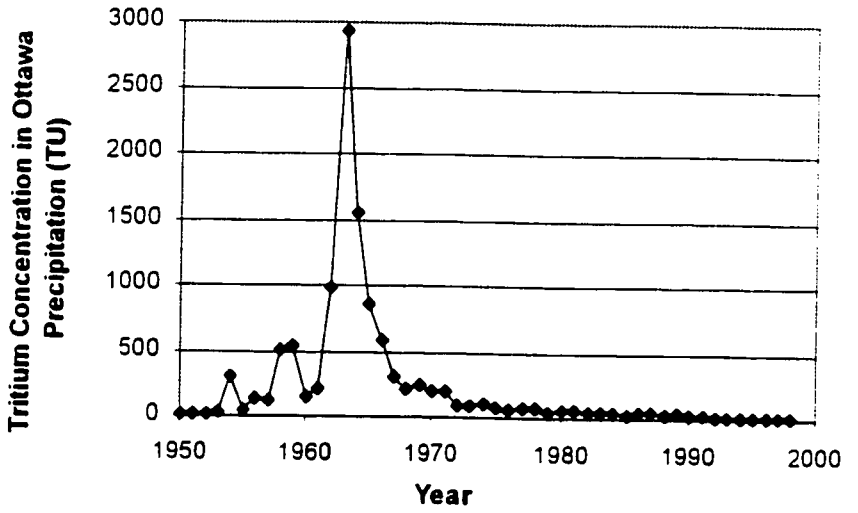

Figure 3. Tritium in Ottawa precipitation from 1953 to 1998. Data collected by R.M.Brown, Atomic Energy Canada Limited (AECL) and are available from the International Atomic Energy Agency (IAEA) (1998).

The $^3H/^3He$ method is based on the concept that as infiltrating water in the subsurface becomes isolated from the unsaturated zone ^3He concentrations from the decay of ^3H will begin to increase as the dissolved gas accumulates in the groundwater. As the time since the groundwater was recharged increases, the dissolved concentration of ^3He will also increase.

If dispersion is negligible, measurement of the dissolved concentrations of ^3H and ^3He in the groundwater can be used to calculate the groundwater age as follows (Poreda et al., 1988):

$$t = \lambda^{-1} \ln\left(\frac{^3He^*}{^3H} + 1\right) \tag{3}$$

where t is the estimated groundwater age, λ is the ^3H decay constant, and ^3H and $^3He^*$ are the measured concentrations of ^3H and tritiogenic ^3He in the groundwater, respectively.

Groundwaters contain dissolved ^3He from a variety of sources, which must be taken into account to determine the tritiogenic component. These include 1) dissolved ^3He in equilibrium with the atmosphere; 2) ^3He due to the presence of excess air entrained by infiltrating water and during sampling; 3) lithogenic (from the n,α reactions on ^6Li) and mantle ^3He. In general, lithogenic and mantle helium are negligible in shallow groundwater systems and corrections need only be made for the atmospheric and excess ^3He (Poreda et al., 1988; Schlosser et al., 1989).

The measurement of the dissolved concentration of Ne is essential to determine the correction of the dissolved ^3He concentration. The component of tritiogenic ^3He can be calculated as follows:

$$^3He^* = {}^3He_{\text{measured}} - {}^3He_{\text{storage gain}} - {}^3He_{\text{equilibrium - excess}} \tag{4}$$

where $^3He_{\text{measured}}$ is the total measured ^3He, $^3He_{\text{storage gain}}$ is the amount of ^3He accumulated in the copper tube sample from the decay of ^3H during sample storage, and $^3He_{\text{equilibrium - excess}}$ is the amount of ^3He present from atmospheric equilibrium and excess air entrapped during infiltration or sampling. The ^3He present due to atmospheric equilibrium and excess air is

calculated using the dissolved neon concentrations (Schlosser et al., 1989). Assuming that the ratio of atmospheric ^3He to Ne is constant the following calculation can be made:

$$^3He_{equilibrium - excess} = R_{He/Ne} * Ne_{measured} \quad (5)$$

where $R_{He/Ne}$ is the ratio of the ^3He to Ne atmospheric solubilities and $Ne_{measured}$ is the total Ne measured in the sample.

The solubility relationships of Ne and He were determined by Weiss (1971). At a recharge temperature of 3 °C, the solubility of neon is $2.23 * 10^{-7}$ ccSTP/g and for ^3He it is $6.71 * 10^{-14}$ ccSTP/g. The solubility of ^3He is determined using the ratio of $^3He/^4He$ in air determined by Clarke et al. (1976) with a correction for the 1.2 % fractionation that occurs when helium dissolves in water (Weiss, 1970).

2.3 Recharge Rates

Groundwater recharge can be defined as the amount of water added to the groundwater system in excess of soil water deficits, evapotranspiration, runoff and the changes in storage by the infiltration of precipitation through the unsaturated zone to the water table (Lerner et al., 1990). In this context, the groundwater recharge rate is direct recharge and does not include groundwater input that may occur as the result of water infiltration following runoff, ponding in low lying areas, and anthropogenic sources of recharge such as irrigation.

$$\text{recharge} = \text{precipitation} - \text{runoff} - \text{evapotranspiration} \pm \text{storage change} \quad (6)$$

There are many different methods for estimating groundwater recharge and include direct measurement, water balance methods, Darcy flux calculations, and tracer techniques. In practice, groundwater recharge rates are often estimated using the water balance method.

The principle is that groundwater recharge can be calculated by using readily available data such as rainfall, runoff, and evapotranspiration estimates to determine the residual amount of precipitation available for recharge (Lerner et al., 1990). While this method is practical, the estimated recharge rate has a high uncertainty due to the magnitude of the errors associated with the estimation of the parameters such as evapotranspiration. Similarly, the use of hydraulic head data and the hydraulic conductivity of the aquifer material to determine the Darcy flux of groundwater can be uncertain. Hydraulic conductivities can vary over several orders of magnitude and are difficult to measure precisely, resulting in large ranges in recharge estimates. The use of environmental tracers to quantify groundwater recharge has been used extensively in the past and is accepted as a more accurate method to determine recharge than the above methods (Lerner et al., 1990; Robertson and Cherry, 1989; Solomon and Sudicky, 1991).

The use of environmental tracers such as tritium, ^{3}He, and CFCs to quantify groundwater recharge rates has been well documented (Solomon et al., 1993; Ekwurzel et al., 1994; Solomon et al., 1995; Szabo et al., 1996). Solomon and Sudicky (1991) found that ^{3}H/^{3}He age gradients measured near the water table could be used to obtain reliable estimates of spatial variations in recharge rates. Similarly, Ekwurzel et al. (1994) found that recharge rates determined using ^{3}H/^{3}He and CFCs were comparable to recharge rates estimated from detailed studies of the hydrology of the area.

2.3.1 Recharge Rate Methods

Groundwater recharge rate estimates using the tracer method can be calculated as follows:

$$r = V_z\theta \tag{7}$$

where r is the recharge rate (mm/yr), V_z is the vertical component of the groundwater velocity (mm/yr), and θ is the effective porosity of the aquifer material (m^3/m^3) (Solomon et al., 1993). The first step in using $^3H/^3He$ and CFCs to estimate groundwater recharge rates is to determine groundwater ages with depth in the aquifer. Assuming that one-dimensional vertical flow dominates in an unconfined aquifer at or near the groundwater divide, the vertical groundwater velocity can be calculated by dividing the depth of a piezometer below the water table by the groundwater age. In the case where there is a nest of piezometers completed at different depths, the vertical velocity can also be calculated by taking the vertical distance between two piezometers and dividing it by the difference in groundwater ages.

Inherent in the calculation of vertical groundwater velocities using groundwater ages is the assumption that there is no groundwater mixing and that dispersion of the dissolved gases and tritium is minimal. Groundwater ages will then be representative of the advective groundwater transport time and a reasonable approximation of the groundwater velocity can be obtained (Solomon and Sudicky, 1991; Solomon et al., 1993; Ekwurzel et al., 1995). In reality, groundwater is generally a mixture of several years of groundwater recharge and the estimated tracer groundwater age is closer to a mean groundwater residence time and therefore a mean groundwater velocity.

3.0 Study Area

The study area is located on the Sandilands glaciofluvial ridge, which encompasses the Sandilands Provincial Forest approximately 80 km southeast of Winnipeg in southeastern Manitoba. The piezometer nests were installed near the Bedford Ridge, which is the highest topographic point in the Sandilands (Figure 1). The ridge is characterized by a steep decline in elevation from 396 m.a.s.l. to less than 335 m.a.s.l. below the ridge. A large percentage of the Sandilands area is a plateau at approximately 384 m.a.s.l. with a more subdued decrease in topography observed to the north, south, and east of the study area. Variable thicknesses in the surficial deposits in the region are the primary control on the topography of the area.

The Sandilands is characterized by a continental temperate climate with large seasonal variations in temperature and precipitation. Total annual precipitation is 574 mm and average annual snowfall is approximately 114 cm. Air temperatures vary annually from an average of −18 °C in January to 19.3 °C in July, with an average annual air temperature of 3.0 °C (Environment Canada, 1999).

Land use in the area is dominated by forested land managed by the Forestry Branch of the Manitoba Ministry of Natural Resources. The forest type surrounding the piezometer nests is a mature monoculture of jack pine. Additional land uses in the region include rural residential communities and small-scale agricultural and livestock farming.

The Bedford Ridge is drained by the Seine, Sand and St. Labre rivers. The ridge area appears to be well drained although wetlands comprise a large percentage of the land cover surrounding the ridge and extend tens of kilometers to the north, south, east and west.

Agricultural areas surrounding the Sandilands generally rely on extensive drainage ditches to enable farming in the wetland regions (Betcher et al., 1995).

The study area borders on three distinct bedrock units; 1) Paleozoic carbonates, sandstones and evaporites in the northwest and west. 2) Precambrian igneous and metamorphic rocks in the east. 3) Jurassic shales and sandstones in the southwest. The Paleozoic carbonate unit is the major bedrock aquifer in southeastern Manitoba with a secondary Paleozoic sandstone aquifer underlying the carbonates in this region (Betcher, 1995).

Bedrock in the Sandilands is overlain by surficial deposits that range in thickness from 76 meters on the periphery of the Bedford Ridge to over 152 meters on the ridge. Much of the Sandilands glaciofluvial ridge was formed as an ice-free region between two ice lobes during the Late Wisconsinan glaciation followed by a succession of glacial advances and retreats and subsequent glacial lake formation which left a complex layering of sand, gravel, tills, and clay (Teller and Fenton, 1980). The surficial deposits in the study area are predominantly subaqueous outwash sands and gravels with minor clay interbeds in the central, northern and western sections with glacial tills primarily in the east and south (Figure 4). The groundwater flow system within the surficial deposits has not been described previously and was investigated as part of this study. Results and interpretations of groundwater flow in the study area are presented in section 5.1.

Instrumentation installed as part of this investigation included five piezometer nests and one single piezometer. Piezometers were installed using a solid stem auger and PVC drive points to eliminate the use of any drilling fluids that could cause CFC contamination

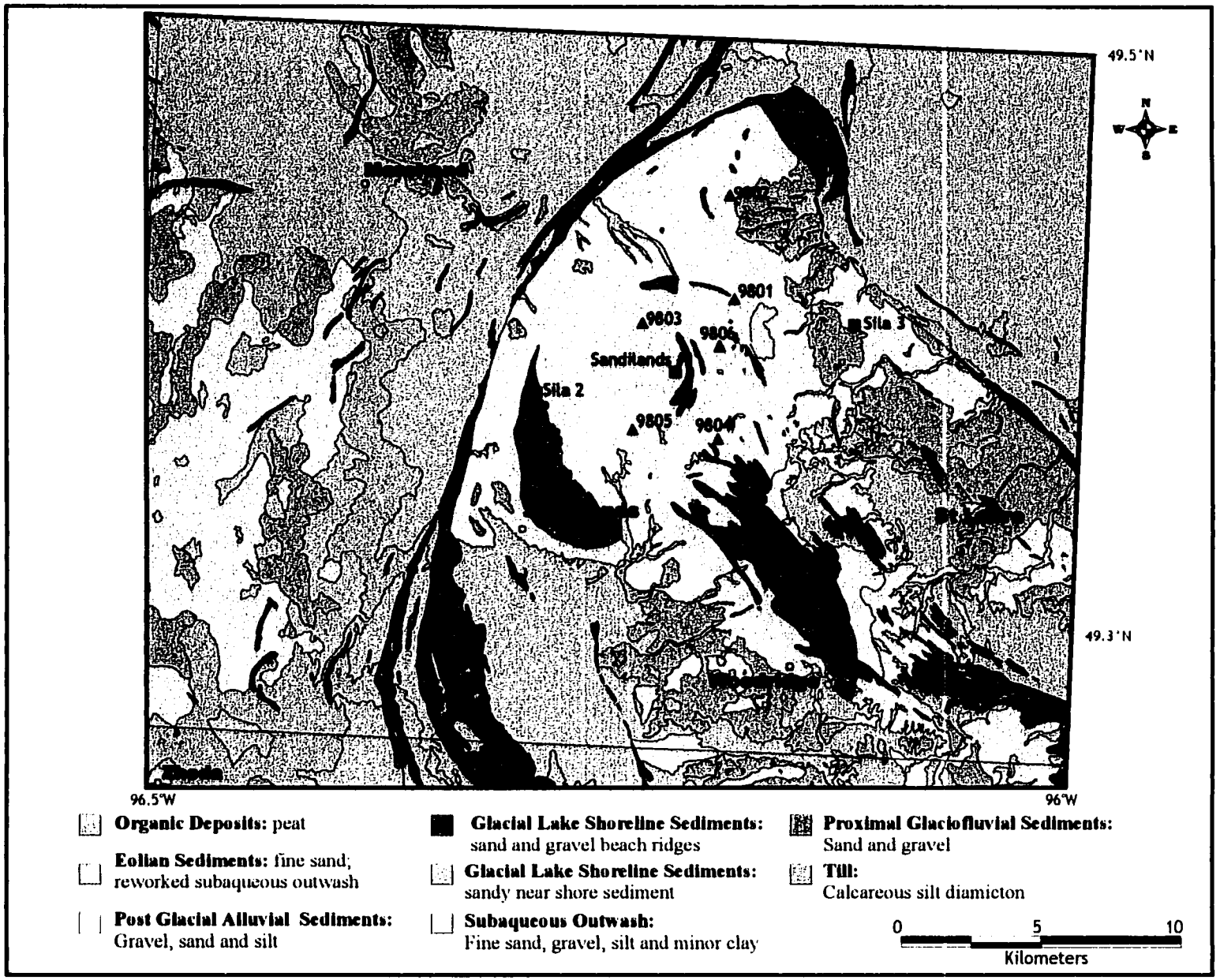

Figure 4. Surficial geology of the study area.

(Figure 1). Each nest consists of 3 piezometers completed approximately 3, 6 and 9 meters below the water table. Piezometers were constructed with polyvinyl chloride tubing with 24 cm screens. Details of piezometer installation and construction are given in Appendix I. In addition to the piezometers installed for this study, several provincial wells managed by the Manitoba Water Resources Branch were used to obtain piezometric data and groundwater samples. The field study also included the sampling of domestic wells in rural towns in and on the periphery of the Sandilands.

4.0 Field Sampling and Analytical Methods

Groundwater samples were collected from the piezometer nests, provincial wells, and domestic wells for major ion and stable isotope analyses. The provincial and domestic wells were sampled in July, 1998 and the piezometer nests were sampled in September, 1998. Groundwater samples were collected after a minimum of three well volumes were purged from each piezometer and well. Domestic wells were selected on the basis that a drilling record could be found in the provincial well data base and samples were collected from house taps upstream of any water softening or iron filtering systems. Temperature, pH, dissolved oxygen, and electrical conductivity measurements were taken during the July sampling with the addition of redox potential and alkalinity measurements to the September sampling.

Samples collected for major ion analyses were filtered using 0.45 μm cellulose acetate membranes and collected in 125 ml high-density polyethylene bottles. Cation samples were acidified by adding 1.5 ml of ultra-pure HNO_3 to the sample and were analyzed by ICP-OES with an analytical uncertainty of ± 7 %. Anions were analyzed using a DX-100 ion chromatograph with an uncertainty of ± 10 %. All analyses were performed by the Geological Survey of Canada Analytical Chemistry Laboratory. Alkalinity was determined in the laboratory with an automated titration system. Samples were acidified using 0.1N H_2SO_4 and pH was plotted versus acid added. Field and laboratory alkalinity results were comparable to within 10 %.

Water samples for ^{13}C analyses in dissolved inorganic carbon ($\delta^{13}C_{DIC}$) and ^{18}O in water were collected in 500 ml amber glass bottles and 100 ml HDPE bottles, respectively. $\delta^{13}C_{DIC}$ samples were preserved with mercuric chloride. $\delta^{13}C_{DIC}$ analyses were performed by reacting the water sample with 85% phosphoric acid under vacuum. Carbon dioxide produced by the reaction was analyzed on an automated triple collector VG SIRA 12 gas source mass spectrometer with a precision of ± 0.10 ‰. $\delta^{18}O$ analyses were done on CO_2 in equilibrium with the water on the VG SIRA 12 gas source mass spectrometer. Both analyses were performed at the G.G. Hatch Isotope Laboratories at the University of Ottawa. Results are expressed in standard δ-‰ notation with respect to VPDB (Vienna Peedee Belemnite) for $\delta^{13}C$ and VSMOW (Vienna Standard Mean Ocean Water) for $\delta^{18}O$.

Groundwater was sampled for CFC analyses from each piezometer and selected provincial wells and from the shallowest and deepest piezometers for ^{3}He, ^{4}He and Ne. CFC and He and Ne samples were collected using a down hole copper tube sampling apparatus (refer to Appendix III) (Solomon, 1998; Kotzer, 1998). Metal sampling equipment was used to minimize CFC sample contamination associated with plastics and rubbers and the samples were isolated from contact with the atmosphere.

Samples were taken in deep piezometers by pressurizing the sampling apparatus and lowering it down the piezometer to within 20 cm of the bottom. Once at depth, the pressure was released, the samples were collected and the system was repressurized prior to bringing the samples to surface. At the surface, the samples were sealed by cold welding the ends of the copper tubes using a hand held crimper for CFC samples and refrigeration clamps for the $^{3}H/^{3}He$ samples. Samples collected in shallow piezometers followed the same procedure with

the exception that the system was placed under partial vacuum while down hole to increase the groundwater volume that could be collected.

Quadruplicate CFC samples were collected and analyzed by Y. Sun at the CFC Laboratory in the Department of Earth Sciences at the University of Waterloo. Dissolved CFC-11, CFC-12, and CFC-113 concentrations were measured using a purge and trap gas chromatograph with an electron capture detector with a detection limit of 3 pg/l and an analytical uncertainty of 1% based on daily calibrations of NOAA air standards.

Analyses for dissolved helium and neon isotopes were performed by Dr. Tom Kotzer at the Chalk River Laboratories, Atomic Energy Canada Limited in Chalk River, Ontario. The dissolved gas concentrations were determined using a double collector static-source mass spectrometer system in combination with a cryogenic gas-separation system (Kotzer and Gascoyne, 1995; Noack, 1995) Analytical error was within ± 10%.

Tritium samples were collected in conjunction with the ^{3}He samples in four 125 ml HDPE bottles for a total of 500 ml. Analyses were done by the Environmental Isotope Lab at the University of Waterloo, Waterloo, Ontario. All samples were analyzed by scintillation counting after electrolytic enrichment with a detection limit of 0.8 TU and an analytical uncertainty of less than 10%.

5.0 Results and Discussion

5.1 Groundwater Flow

Piezometeric data were collected from the piezometer nests and provincial wells in the study area to assess the groundwater flow system in the surficial deposits and are tabulated in Appendix II. A generalized configuration of the water table based on piezometric data and the locations of lakes, streams, and wetlands in the region is shown in Figure 5. The data were compiled in a Geographic Information Systems (GIS) program and interpolated to produce water table elevation contours. While this map is an approximation of water table elevations in the Bedford Ridge area, it is useful for general groundwater flow observations.

In general, the water table follows the topographic outline of the region with a shift in the groundwater divide to the east of the topographic high. The steep decrease in topography at the Bedford Ridge appears to be drawing the water table down in the west and offsetting the groundwater divide from the topographic high. The presence of thick units of near surface clayey tills in the eastern region of the study area in contrast to predominantly highly permeable sands, which characterize the topographic high, may also be influencing the water table elevation (Figure 6).

Similar to the topography, the central portion of the study area is characterized by the highest water table elevations (381 m.a.s.l.), which decrease gently outwards. In general, the water table decreases by less than 10 meters over several kilometers resulting in horizontal gradients on the order of 0.003 in the central plateau region. Water table gradients rapidly increase where there is a steep decrease in topographic elevations, most notably at the

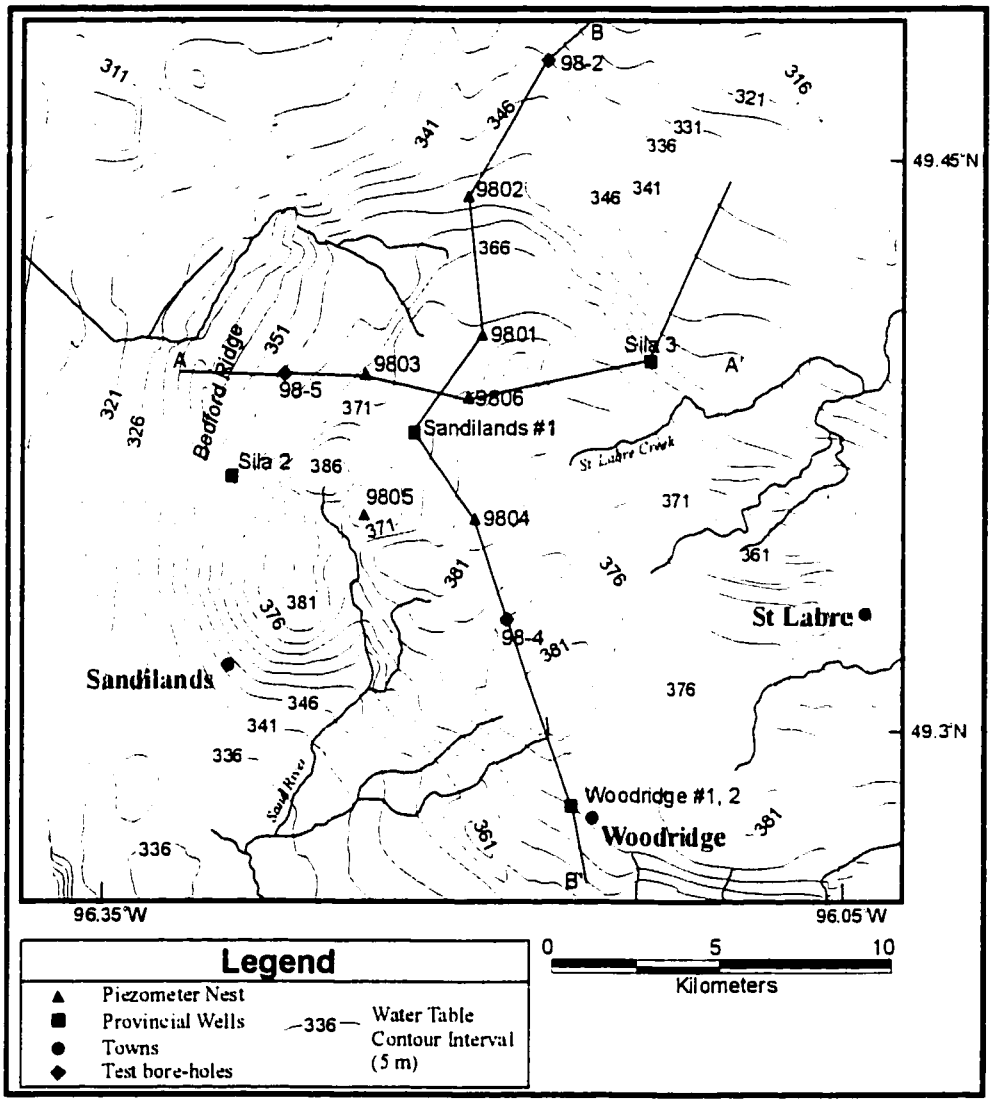

Figure 5. Water table map showing peak water table elevations (381 m.a.s.l) in the center of the study area, to the southeast of the Bedford Ridge and cross-sections A-A' and B-B'. The area containing the higher water table elevations in the region include piezometer nests 9804, 9806, and to some degree 9801.

Bedford Ridge. Shallow groundwater likely follows the slope of the water table and flows outward from the central high points towards the north, east, and west.

A primary objective in the evaluation of groundwater flow in the Sandilands was to determine flow conditions at the piezometer nests where CFC and $^{3}H/^{3}He$ data were collected. In particular, it was a goal to determine whether groundwater flow at the nests is predominantly vertical. Due to the small vertical spacing of the piezometers at each nest and hydraulic conductivities in the sand that exceed $1 * 10^{-5}$ m/s, it was not possible to use piezometric data to determine vertical hydraulic gradients at most of the sites Sites 9804 and 9803 do, however, indicate that downward gradients range between 0.135 and 0.014 within the study area (Table 1). In addition, sites such as 9804 and 9806 are located approximately on the groundwater divide and shallow groundwater flow is likely to be predominantly vertical.

Table 1
Downward Vertical Hydraulic Gradients Measured at Two Locations in the Study Area

Piezometer #	Hydraulic Head (m.a.s.l)	Head Difference (m)	Vertical Distance (m)	Vertical Gradient	Flow Direction
9804-2	381.61	0.951	7.044	0.135	down
9804-3	380.659				
9803-1	366.808	0.697	48.292	0.0144	down
9803-4	366.111				

Water table elevations and the comparison of vertical to horizontal hydraulic gradients were used to infer groundwater flow conditions at the piezometer nests. Horizontal

gradients were calculated at each nest with respect to the water table elevation and its distance from site 9804, located approximately on the groundwater divide, and compared to the vertical gradient measured at site 9803. Sites 9804, 9806 and 9801, located on or near the groundwater divide, likely have predominantly vertical flow with vertical gradients between 8 and 10 times greater than the horizontal gradients between sites. In contrast, sites 9802, 9803 and 9805 have increasing components of horizontal flow (Table 2).

Table 2
Comparison of Vertical to Horizontal Gradients

*Site 9804: Water Table Elevation (m.a.s.l.) = 381.610
Site 9803: Vertical Gradient = 0.0144

Site #	Horizontal Distance to 9804 (km)	Water Table Elevation (m.a.s.l.)	Head Difference Compared to 9804	Horizontal Gradient from site # to 9804	Ratio of Vertical to Horizontal Flow**
9806	3.53	376.626	4.984	0.0014	10
9801	5.50	371.642	9.968	0.0018	8
9802	9.58	360.627	20.983	0.0022	6.5
9803	4.67	366.808	14.802	0.0032	4.5
9805	3.29	367.884	13.721	0.0033	3.5

* Site 9804 located approximately on the groundwater divide
** Vertical gradient at site 9803 compared with horizontal gradient between site 9804 and the site # indicated.

Geologic information was compiled from drilling during the study site instrumentation and the provincial well data base to produce two conceptualized geologic

cross sections through the study area (Figure 6). In some cases, where the sand and till are illustrated as thick units they have been simplified from drilling logs and may contain thin interbeds of till and clay, however, the predominant unit was used for illustrative purposes. Hydraulic conductivities of the sediments were found to range over five orders of magnitude from $2.4*10^{-4}$ m/s for sands to $8.3 * 10^{-9}$ m/s for the clayey tills (Table 3) (refer to Appendix II for complete tabulation of hydraulic conductivities). It is proposed that the distribution of the sediment types may significantly affect regional groundwater flow patterns in the Sandilands and it was a concern that this would complicate the interpretation of groundwater ages. As indicated in Figure 6, with the exception of sites 9804, 9802 and Woodridge, the piezometer nests are located in shallow sand units and are likely not influenced by the channeling of groundwater flow around the tills.

Table 3
Range of Hydraulic Conductivities (K) of Sediments in the Study Area

Piezometer #	Sediment Type	*$K_{average}$ (m/s)
9806-3	coarse sand	$2.4 *10^{-4}$
9802-3	medium sand	$6.8 * 10^{-5}$
9803-1	very fine sand	$8.2 * 10^{-6}$
9802-1	silty, sandy till	$6.8 * 10^{-6}$
9804-2	sandy, clayey till	$3.5 * 10^{-8}$
9804-3	clayey till	$8.3 * 10^{-9}$

* an average of hydraulic conductivities determined using the Hvorslev method on multiple bail tests at each piezometer.

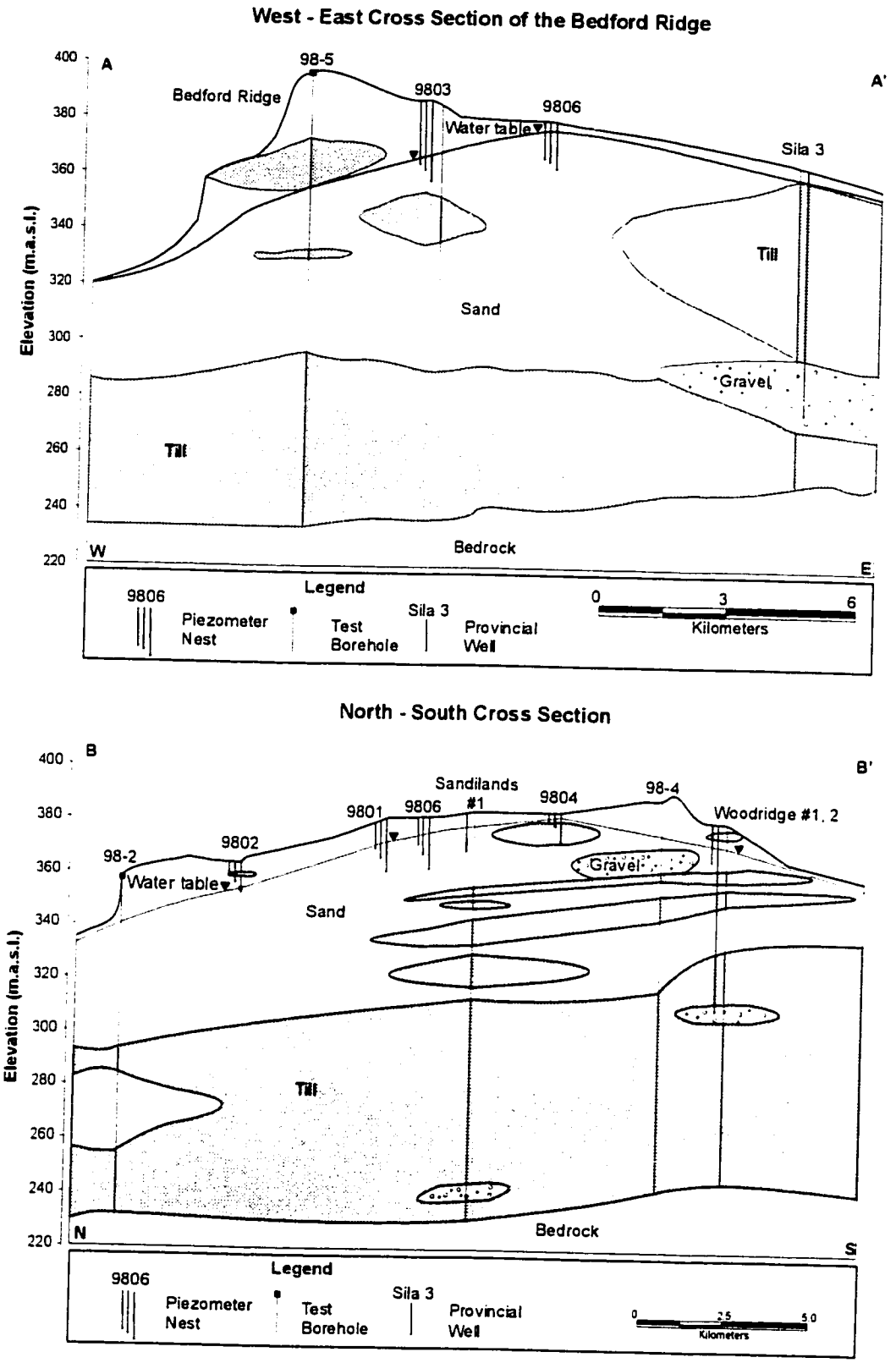

Figure 6. Conceptualized geologic cross sections through the study area showing the location of piezometer nests, wells, test bore holes and water table elevation. The distribution of the sediments is an approximation as geological data was only available from bore holes in select locations. In many cases, where the sand and till are illustrated as thick units they have been simplified from drilling logs and in reality contain many thin layers of till and sand, however, the predominant unit was used for illustrative purposes.

5.2 Groundwater Geochemistry

5.2.1 Groundwater Geochemistry of the Piezometer Nests

Groundwater from the piezometer nests is dominated by a Ca-Mg-HCO_3 geochemical facies with pHs between 7.8 and 8.2 (Figure 7, Table 4). Tills and sands in the region are high in calcite and dolomite (Teller and Fenton, 1980) and account for the observed distribution of the major cations.

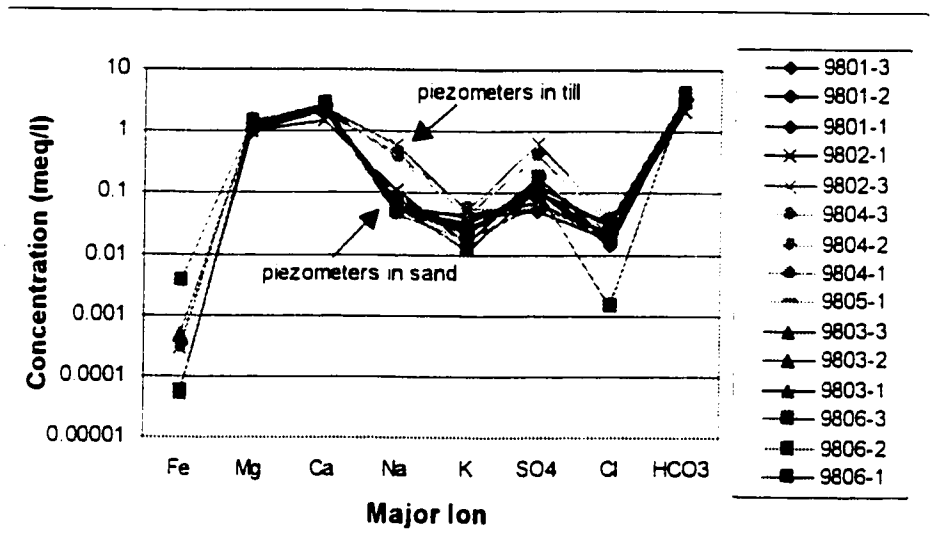

Figure 7. Groundwater geochemistry of the piezometer nests illustrating a predominantly Ca-Mg-HCO_3 facies and the difference in Na^+ and SO_4^{2-} concentrations in groundwater found in the till versus the sand.

Secondary constituents include Na^+ and SO_4^{2-}, with higher concentrations (up to 8 ppm higher in Na^+ and 20 ppm SO_4^{2-}) associated with piezometers screened in the clayey till. The source of the increased Na^+ may be from feldspar weathering in the till as Cl^- concentrations increase very slightly and do not support a saline source for Na^+. This phenomenon is also seen on a regional scale with the geochemistry of the domestic wells. Generally, if groundwater has come into contact with till it has a higher concentration of Na^+

Table 4
Field Measurements and Groundwater Geochemistry of the Piezometer Nests

Piezometer #	Depth b g s (m)	Depth below water table (m)	Geologic Unit	Field Measurements: Cond (uS/cm)	T (°C)	pH	DO (mg/l)	Redox (mV)	TDS[a]	Major Anions: $^{b}HCO_3^-$ (mg/l)	SO_4^{2-} (mg/l)	Cl^- (mg/l)	NO_3^- (mg/l)	Major Cations: Ca^{2+} (mg/l)	Mg^{2+} (mg/l)	Na^+ (mg/l)	K^+ (mg/l)	Fe_{tot} (mg/l)	Si (mg/l)	Sr (mg/l)
9801-1	10 175	1 725	sand	280	6 6	8 10	11 57	350	242	181	2 39	0 63	0 23	42	12	1 4	1 6	<0 003	3 9	0 034
9801-2	13 437	4 987	sand	300	10 6	8 14	11 12	313	262	195	3 44	0 71	0 34	46	13	1 2	1 7	<0 003	4 1	0 035
9801-3	16 448	7 998	sand	301	9 2	7 72	9 70	326	257	194	5 45	0 51	0 25	44	12	1 2	1 3	<0 003	4 1	0 034
9802-1	4 23	perched	sand	198	9	8 00	5 45	225	188	137	8 40	0 79	0 06	30	12	2 5	0 6	<0 003	6 3	0 035
9802-3	10 416	0 581	sand	338	7 1	8 12	10 13	268	309	221	31 4	1 39	0 14	48	18	14	2	0 008	5 9	0 058
9803-1	21 032	1 393	sand	340	9 2	7 97	11 52	245	274	206	4 85	1 19	0 18	46	14	1 7	1	<0 003	4 6	0 037
9803-2	23 712	4 073	sand	329	11 9	7 85	11 20	242	284	215	5 13	0 72	0 10	48	14	1 3	0 85	<0 003	4 6	0 037
9803-3	27 025	7 386	sand	335	8 3	7 90	11 36	244	270	199	6 58	0 98	0 20	49	15	1 5	0 93	0 014	4 6	0 037
9804-1	3 318	1 248	sand	293	20 3	8 06	7 37	220	277	207	3 09	0 63	0 37	48	15	1	0 71	<0 003	4 1	0 033
9804-2	5 095	3 025	clayey till	376	9 3	7 93	2 59	275	309	228	18 8	1 20	<0 05	46	17	8 5	1 7	<0 003	7 5	0 082
9804-3	12 139	10 069	clayey till	343	6 9	7 88	2 71	207	307	227	2 74	1 39	0 64	39	18	10	2 2	0 008	10	0 17
9805-1	21 702	2 866	sand	316	11 6	7 94	8 54	223	268	198	8 57	0 77	<0 05	47	15	2 1	0 88	0 009	5 4	0 045
9806-1	7 009	1 888	sand	370	9 6	7 81	12 08	242	317	235	5 65	< 001	2 16	55	17	1 6	0 45	0 098	4 8	0 042
9806-2	10 313	5 192	sand	332	7 5	7 97	8 80	245	261	193	5 15	0 62	0 71	47	14	1 4	0 49	<0 003	4 6	0 038
9806-3	13 508	8 387	sand	323	8	8 02	3 17	240	273	205	8 30	0 63	0 12	46	14	1 8	0 89	<0 003	5 1	0 043

[a] TDS calculated as a sum of dissolved ions and silica
[b] calculated from alkalinity

(Figure 8). Site 9804 suggests that cation exchange may be influencing the Ca^{2-} and Na^{-} concentrations of groundwater in the till. As groundwater flows from the sand down through the till there is a decrease in the concentration of Ca^{2-} as Na^{-} subsequently increases (Figure 9).

In general, groundwater from the piezometer nests is saturated with respect to calcite and in some cases with respect to dolomite as well (Table 5). $\delta^{13}C_{DIC}$ values for groundwater in the piezometers range from –9.4 ‰ to –12.9 ‰, with an average of –10.7 ‰. The $\delta^{13}C$ of soil CO_2 where the vegetation is predominantly trees and shrubs (C3 vegetation) is generally about –23 ‰ (Clark and Fritz, 1997). As the soil CO_2 with a $\delta^{13}C$ of –23 ‰ is hydrated and dissolved in groundwater it is enriched by approximately 10.2 ‰ at 3 °C and so the resulting $\delta^{13}C_{DIC}$ values in groundwater are close to -12.8 ‰. $\delta^{13}C_{DIC}$ values of groundwater in the Sandilands are enriched above -12.8 ‰ and are likely influenced by the dissolution of calcite. The $\delta^{13}C$ measured on carbonate in sand samples (Table 6) from the study area is on average -0.7 ‰. Dissolution of this carbonate would enrich the $\delta^{13}C_{DIC}$ derived from the dissolution of soil CO_2 to values closer to those observed in much of the groundwater in the piezometer nests. The final $\delta^{13}C_{DIC}$ of the groundwater is dependent on whether or not the system is open to the continual input of soil CO_2, with closed systems evolving to $\delta^{13}C_{DIC}$ values between the soil CO_2 and the $\delta^{13}C$ of the carbonate.

It appears that there may be a combination of open and closed system dissolution of calcite in the piezometer nests. In particular, there are notable differences in the $\delta^{13}C_{DIC}$

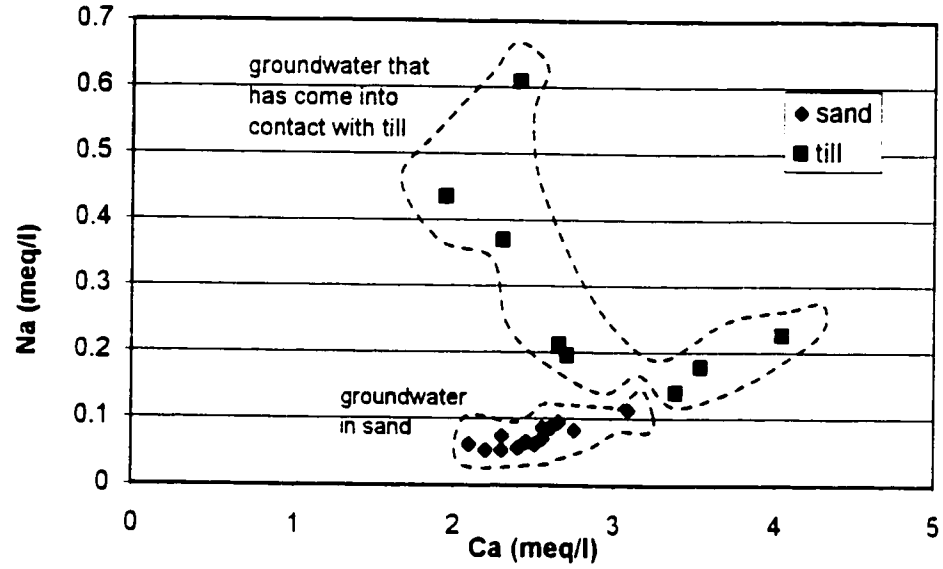

Figure 8. Na^{+} vs Ca^{2+} in groundwater from the piezometer nests, provincial and domestic wells that has flowed through till compared with groundwater in sand (excluding the domestic wells in the towns of Zhoda and La Broquerie which are discussed in the following section).

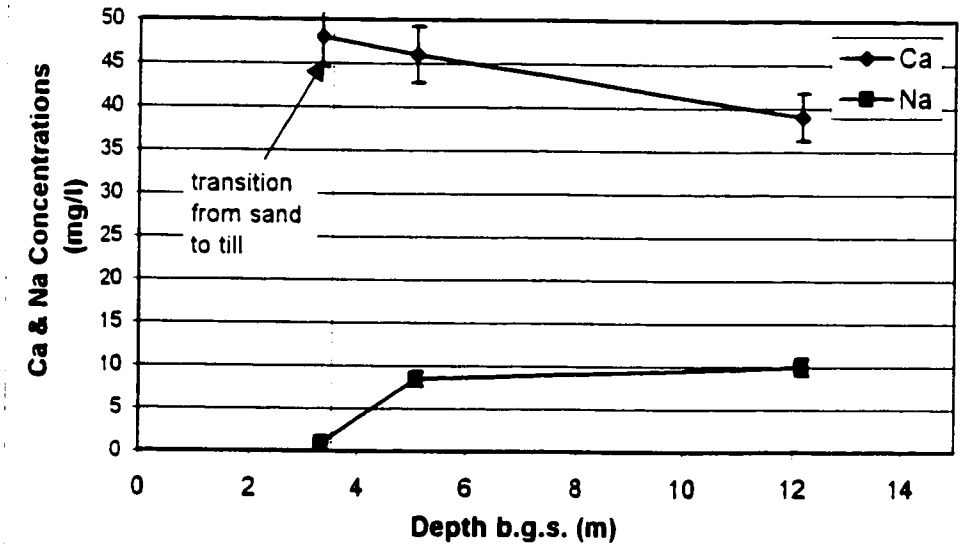

Figure 9. Ca^{2+} and Na^{+} versus depth at site 9804. Evidence of possible cation exchange in the till.

values where the water table is perched (site 9802, Table 5) and the $\delta^{13}C_{DIC}$ values where the groundwater flow times in the saturated zone are greater and therefore more likely to be representative of closed system conditions (site 9806, Table 5). An average $logP_{CO2}$ value of −2.75 also indicates that there is likely some closed system weathering occurring.

Table 5

Alkalinity, DIC and $\delta^{13}C_{DIC}$ for selected piezometers and provincial wells

Piezometer #	Depth below water table (m)	pH	Alk. $CaCO_3$ (mg/l)	DIC[a] (mgC/l)	$\delta^{13}C$ DIC	[b]$logP_{CO2}$	LogSI Calcite	LogSI Dolomite
Piezometer Nests								
9801-1	1.73	8.10	148	186	-10.9	-2.94	0.29	-0.01
9801-2	4.99	8.14	160	200	-10.7	-2.93	0.45	0.29
9801-3	8.00	7.72	159	205	-10.5	-2.52	-0.01	-0.64
9802-1	perched	8.00	112	141	-11.3	-2.95	-0.03	-0.51
9802-3	0.58	8.12	181	227	-12.9	-2.88	0.43	0.38
9803-1	1.39	7.97	169	213	-10.2	-2.75	0.28	-0.01
9803-2	4.07	7.85	176	223	-10.1	-2.60	0.24	-0.14
9803-3	7.39	7.90	173	219	-11.3	-2.68	0.25	-0.07
9804-1	1.25	8.06	170	213	-11.7	-2.78	0.56	0.47
9804-2	3.03	7.93	187	236	-9.8	-2.67	0.27	0.06
9804-3	10.07	7.88	186	236	-9.8	-2.63	0.12	-0.14
9805-1	2.87	7.94	162	204	-9.9	-2.72	0.28	-0.01
9806-1	1.89	7.81	193	246	-11.6	-2.53	0.25	-0.07
9806-2	5.19	7.97	158	199	-9.8	-2.78	0.24	0.09
9806-3	8.39	8.02	175	219	-9.4	-2.89	0.43	0.29
Provincial Wells								
Sandilands #1	2.86	8.25	185.21	231	-9.7	-3.00	0.61	0.69
Woodridge #2	8.04	7.78	192.83	247	-10.2	-2.51	0.17	-0.20
Woodridge #1	61.10	8.31	191.8	239	-11.9	-3.04	0.46	0.65
Sila #3	81.52	8.18	181.8	227	-10.8	-2.94	0.51	0.46
Zhoda #1	119.44	8.40	242.03	302	-18.6	-3.03	0.33	0.26

[a] DIC calculated from alkalinity and pH.
[b] $logP_{CO2}$ calculated from alkalinity.

Table 6 $\delta^{13}C$ of Carbonate in Sand			
Site # of sand sample	Depth b.g.s. (m)	% cc $CaCO_3$	$\delta^{13}C_{VPDB}$ ‰
9805	9.2	4	-0.88
9805	13.1	10	-0.69
9802	5.8	5	-0.53

Redox conditions in the piezometer nests are of particular importance with respect to the CFC dating method as CFC degradation may occur under anoxic conditions. Dissolved oxygen levels in the groundwater are generally close to saturation near the water table and decrease with depth. In particular, at sites 9806 and sites 9804 there is a rapid decrease in dissolved oxygen with depth in the aquifer (Table 4). This decrease in dissolved oxygen is accompanied by an increase in SO_4^{2-} suggesting that pyrite oxidation may be occurring and is most pronounced at site 9804 where groundwater is in contact with the till (Figure 10) Examination of site 9804, however, indicates that while SO_4^{2-} may initially be produced from the oxidation of pyrite, at greater depths it is possibly being consumed due to sulphate reduction, as indicated by the SO_4^{2-} peak in Figure 10. Dissolved oxygen measurements at this site are presumed to be too high, as continuous flow measurements were not possible and may be lower than the measured 2.5 mg/l. Previous studies have indicated that CFC degradation does not start until dissolved oxygen levels fall below 0.5 mg/L (Cook et al. 1995). The possibility of sulphate reduction at site 9804 would suggest that dissolved oxygen concentrations are below 0.5 mg/l and CFCs may not behave conservatively in the deeper piezometer.

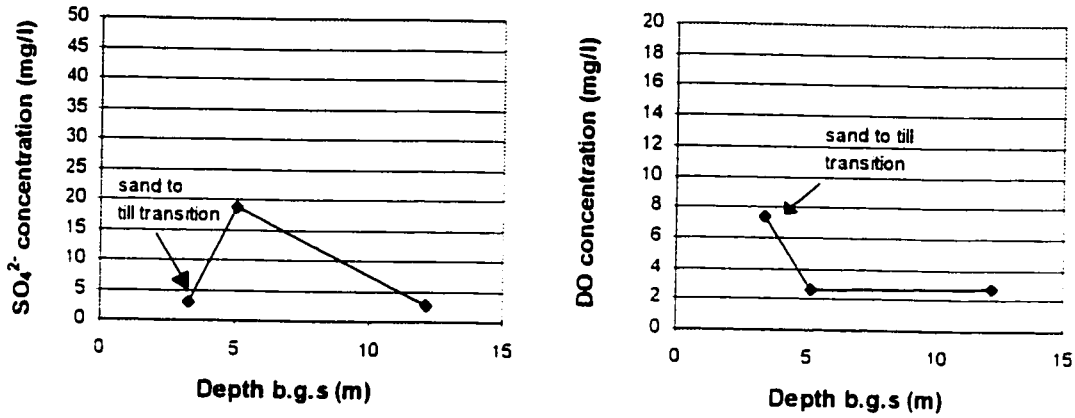

Figure 10. SO_4^{2-} and dissolved oxygen versus depth at site 9804. Dissolved oxygen values at 5 and 12 meters depth may be lower than 2.5 mg/l as measurements were not taken on continuous flow groundwater.

5.2.2 Regional Groundwater Geochemistry

Provincial and domestic wells within the area were sampled to define the regional groundwater geochemistry and demonstrate the geochemical evolution of groundwater within and on the periphery of the Sandilands (Tables 7 & 8). The provincial wells are part of the Manitoba Water Resource Branch's monitoring network. Domestic well samples were collected from four communities within the Sandilands and three communities on the outskirts of the Sandilands (Figure 1).

Comparison of the groundwater geochemistry of the piezometer nests with over 40 regional provincial and domestic well samples indicates that there is much greater geochemical variability over the regional scale (Figure 11). Variations include higher concentrations of the major constituents, Mg^{-}, Ca^{2-}, and HCO_3^{-}, and in particular large increases in Fe. In addition, the ranges of Na^{-}, SO_4^{2-}, and Cl^{-} concentrations are much larger. These variations are likely representative of the geochemical evolution of groundwater from

Table 7
Field Measurements and Groundwater Geochemistry of the Provincial Wells

Provincial Well #	Depth b.g.s. (m)	Depth below water table (m)	Geologic Unit	Field Measurements: Cond (us/cm)	T (°C)	pH	DO (mg/l)	TDS[a]	Major Anions: $^{b}HCO_3^-$ (mg/l)	SO_4^{2-} (mg/l)	Cl^- (mg/l)	NO_3^- (mg/l)	Major Cations: Ca^{2+} (mg/l)	Mg^{2+} (mg/l)	Na^+ (mg/l)	K^+ (mg/l)	Fe_{tot} (mg/l)	Si (mg/l)	Sr (mg/l)
Woodridge #2	15.54	8.04	sand	390	7.4	7.78	2.75	316	235	9.43	4.00	0.402	54	17	2.5	0.84	0.063	5.5	0.059
Woodridge #1	68.60	61.10	gravel	353	8.3	8.31	0.15	313	234	<0.05	0.81	0.186	29	17	21	3.1	0.45	8.2	0.21
Sandilands # 1	7.62	2.86	sand	302	7.4	8.25	3.66	316	226	12.1	1.54	0.383	51	17	1.6	0.48	0.55	5	0.047
Sila # 3	86.50	81.52	gravel	346	7.2	8.18	0.11	300	222	2.98	0.67	<0.05	48	15	2.8	1.4	0.72	6.3	0.069
Zhoda # 1	119.94	119.44	shale	501	8.4	8.4	0.25	436	295	8.79	6.42	<0.05	14	6.4	92	8.2	0.37	3.7	0.44

[a] TDS calculated as a sum of dissolved ions and silica
[b] calculated from alkalinity

Table 8

Field Measurements and Groundwater Geochemistry of the Domestic Wells

Sample I.D. #	Depth b.g.s. (m)	Geologic Unit	Field Measurements: Cond (us/cm)	T (°C)	pH	DO (mg/l)	TDS (mg/l)	Major anions: HCO_3^- (mg/l)	SO_4^{2-} (mg/l)	Cl (mg/l)	NO_3^- (mg/l)	Major Cations: Ca^{2+} (mg/l)	Mg^{2+} (mg/l)	Na^+ (mg/l)	K^+ (mg/l)	Fe_{tot} (mg/l)	Si (mg/l)	Sr (mg/l)
Town/Region																		
Marchand																		
M982021	54.41	gravel	352	16.5	7.89	0.53	227	226.902	<0.05	1.48	<0.05	46	15	8	1.7	1.4	9.4	0.17
M982014	76.20	sandstone	465	9.9	7.82	0.29	294	294.101	<0.05	6.07	<0.05	43	22	24	4.4	1.9	8.2	0.3
Sandilands																		
M982031	30.63	sand	372	11.4	7.58	0.5	228	227.509	11.8	0.65	<0.05	55	16	1.9	1.3	0.013	9.1	0.057
M982032	31.24	sand	362	7.7	7.73	0.52	225	224.765	9.79	0.60	<0.05	53	17	2.2	1.4	0.34	7.5	0.05
M982033	10.52	sand	358	9.9	7.72	0.48	222	222.3	9.60	0.64	<0.05	51	16	2	1.4	0.43	6.9	0.051
M982034	30.02	sand	363	12.2	7.69	0.52	224	223.615	9.44	0.58	<0.05	52	16	2	1.2	0.43	5.9	0.051
Woodridge																		
M982022	17.53	sand	487	8.9	7.63	0.5	305	304.529	14.5	0.89	0.295	73	22	2.6	1.1	3.1	9.1	0.064
M982023	19.05	sand	600	9.8	7.5	0.42	308	307.52	7.06	33.0	<0.05	81	25	5.2	1.1	3.2	7.9	0.082
M982036	21.03	sand	488	10.9	7.67	0.61	289	288.928	18.8	8.01	<0.05	71	22	4.1	1.4	0.84	8.4	0.077
M982037	20.88	sand	412	10.6	7.7	0.53	256	255.997	7.14	1.62	<0.05	62	18	2.6	1	0.74	7.6	0.059
Kerry																		
M982024	15.39	sand/gravel	363	10.9	7.78	6.82	215	215.306	7.43	1.84	7.482	51	17	1.6	0.64	0.041	4.9	0.039
M982025	------	------	450	16.6	7.61	6.97	254	254.28	11.5	7.20	10.48	65	20	1.9	1.2	0.086	6.4	0.055
M982026	------	------	500	9.9	7.53	0.56	321	320.529	4.73	1.10	<0.05	70	23	5	1.5	4.5	9.4	0.11
M982027	47.09	sand	439	12.1	7.54	0.57	288	287.772	0.15	0.76	<0.05	68	17	3.2	1.1	3.3	8.9	0.066
M982045	61.42	sand/gravel	605	8.1	7.31	-----	232	232.4	0.06	1.95	<0.05	53	15	4.8	1.4	1.4	9.6	0.11
M982046	------	------	369	12.5	7.84	-----	395	395.023	9.79	3.24	<0.05	85	29	3.8	0.99	3.3	8.4	0.081
M982047	24.84	sand	369	12.5	7.84	-----	246	245.855	<0.05	0.74	<0.05	53	16	4.9	1.5	1	11	0.13
M982048	30.94	sand	370	11.6	7.87	-----	240	239.705	<0.05	0.75	0.282	54	15	4.5	1.4	0.83	10	0.11
St. Labre																		
M982028	10.06	sand	566	9.9	7.49	1.02	366	365.725	6.40	3.55	3.91	85	26	4.8	0.92	0.014	6.3	0.072
M982029	19.96	sand	443	8.1	7.86	0.5	278	277.993	8.64	1.63	0.244	64	20	3.3	1.5	1.3	8.1	0.12
M982030	40.69	sand/gravel	372	11.5	7.87	0.27	239	239.119	<0.05	0.88	<0.05	41	15	23	2.5	0.7	11	0.22
M982038	26.97	sand	199.4	9.5	7.88	0.5	218	218.437	0.20	0.66	0.866	43	14	12	2.3	0.54	12	0.18
M982039	23.32	sand/gravel	317	10.8	7.61	0.51	208	208.267	0.31	0.58	<0.05	45	13	4.4	1.2	0.55	9.7	0.088
M982040	46.18	sand	360	7.8	8.03	0.63	239	239.301	<0.05	1.57	<0.05	44	16	12	2.3	0.35	8.6	0.21
M982041	41.15	gravel	363	8.1	7.88	0.42	235	235.363	<0.05	1.35	<0.05	45	16	11	2.4	0.56	9.2	0.21
M982042	53.34	sand	613	11.8	7.27	0.4	242	241.771	<0.05	2.07	2.708	45	16	13	2.3	1	9	0.2
M982043	8.53	------	579	12	7.36		409	409.084	4.74	1.07	<0.05	81	36	4.7	1.3	1.7	8.5	0.15
M982044	3.05	------	360	12.6	7.67		388	388	0.96	0.98	<0.05	85	29	1.4	0.62	3.1	7	0.072
La Broquerie																		
M982015			363	6.9	7.81	0.5	215	214.798	1.32	9.50	<0.05	49	18	15	2.4	1.1	8.2	0.21
M982016	35.81	gravel	365	7	7.88	0.38	213	213.055	2.05	10.8	<0.05	42	15	14	2.2	0.7	8.2	0.19
M982017	23.93	sand/gravel	407	13.7	7.75	0.27	244	244.21	<0.05	9.13	<0.05	42	17	22	3.1	1.4	7.7	0.23
Zhoda																		
M982012	17.98	sand/gravel	385	11	8.08	0.76	246	245.877	5.52	1.78	<0.05	23	16	41	2.6	0.13	7	0.22
M982013	46.63	sand	427	10.8	7.96	0.37	274	274.278	0.91	5.00	<0.05	32	14	43	2	0.52	9	0.22

[a] TDS calculated as a sum of dissolved ions and silica.

[b] calculated from alkalinity

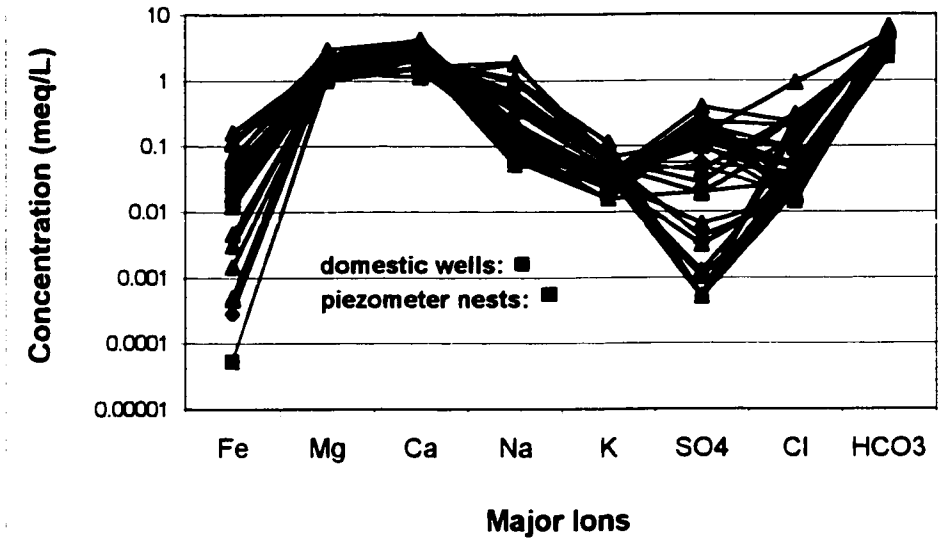

Figure 11. Geochemical variability of groundwater on a regional scale as shown by a comparison of the geochemistry of the piezometer nests to the geochemistry of the domestic wells.

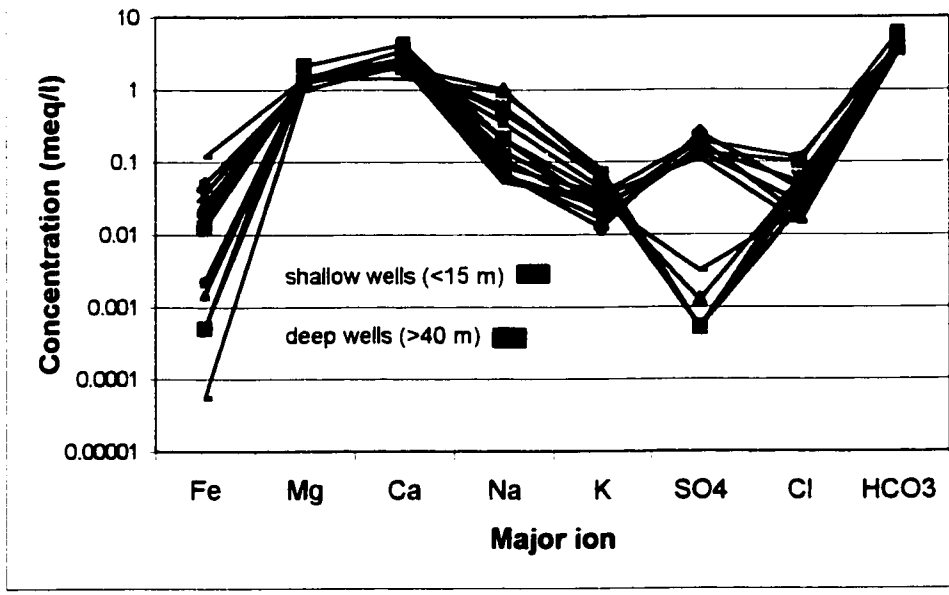

Figure 12. Geochemical groundwater evolution with depth characterized by increased concentrations of Fe, Na+, and K+ and decreased SO_4^{2-} concentrations.

the recharge areas through to the groundwater geochemistry found at greater distances along the regional scale flow path and are discussed below.

Similar to the piezometer nests, the groundwater geochemistry on a regional scale in the Sandilands is dominated by a Ca-Mg-HCO_3 facies, which evolves towards a Ca-Mg-Na-HCO_3 facies at greater depth. As discussed previously, this pattern is associated with the weathering of feldspars present in the till. The controls on the groundwater geochemistry are related to depth (i.e. length of groundwater flow path) and to some degree by region. Examination of groundwater with depth in the Sandilands indicates that groundwater progresses to increased concentrations of Fe, Na^+, K^+, and lower SO_4^{2-} concentrations (Figure 12). In most cases groundwater at greater depth will have come into contact with the till which results in increased concentrations of Na^+.

Shallow groundwater in the sand is generally saturated with dissolved oxygen (10-12 mg/l DO), however, oxygen is quickly consumed with depth and groundwater contains less than 0.5 mg/l of oxygen at depths of 20 m and greater (Figure 13).

Redox conditions continue to evolve with depth in the Sandilands. Fe concentrations increase and finally SO_4^{2-} concentrations reach detection limit levels (50 ppb) at depths of 40 m and greater (Figure 14). Sulphate reduction appears to be the dominant redox buffer in the deeper groundwater flow systems in the Sandilands although $\delta^{34}S$ isotope analyses would be required to determine this conclusively. Sulphate reduction in the deeper groundwater of the surficial aquifer could limit the use of the CFC dating method in the Sandilands although groundwater at this depth may exceed the limits of the dating method.

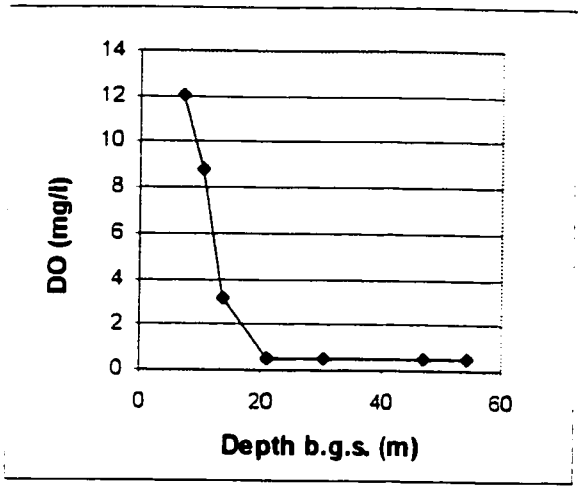

Figure 13. Dissolved oxygen versus depth. Data between 2-16 m are from piezometer nest 9806 and at 20 m and greater are from selected domestic wells.

The geochemistry in regions that are located on the periphery of the Bedford Ridge (towns of Zhoda and LaBroquerie) differs from the other regions in the Sandilands (town of Sandilands) (Figure 15). Much higher concentrations of Na^+ and lower concentrations of Ca^{2+} characterize groundwater in the town of Zhoda. It is possible that surficial sediments in this region are derived from shale, which underlies the surficial deposits, and have a different mineralogical composition than sediments in the Sandilands. Groundwater in Zhoda from the shale unit has a unique Na/Ca ratio, and increased K^+ and Cl^- concentrations, which are attributed to contributions of saline pore water in the shale. Groundwater from the surficial aquifer in this area appears to reflect this type of geochemistry as well. Similarly, the geochemistry of groundwater in the town of LaBroquerie is characterized by higher concentrations of Na^+ and Cl^- and may be reflecting a different till composition derived from the bedrock unique to the area.

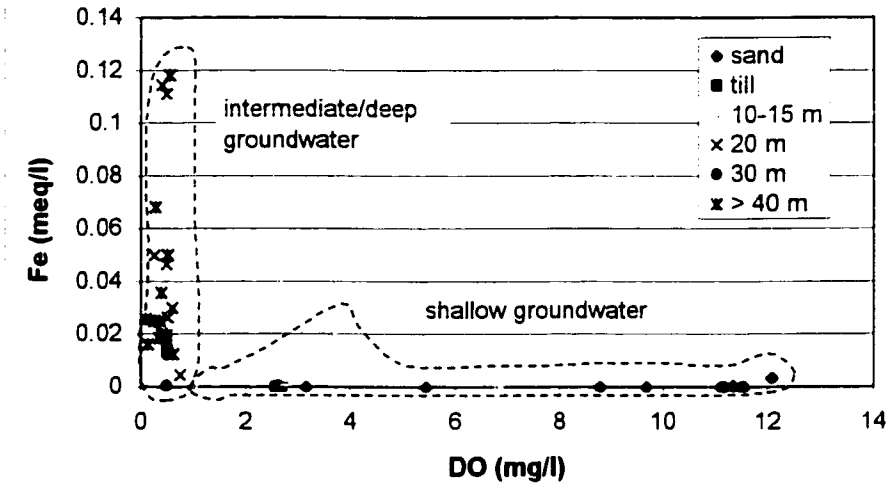

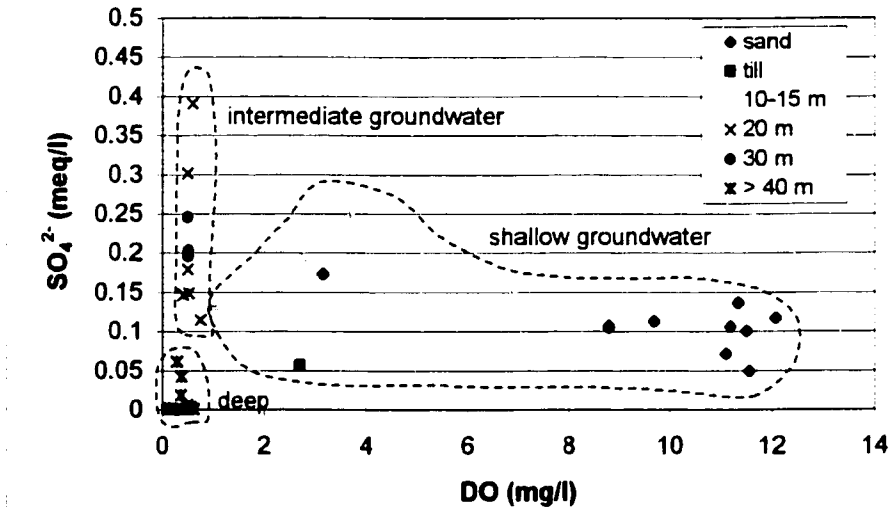

Figure 14. Fe and SO_4^{2-} concentrations versus dissolved oxygen for three different flow regimes: shallow (0-15 m), intermediate (20-30 m), and deep (>40 m).

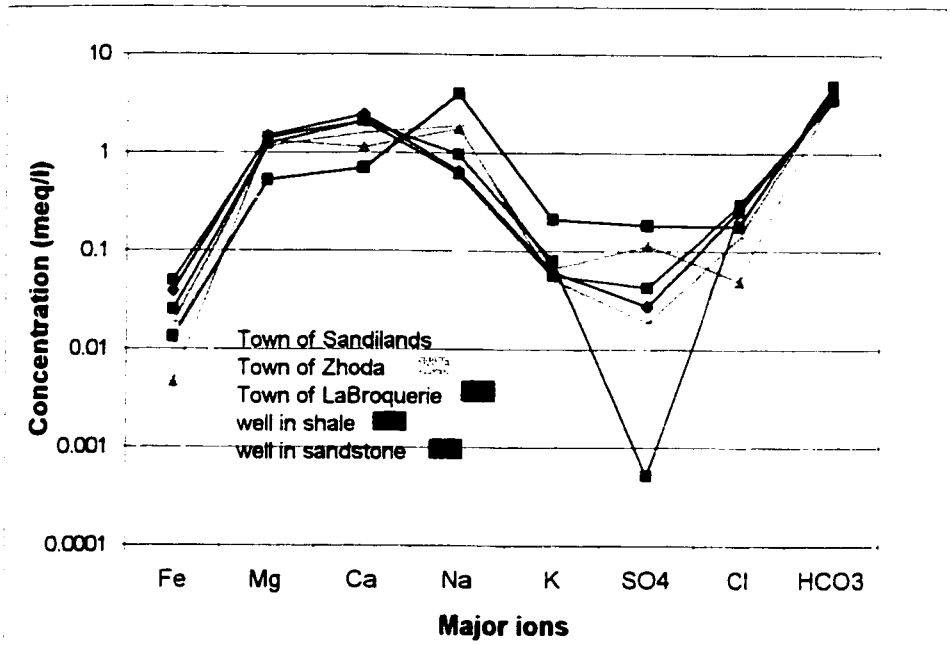

Figure 15. Geochemical characteristics of regions on the periphery of the Sandilands (Zhoda. La Broquerie) compared to those in the Sandilands.

5.3 Groundwater Ages

5.3.1 Estimation of Recharge Temperature

An integral component of the CFC and $^{3}H/^{3}He$ groundwater dating methods is to accurately estimate the groundwater recharge temperature. While dissolved ^{3}He and low CFC concentrations are not as sensitive to the temperature estimate, CFC age estimates for groundwater recharged in the last 15 years are quite sensitive to changes in the recharge temperature. For example, a 3 °C decrease in the recharge temperature for dissolved CFC concentrations that would be in equilibrium with air in 1990 would result in CFC-12, CFC-11, and CFC-113 groundwater age estimates that are 4.1, 4.5 and 2.2 years younger, respectively.

Three different approaches were used in this study to estimate the groundwater recharge temperature in the Sandilands. Groundwater temperatures were measured in the field on rapidly bailed groundwater samples from the shallow piezometers using the temperature function on a specific conductance meter. An average groundwater temperature of 6 °C was determined using this method. The second method measured subsurface temperatures in 8 thermistors on a temperature cable installed down a PVC tube (M. Hinton, personal communication, 1999). Temperature data that were collected at eight depths over a period of twelve months indicates that the subsurface air temperatures fluctuate in the first 10 meters of the unsaturated zone but are attenuated to a constant value of 5.9 °C at depths greater than 10 meters (Figure 16). Although, these data suggest that a recharge temperature of 6 °C would be a reasonable estimate for groundwater in the Sandilands, a discrepancy between these data and the average annual air temperature is discussed below.

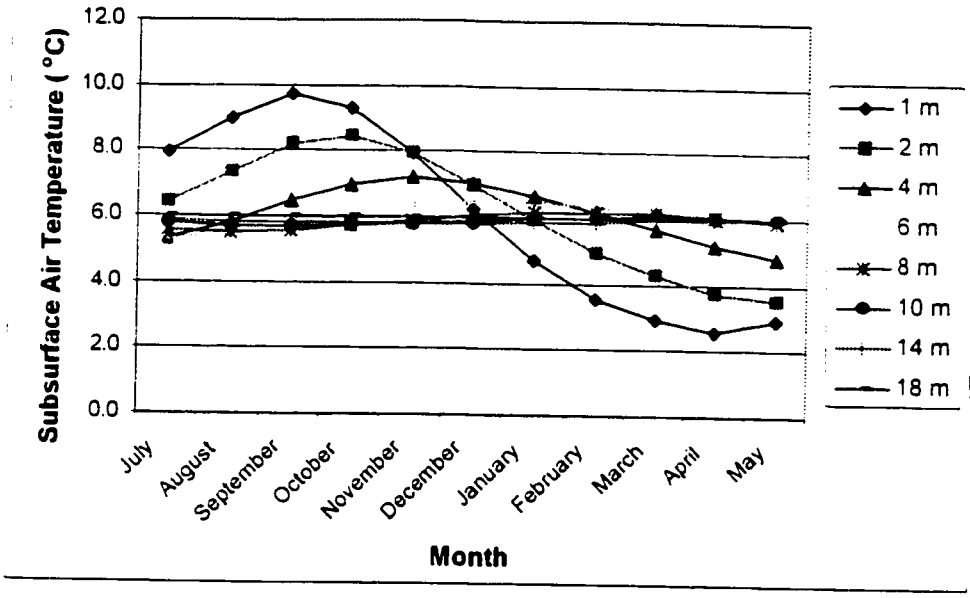

Figure 16. Subsurface air temperatures versus depth monitored over a one year time period illustrate a damped temperature signal at depths of 10 m and greater.

The average annual air temperature of 3 °C at the Winnipeg Airport weather station (Environment Canada, 1999) is 3 °C lower than the estimates using the above methods $\delta^{18}O$ data and dissolved CFC concentrations were used to provide insight into this discrepancy

$\delta^{18}O$ measurements on groundwater can provide information on the seasonality of groundwater recharge. The $\delta^{18}O$ values of groundwater in the piezometer nests and provincial and domestic wells in the Sandilands are reported in Table 9 and range from −12.3 ‰ to −15.3 ‰, with an average of -14.2 ‰. The five year weighted average of $\delta^{18}O$ in precipitation from the closest IAEA monitoring station in Atikokan, Ontario is -12.4 ‰. Comparison of the average $\delta^{18}O$ value of groundwater with the average $\delta^{18}O$ in precipitation shows that the groundwater value is lower. This difference suggests that recharge occurs predominantly in the spring and/or fall when the recharge temperature may be lower than the

average annual subsurface temperature. Figure 16 shows that for a thin unsaturated zone the soil air temperature is as low as 2.6 °C in the spring.

Table 9
$\delta^{18}O$ of Groundwater in the Study Area

Piezometer #	Depth b.g.s (m)	$\delta^{18}O_{VSMOW}$ ‰
Piezometer Nests		
9801-3	16.45	-13.6
9802-1	4.23	-15.0
9802-3	10.42	-13.8
9803-1	21.03	-14.4
9803-2	23.71	-14.3
9803-3	27.03	-13.7
9803-3 (dup)	27.03	-13.8
9804-1	3.32	-14.2
9804-2	5.10	-14.5
9804-3	12.14	-14.0
9805-1	21.70	-14.4
9806-1	7.01	-13.6
9806-2	10.31	-14.3
9806-2 (dup)	10.31	-14.3
9806-3	13.51	-14.8
9806-3 (dup)	13.51	-15.0
Provincial Wells		
Sandilands #1	7.62	-14.3
Woodridge #2	15.54	-14.1
Woodridge #1	68.60	-13.9
Zhoda #1	119.24	-14.9
Domestic Wells		
M982032	31.24	-14.5
M982013	46.63	-15.3
M982014	72.20	-14.1
M982021	54.40	-13.6
M982022	17.50	-13.7
M982024	15.40	-13.8
M982029	19.96	-14.1
M982030	40.69	-13.7
M982034	30.02	-14.5
M982037	20.89	-14.4
M982048	30.93	-12.3
average $\delta^{18}O$ of groundwater =		-14.2

Dissolved CFC concentrations in the shallow groundwater in the study area also provide an indication that the dissolved gas recharge temperature may not be the same as the subsurface air temperature and the measured groundwater temperature. As previously discussed, higher dissolved CFC concentrations are more sensitive to temperature differences. High dissolved CFC concentrations in the shallow piezometers (younger groundwater) are well above those expected from atmospheric equilibrium at a temperature of 6 °C suggesting that the dissolved gas recharge temperature is closer to 3 °C.

The reason for the discrepancy in subsurface temperatures and the average annual air and CFC recharge temperatures in the Sandilands is not known. However, a review of the literature indicates that this phenomenon has been previously documented. Studies of groundwater recharge temperatures indicate that dissolved noble gases can be used to effectively estimate the temperature at which dissolved gases are isolated from the soil air (Heaton and Vogel, 1981; Andrews and Lee, 1979; Herzberg and Mazor, 1979). Heaton and Vogel (1981) found that groundwater recharge temperatures (in areas with unsaturated zones varying from 1-17 m) determined using dissolved noble gases were generally 1 °C lower than the average annual air temperature and up to 2 °C lower than the temperature of the groundwater measured in the field. Similarly, Busenberg and Plummer (1992) reported that groundwater recharge temperatures determined using dissolved noble gases may be less than the mean annual subsurface temperature. Comparison of a CFC groundwater study by Cook et al. (1995) in Sturgeon Falls, Ontario located in a similar climate to the Sandilands found that the noble gas recharge temperature was 2 °C, approximately 1 °C lower than the average annual air temperature.

Given the discrepancy in temperature data it was difficult to constrain the dissolved gas recharge temperature. If recharge occurs predominantly in the spring a dissolved gas recharge temperature of 3 °C may be reasonable. However, shallow subsurface temperatures range from 9.9 °C in the fall to 2.6 °C in the spring and the recharge temperature could fall between those values. Error in the recharge temperature propagates to the CFC groundwater age estimate through the calculation of K, Henry's Law constant, which is temperature dependent. The difference between estimating a 3 °C CFC recharge temperature compared with a 6 °C recharge temperature is a large possible source of error for CFC groundwater ages 19 years and younger. Because He and Ne are only sparingly soluble in water, it was not possible to use them to constrain the recharge temperature for dissolved gases for this study. However, based on the idea that recharge occurs during the cooler months, it was concluded that a CFC groundwater recharge temperature of 3 °C is the most reasonable estimate.

5.3.2 CFC Groundwater Ages

Dissolved concentrations of CFC-11, CFC-12, and CFC-113, the calculated atmospheric concentrations and the estimated groundwater ages are reported in Table 10. The dissolved CFC concentrations measured in pg/kg are averages of the quadruplicate samples (Appendix III) with the exception of six samples. Individual samples were removed from the quadruplicate sample set used to determine the average concentration if the dissolved CFC concentration was above the equilibrium value for the highest atmospheric concentration or if they did not agree with at least one other sample within 30%. Piezometers where data were removed are indicated in Table 10; no CFC-12 values, three CFC-11 values and six CFC-113

Table 10

CFC Concentrations in Groundwater and Calculated CFC Groundwater Ages

Atmospheric CFC concentrations[g] and the equivalent dissolved concentration @ 3°C in the summer / fall of 1998

Atmospheric CFC-11 (pptv)	Dissolved CFC-11 (pg/kg)	Atmospheric CFC-12 (pptv)	Dissolved CFC-12 (pg/kg)	Atmospheric CFC-113 (pptv)	Dissolved CFC-113 (pg/kg)
269 66[f]	1193 4	539 2	521 1	84 08[f]	162 9

Piezometer Nest #	Piezometer I.D.	Depth of Piezo b.g.s (m)	Water Table Depth (m)	Measured Dissolved CFC Concentration CFC-11 (pg/kg)	CFC-12 (pg/kg)	CFC-113 (pg/kg)	Calculated Atmospheric Conc.* CFC-11 (pptv)	+/-	CFC-12 (pptv)	+/-	CFC-113 (pptv)	+/-	CFC Groundwater Ages** CFC-11 (yrs)	+/-	CFC-12 (yrs)	+/-	CFC-113 (yrs)	+/-
9801	9801-1	10 18	8 451	1170 0	328 6	121 5	264 4	4 3	340 0	10 0	62 7	8 2	9 4	2 5	17 0	3 5	10 3	2 0
	9801-2	13 44		1233 5	326 0	104 7	278 7	4 5	337 3	3 2	54 0	1 8	5 8	5 0	17 2	2 0	11 6	2 0
	9801-3	16 45		1075 2[b]	285 4	81 8	243 0	2 0	295 3	7 4	42 2	4 4	11 6	2 5	19 6	2 2	13 5	2 4
9802	9802-1	4 23	3 183[e]	1126 1	319 7	151 7[d]	254 5	4 3	330 9	1 6	78 3	15 8	10 7	5 0	17 6	2 0	8 2	3 6
	9802-3	10 42	9 835	868 6	243 4	87 4	196 3	0 3	251 8	2 2	45 1	6 4	16 0	2 0	22 0	2 2	13 0	2 8
9803	9803-1	21 032	19 639	1014 9	273 9	91 3	229 3	2 4	283 4	1 5	47 1	1 8	12 7	2 0	20 9	2 8	12 7	2 2
	9803-2	23 712		1101 0	276 6	158 8	248 8	5 6	286 2	8 8	82 0	2 1	11 2	4 5	20 8	2 5	7 5	1 9
	9803-3	27 025		1240 7[b]	313 6	691 9	280 3	5 2	324 5	11 0	357 1	74 7	4 8	5 0	17 9	3 0	C	....
9804	9804-1	3 318	2 070	1196 7	283 5	99 1	270 4	13 8	293 3	3 3	51 1	3 4	8 4	4 0	19 7	1 5	12 0	1 8
	9804-2	5 095		52 8	61 8	23 4	11 9	1 1	63 9	2 1	12 1	2 4	37 7	2 5	32 9	2 0	23 1	2 6
	9804-3	12 139		131 5	62 5	29 9	29 7	1 4	64 7	3 3	15 5	3 8	32 9	1 5	32 9	1 5	21 4	3 5
9805	9805-1	21 702	18 836	448 8	170 1	30 5	101 4	4 1	176 0	4 9	15 8	3 2	25 0	1 2	24 9	1 6	21 2	3 0
9806	9806-1	7 009	5 105	1185 2	304 8	94 3	267 8	16 0	315 4	24 0	48 7	3 8	9 4	4 0	18 5	3 1	12 4	2 0
	9806-2	10 313		451 4	166 3	38 0	102 0	1 7	172 1	8 2	19 6	4 5	24 9	1 3	25 1	1 8	19 6	3 2
	9806-3	13 508		160 7	105 3	31 2[e]	36 3	1 5	109 0	6 5	16 1	....	31 7	1 6	29 0	1 6	21 1	....
Woodridge	Woodridge #2	15 54	8 450	129 7	76 3	22 7[h]	32 0	6 4	79 0	4 9	11 7	3 3	32 4	2 5	31 4	1 9	23 3	4 0
	Woodridge #1	68 20	8 550	43 2	15 3	310 6	9 8	0 8	15 8	2 2	160 3	37 4	39 7	2 5	42 8	6 0	C	....
Sandilands	Sandilands #1	14 91	9 172	584 84[c]	215 9	34 8	132 2	3 1	223 4	2 8	18 0	2 5	22 8	1 3	22 6	1 1	20 3	2 0

*+/- = one standard deviation in pptv

**+/- = Error on groundwater ages as a sum of the error introduced during analysis, error in the atmospheric curve, and a 1 °C error in $T_{recharge}$

[a] = perched water table

[b] = one sample removed from quadrulicate data set as dissolved CFC concentration above equilibrium with atmosphere

[c] = one sample removed from quadruplicate data set as dissolved CFC concentration did not agree with any other measurement within 30 %

[d] = two samples removed from quadruplicate data set as dissolved CFC concentrations were above equilibrium with atmosphere

[e] = three samples removed from quadruplicate data set as dissolved CFC concentrations were above equilibrium with atmosphere

[f] = maximum atmospheric concentrations occurred in 1993 for CFC-11 (276 81 pptv) and 1994 for CFC-113 (85 0 pptv)

[g] = measured by NOAA in Niwot Ridge, Colorado

C = every quadruplicate CFC-113 sample contaminated

samples were removed. Standard deviations are within 5 % for CFC-11 and 7.5 % for CFC-12 indicating the reproducibility of the sampling and analytical methods. CFC-113 groundwater concentrations are more variable with a maximum standard deviation of 19 %.

Calculated CFC-12 and CFC-11 equivalent atmospheric concentrations in parts per trillion volume (pptv) in groundwater are within the range possible for air-water equilibrium at 3 °C (Figure 17). At two piezometers, 9803-3 and Woodridge # 1, calculated CFC-113 partial pressures in groundwater are above peak atmospheric values and groundwater ages

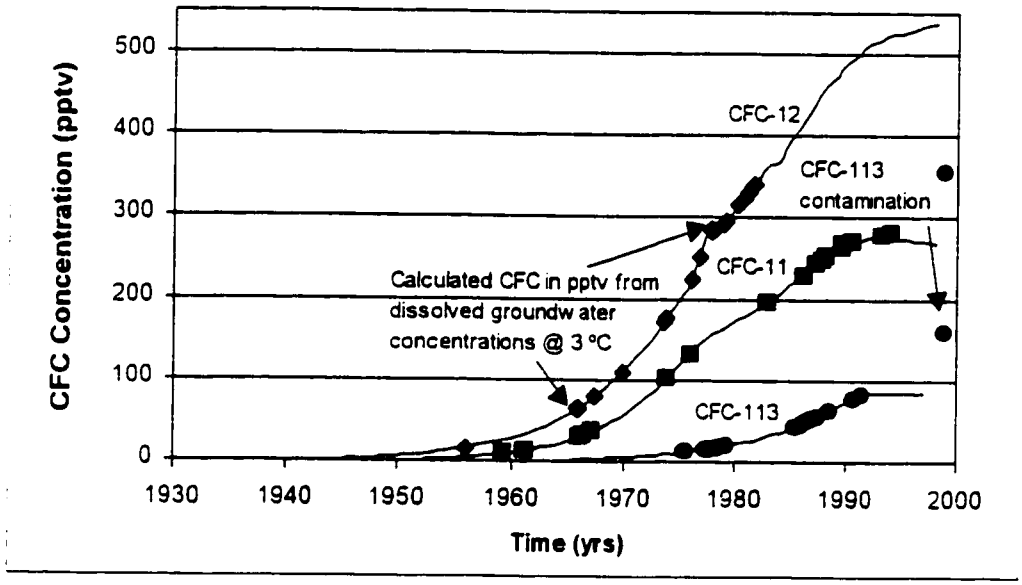

Figure 17. Calculated CFC concentrations in pptv from dissolved CFCs in groundwater compared with the atmospheric curves.

could not be determined. CFC-113 concentrations well above atmospheric values can be indicative of contamination that may have occurred during sampling or from well construction materials while the lower value may be representative of atmospheric contamination (Szabo et al., 1996, Cook et al., 1995). Based on CFC-11, CFC-12 and CFC-

113 concentrations, groundwater ages range from 4 to 40, 17 to 43, and 8 to 23 years, respectively.

Comparison of groundwater ages determined using each CFC compound provided insight into non-conservative processes that may have affected CFC concentrations in Sandilands groundwater. Figure 18 indicates that the degree of agreement between CFC groundwater ages follows trends that are dependent on the range of groundwater ages. CFC-11 and CFC-12 groundwater ages are comparable within the error limits of the method (approximately 3 years) for groundwater between 20 and 35 years. For younger groundwater, CFC-12 groundwater age estimates are significantly older than for CFC-11 and CFC-113. In contrast, CFC-113 groundwater ages are much younger than the CFC-11 and CFC-12 ages for older groundwater.

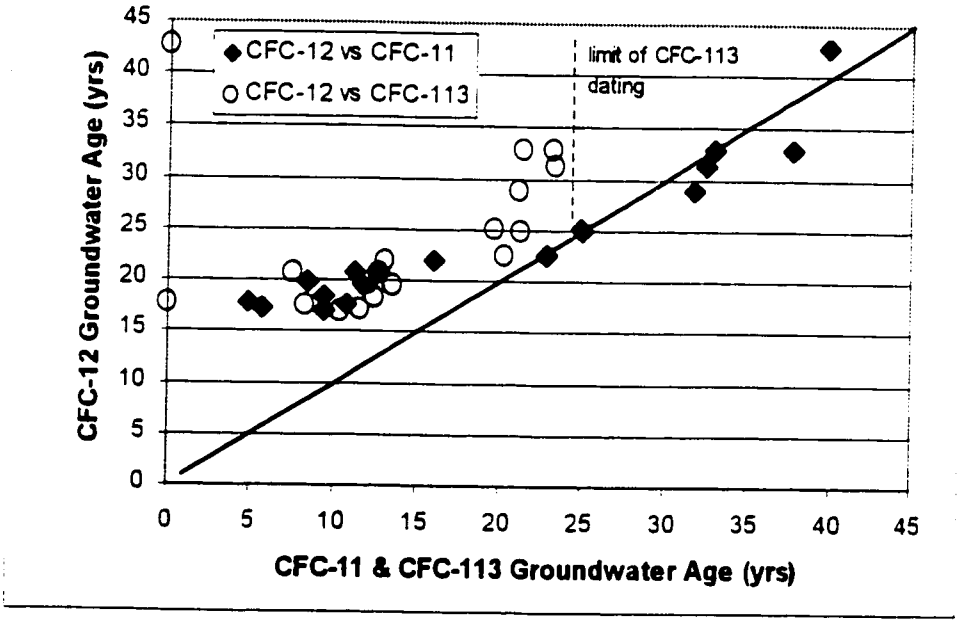

Figure 18. CFC-11 and CFC-113 versus CFC-12 groundwater ages. CFC-113 concentrations that were above atmospheric were assigned a groundwater age of 0 for illustrative purposes.

CFC-12 groundwater ages greater than CFC-11 and CFC-113 ages could be the result of either CFC-11 and CFC-113 contamination or CFC-12 losses. It was not possible to determine conclusively which of the above factors resulted in the discrepancy in ages. However, examination of the CFC-12 ages suggests that they may be overestimated. The younger CFC-12 groundwater ages, which are found in the shallow piezometers less than 2 meters below the water table, are 17 years and greater. The CFC-12 age difference between the shallow and middle piezometers and the middle and deepest piezometers at site 9806 are 5.6 and 3.9 years, respectively over similar vertical distances. In addition, groundwater velocities calculated based on the CFC-12 age in the shallow piezometer and the distance below the water table are an order of magnitude greater than velocities calculated using CFc-12 groundwater ages in other piezometers and CFC-11 and CFC-113 ages. This trend is seen at other piezometer nests and may be indicating that the CFC-12 groundwater ages are overestimated in the shallow piezometers.

Typical non-conservative processes such as anaerobic degradation, adsorption, and diffusional time lags in the unsaturated zone are not the cause of the low CFC-12 concentrations in younger groundwater. If the above processes were taking place they would affect CFC-11 and CFC-113 to a larger extent and would be easily identifiable. In general, CFC-11 undergoes anaerobic degradation to a larger degree than CFC-12 and CFC-113 and groundwater ages that are much larger for CFC-11 in combination with low dissolved oxygen concentrations (<0.5 mg/L) would be an indicator that degradation may have taken place (Cook et al., 1995, Semprini et al., 1991). Similarly, adsorption would likely decrease dissolved CFC-113 concentrations preferentially over CFC-12 and CFC-11 and would result

in older CFC-113 groundwater ages (Cook et al., 1995). One possible explanation for the observed trend is the sampling method of the shallower and subsequently younger groundwater. To increase the volume of groundwater flushing during the CFC sampling of the shallow piezometers, the system was placed under partial vacuum. Dissolved neon concentrations, discussed in detail in the following section, indicate significant gas losses in samples obtained with suction. Weeks et al. (1982) found that CFC-12 is more diffusive in nitrogen than CFC-11 so that it is possible that CFC-12 was preferentially stripped during the sampling process.

CFC-113 groundwater age estimates proved to be the most inconsistent and were particularly problematic for dating groundwater greater than 25 years. Two of the samples collected had dissolved CFC-113 concentrations exceeding those that would be expected from atmospheric equilibrium and suggest that sample contamination may have occurred. Contamination of CFC groundwater samples can occur due to contact with certain types of plastics, grease, rubber, and exposure to the atmosphere and it is not uncommon for one CFC to be affected and not the others (Cook et al, 1995; Szabo et al, 1996, Busenberg and Plummer, 1991). Atmospheric CFC-113 concentrations only increased by 10 pptv (from 1 pptv to 11 pptv) from 1965 to 1975. These low concentrations make it difficult to date groundwater greater than 25 years and the presence of even trace CFC-113 contamination would have a substantial effect on the CFC-113 groundwater age dating technique.

5.3.3 ^{3}H and $^{3}H/^{3}He$ Groundwater Ages

Dissolved concentrations of ^{3}H, ^{3}He ^{4}He, Ne, and the calculated $^{3}H/^{3}He$ groundwater ages are reported in Table 11. Dissolved neon concentrations significantly below those that would be expected from equilibrium with the atmosphere indicate the loss of dissolved gases. The ratio of the measured Ne concentrations to the atmospheric solubility of Ne indicates that gas losses between 20 % and 85 % occurred in all of the samples. Possible reasons for these losses include gas stripping and non-equilibrium conditions during sampling. The significant loss of dissolved ^{3}He in samples 9805-1 and 9803-1 suggests that the sampling method in the shallow piezometers was problemtatic. Suction during sample collection may have stripped the helium and as a result groundwater ages were not determined at these piezometers. In addition, water levels in the sampling apparatus did not reach static groundwater levels and it is probable that the 1 p.s.i check valves used to collect the CFC and $^{3}H/^{3}He$ samples closed before equilibrium conditions were obtained in the copper tubes. Physical non-equilibrium conditions between groundwater in the sampling apparatus and groundwater in the piezometer could have coincided with non-equilibrium dissolved gas conditions. This may have resulted in incomplete dissolved gas sampling.

Assuming that the ratio of Ne/He lost is constant, the Ne ratio can be used to calculate the amount of helium that was lost during the sampling process. However, it is not possible to completely account for the amount of ^{3}He that was lost that was present above atmospheric concentrations. Corrections were made to the measured ^{3}He concentrations to account for the losses prior to calculating the tritiogenic component of the ^{3}He. Duplicate

Table 11
Dissolved Ne, ^3He, ^4He and $^3H/^3He$ Groundwater ages.

Piezometer #	Depth below water table (m)	^3H** (TU)	Ne E-8 (ccSTP/g)	$\frac{Ne_{measured}}{Ne_{atmospheric}}$	$^4He_{measured}$ E-8 (ccSTP/g)	$^4He_{corrected}$ E-8 (ccSTP/g)	$^3He_{measured}$ E-14 (ccSTP/g)	$^3He_{tritiogenic}$ E-14 (ccSTP/g)	$^3He_{tritiogenic}$ (TU)	$^3He/^4He$ E-6	$^3H/^3He$ Age[A] (years)
*9801-3a	7.832	16.1	17.8	0.8	6.4	7.39	9.58	4.1	16.45	1.5	12.6 +/- 1.1
9801-3b	7.832	16.1	9.87	0.44	2.75	5.45	4.94	1.83	7.37	1.8	6.8 +/- .8
9803-1	1.340	16.2	10.5	0.47	2.96	5.52	4.13	0.819	3.29	1.4	NA
9803-3	7.347	12.3	10.1	0.45	2.8	5.45	4.05	0.886	3.56	1.44	NA
9804-3	9.134	0.8	10.4	0.47	4.7	7.28	4.53	1.38	5.55	0.96	37.14 +/- 3.5
9805-1	2.866	50.6	3.29	0.15	2.51	6.64	5.92	4.48	18.01	2.36	NA
9806-3a	8.387	56.3	15	0.67	6.06	7.64	38.2	33.2	133.49	6.31	21.8 + 2.2
9806-3b	8.387	56.3	8.27	0.37	3.07	6.12	35.7	32.7	131.57	11.6	21.6 +/- 2.2

* Samples a & b are duplicate samples

** Tritium concentrations corrected for decay during storage.

$^4He_{corrected}$ corrected for excess air from recharge and sampling based on the measured to atmospheric Ne ratio. $^4He_{corrected} = {}^4He_{measured} - 4.85*10\text{-}7*(Ne_{meas}/Ne_{atm})\text{-}1)$, where 4.735 *10-8 ccstp/g is the solubility of ^4He

$^3He_{tritiogenic}$ calculated after correcting for excess air and ^3He gain during sample storage

$^3H/^3He$ Age: NA no age was calculated because helium was stripped during sampling and the corrected $^3He_{tritiogenic}$ concentrations were low in comparison to ^3H concentrations (not the case in piezometers 9801-3b and 9806-3b)

* = =/- error on age based on analytical uncertainty and uncertainty in estimation in tritiogenic component of helium

samples, 9806-3b and 9801-3b, may give some insight into the validity of the corrections made for the gas losses. While the calculated tritiogenic ^3He is very comparable for the 9806-3 duplicates, the 9801-3 duplicates indicate that the correction may not always yield consistent results. In this case the sample with only 20 % gas losses was taken as the most reliable groundwater age. Difficulty in preserving the dissolved gas concentrations while sampling of the groundwater was the most significant limitation on the use of $^3H/^3He$ method for determining groundwater ages in the Sandilands and groundwater age estimates should be regarded as minimum ages.

The groundwater age estimate at piezometer 9804-3 is considered a minimum as the ^3H concentration is a detection limit value and not an absolute value. The $^3He/^4He$ value is lower (0.96 * 10-6) than the equilibrium value in rain of 1.37 * 10^{-6} and provides some insight into the groundwater age. Dissolved concentrations of ^4He in excess to those expected from atmospheric equilibrium have been documented in several studies (Bottomley et al., 1984; Gascoyne and Kotzer, 1995) and are attributed to the α decay of uranium and thorium present in the bedrock or sediments of the aquifer. Dissolved ^4He concentrations accumulate in the groundwater as the uranium and thorium undergo radioactive decay. In this context, dissolved ^4He concentrations can be used to deterime if there is a radiogenic source of helium and in some circumstances can be used to aid in constraining the groundwater age. The time to accumulate detectable concentrations of radiogenic ^4He in groundwater can be on the order of hundreds of years (Andrew et al., 1989a; Torgersen and Clark, 1985) suggesting that groundwater at this site may be much older than the calculated $^3H/^3He$ age of 37.1 years. In a physical groundwater flow context, using a Darcy's Flux of 35 mm/yr and a porosity of 0.3

the groundwater age at that depth in the till is on the order of 60 years. This provides some evidence that $^{3}H/^{3}He$ groundwater ages on the order of 37 years may be underestimating the actual groundwater travel times.

5.3.4 ^{3}H Groundwater Ages

Tritium concentrations were determined at 15 piezometers and range from the detection limit of 0.8 to 56.3 TU (Table 12). Qualitatively this suggests that groundwater ages in the Sandilands vary from pre-bomb through to recently (0-10 years) recharged groundwater with a few piezometers indicating predominantly 1960s recharge.

A lumped parameter mathematical model for estimating groundwater ages from tritium data was used to estimate groundwater ages. The model was chosen using the assumption that simple plug flow with negligible molecular diffusion, hydrodynamic dispersion and mixing could represent the shallow groundwater flow system in the Sandilands. The equation used to represent the system is as follows:

$$C(t) = C_{in}\,(t\text{-}t_t)^{*}\exp(-\lambda * t_t) \qquad (8)$$

where $t\text{-}t_t$ represents the time the tracer entered the system, t is the time the groundwater sample was taken, t_t is the transit time of the tracer (or groundwater age), C_{in} is the initial input tritium concentration and C(t) is the measured tritium concentration at time t. Inserting λ equal to $\ln 2/t_{1/2}$ (the decay constant) yields the basic tritium radioactive decay equation (Maloszewski and Zuber, 1996). The input values used for the model are measured tritium values in Ottawa precipitation for the years 1953 through 1994. Pre-1953 values were given a

value of 10 TU and 1994 through 1998 values were assumed to be constant at 15 TU (Figure 2).

Groundwater ages estimated using the plug flow model range from 12.8 to 49 years (Table 12). Groundwater ages were not determined for the range of tritium concentrations from 8 to 14 TU as the relatively constant tritium concentrations over the past 10 years make

Table 12
Measured ^{3}H Concentrations and Estimated Model Ages.

Piezometer #	Depth b.g.s. (m)	$^{3}H_{measured}$ (TU)	+/- (TU)	$^{3}H_{corrected}$ (TU)	^{3}H Model Age* (years)
9801-1	10.18	10.2	1	10.3	---------
9801-3	16.45	15.9	1.3	16.1	12.8
9802-1	4.23	9.3	1	9.4	---------
9802-3	10.42	10.3	1	10.4	---------
9803-1	21.032	16	0.3	16.2	12.8
9803-3	27.025	12.1	1.1	12.3	---------

9804-1	3.318	8.1	0.9	8.2	---------
9804-3	12.139	0.8	0.6	0.8	> 49**
9805-1	21.702	49.9	3.4	50.6	39.5
9806-1	7.009	12.2	1.1	12.4	---------
9806-3	13.508	55.5	3.8	56.3	31.1
9806-3 (dup)	13.508	49.5	3.4	50.2	31.1
Woodridge # 2	15.54	50.8	3.5	52.5	31
Woodridge # 1	68.20	0.8	0.5	0.8	> 49**
Sandilands # 1	14.91	29.9	2.1	30.9	25

* Groundwater ages not modelled for concentrations between 8 and 15 TU.
** Groundwater age is a minimum because 0.8 TU is the detection limit and therefore a maximum concentration.
$^{3}H_{corrected}$: Measured concentrations corrected for ^{3}H decay during storage

it difficult to constrain the groundwater age. Groundwater ages that are of particular interest are those that fall in the range of the detection limit (0.8 TU) and those with concentrations of 50 TU and greater. The groundwater age estimates at piezometers 9804-3 and Woodridge # 1 suggest that groundwater only 7 meters deep in the till and deeper groundwater in sand and gravel (60 meter) is at least 49 years old. Groundwater that was recharged predominantly in the late 1960s (55 TU) was found in piezometers 9806-3, Woodridge #2, and 9805-1 at depths between 13.5 and 22 meters below ground surface.

5.3.5 Groundwater Age Comparison

Due to the difficulties with the $^{3}H/^{3}He$ groundwater age dating method in the shallow piezometers a comparison with the ^{3}H and CFC methods was only possible at the deepest piezometers at three sites. Figure 19 illustrates the groundwater ages determined using each tracer method. Coefficients of variation between the tracer ages range from 19 % to 22 %. The variation that would be expected based on a three year uncertainty in the groundwater ages is approximately 15 %. While the observed variations in the groundwater ages are slightly greater than 15 %, they do provide a greater level of confidence in the age estimates than if only one method had been used to determine groundwater ages. All of the groundwater ages appear to be reasonable based on the hydraulic conductivities and precipitation in the region. Variations in groundwater ages may be reflecting subsurface processes that affect the dating methods differently.

No clear trend was observed with respect to groundwater ages estimated using the different tracer methods. However, gas losses during the ^{3}He sampling and difficulties dating

older groundwater using CFC-113 may be responsible for some of the variation. Detection limit concentrations of tritium at piezometer 9804-3 made it difficult to quantitatively compare the groundwater ages.

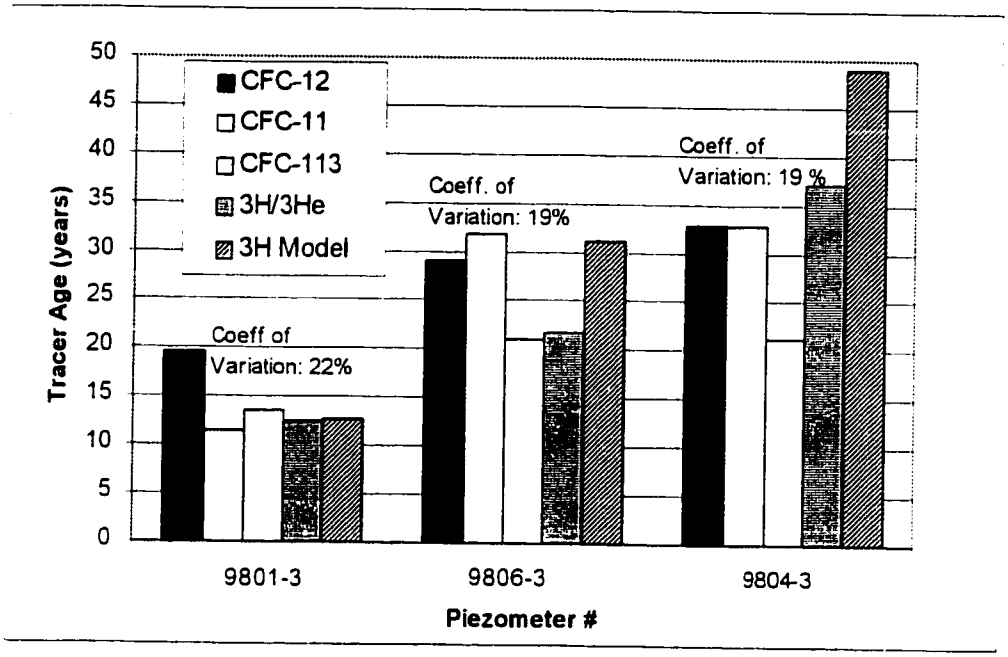

Figure 19. Tracer age comparison. ^{3}H model and $^{3}H/^{3}He$ ages at site 9804 are minimum ages (detection limit ^{3}H). The coefficient of variation in groundwater ages would be approximately 15 % based on an uncertainty in the groundwater ages of ± 3 yrs.

As discussed previously, comparison of the CFC groundwater ages suggest that subsurface processes such as anaerobic degradation and adsorption do not appear to be affecting the age estimates. Subsurface processes such as dispersion can affect ^{3}H model and $^{3}H/^{3}He$ groundwater ages. Previous studies have used the comparison of $^{3}H/^{3}He$ groundwater ages to CFC ages to assess if dispersion affected the $^{3}H/^{3}He$ age estimates (Ekwurzel et al., 1994). Generally, dispersion should affect CFC ages less than $^{3}H/^{3}He$ age estimates because of the relatively steady CFC atmospheric concentrations and so the effects of dispersion on

^3H and ^3He should dominate a plot of $^3H/^3He$ versus CFC ages. Ekwurzel et al. (1994) found that modeled $^3H/^3He$ groundwater ages versus CFC ages with a dispersion of 0.5 m^2/yr resulted in similar groundwater ages from 0-14 years, older $^3H/^3He$ ages between 14 –25 years and younger $^3H/^3He$ age estimates for groundwater greater than 25 years. In addition, the effects of dispersion on the age estimates are most pronounced for groundwater recharged in the mid 1960's due to the large input of ^3H in precipitation (Solomon and Sudicky, 1991; Ekwurzel et al., 1994). In the case of the three deepest piezometers where groundwater ages are compared in Figure 19, site 9806 which has a component of 1960's recharge (56.3 TU) would be the most likely to be affected by dispersion. The $^3H/^3He$ groundwater age is younger than the CFC-12 and CFC-11 groundwater ages by approximately 7 years and may be reflecting some dispersion affect on the $^3H/^3He$ age estimates. However, as previously discussed the $^3H/^3He$ ages can also be regarded as minimum ages due to dissolved gas losses.

CFC and $^3H/^3He$ groundwater ages can be compared, but travel times through the unsaturated zone must be considered with the ^3H model ages. CFC groundwater ages are based on the time the dissolved CFCs are isolated from the unsaturated zone (water table) while ^3H ages are based on water travel times through the unsaturated and saturated zones. Using the average CFC and $^3H/^3He$ groundwater age at site 9801 and the depth below the water table, the vertical velocity in the saturated zone is on the order of .58 m/yr. Based on this value and an estimated unsaturated zone soil moisture content of 0.1, infiltration of water through the unsaturated zone may be on the order of 1.7 m/yr. At this rate of infiltration ^3H groundwater travel times through the unsaturated zone would be approximately 4.5, 2.8 and 1 years at sites 9801, 9806 and 9804, respectively. ^3H groundwater ages at sites 9801 and 9806

are not substantially larger than the CFC ages, although based on the unsaturated zone travel times the ^{3}H ages should be greater. If the affect of dispersion was not negligible it would lower ^{3}H groundwater ages in the range of the mid 1960s bomb peak (Solomon and Sudicky, 1991). Taking into account a 2 year travel time in the unsaturated zone, groundwater from this age range at site 9806 appears to be only minimally affected by dispersion. Similarly, dispersion does not appear to be lowering ^{3}H groundwater ages at site 9804 where it is possible to make a more direct comparison of CFC and ^{3}H groundwater ages due to a thin unsaturated zone.

Groundwater velocities based on the average ages in the piezometers and travel distances of 8 meters below the water table are on the order of 0.58 m/yr and 0.31m/yr at sites 9801 and 9806, respectively. A study of the longitudinal dispersivity of ^{3}H in a shallow sandy silt aquifer where groundwater flow was vertical found that the dispersivity was on the order of 0.02 m over a travel distance of 10 m (Robertson and Cherry, 1989). Given those parameters Solomon and Sudicky (1991) estimated that the difference between groundwater travel times and the estimated $^{3}H/^{3}He$ ages for velocities on the order of 0.5 m/yr would be negligible. The groundwater flow system described above is not that unlike the flow conditions found at site 9801 and 9806 and may support the CFC, $^{3}H/^{3}He$ and ^{3}H age comparison that suggests that dispersion is at a minimum. A much lower velocity at site 9804 through the till may be important in terms of the molecular diffusion component of dispersion and is discussed in more detail in the following section.

The relationship in the groundwater ages can also be explained by examining site specific characteristics such as sediment type and unsaturated zone thickness which are discussed in detail in the interpretation of the groundwater age profiles.

CFC and ^{3}H ages were compared at three additional piezometers where ^{3}He samples were not collected and show that the groundwater ages at two of the locations are comparable within 15 % (Figure 20). As discussed previously, non-equilibrium conditions during sampling for CFCs and ^{3}He may have resulted in gas losses. ^{3}H ages that are larger than CFC

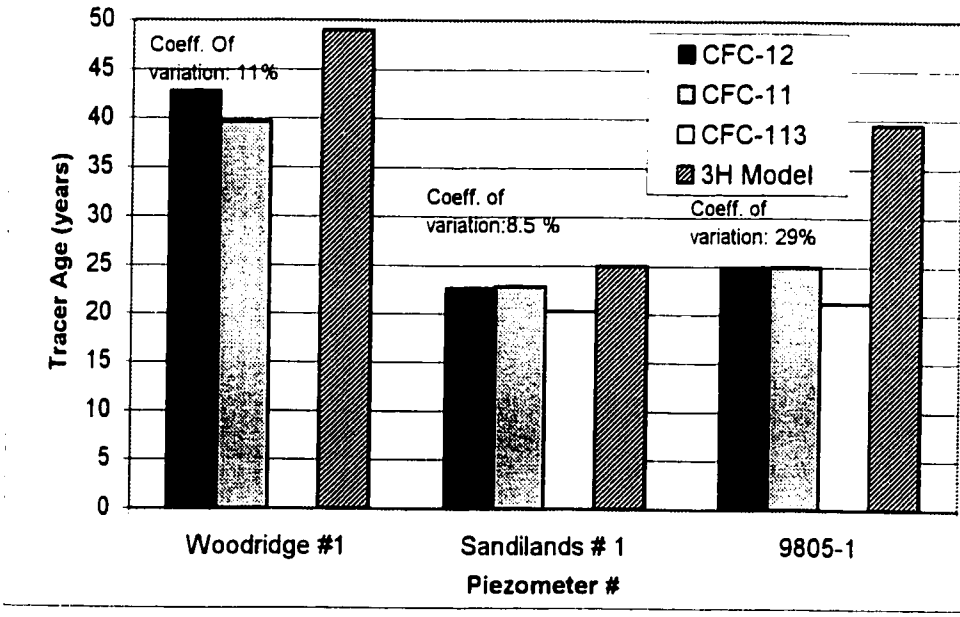

Figure 20. CFC and ^{3}H age comparison at sites where ^{3}He was not sampled.

groundwater ages, on the order of travel times through the unsaturated zone, suggests that dissolved gas losses may not have significantly influenced the CFC ages. Site 9805 is characterized by a thick unsaturated zone (> 18 m) and the difference in the CFC and ^{3}H groundwater ages observed at this location is likely due to the travel time associated with

groundwater infiltration through the unsaturated zone (approximately 10 yrs) and is discussed further in the following section.

5.3.6 Groundwater Age Profiles

Application of the CFC and $^{3}H/^{3}He$ groundwater dating methods to determine groundwater velocities and recharge rates in the Sandilands was assessed by examining groundwater age profiles with depth at the piezometer nests. Although these tracer methods have been extensively studied in well-characterized aquifers, this study attempted to apply the methods to a region where limited information was available on the groundwater system. Provided that groundwater flow is predominantly vertical at the piezometer nests, groundwater ages should increase with depth and can be used to determine vertical groundwater velocities. This trend was not observed at all of the sites and is discussed with respect to the hydrogeological conditions in the Sandilands that complicate the use of CFCs and $^{3}H/^{3}He$ to estimate groundwater velocities and recharge rates.

Figure 21 illustrates three piezometer nests where groundwater ages generally increase with depth. Site 9806 is located in close proximity to the groundwater divide with an unsaturated zone thickness of 5 meters making this site ideal for both one dimensional vertical flow and the CFC groundwater age dating method. As illustrated in Figure 21, this ideality seems to be confirmed by a groundwater age profile where all of the CFC ages increase (between 9 and 22 years) with depth and were used to calculate a vertical groundwater velocity on the order of 0.8 m/yr at depth in the aquifer.

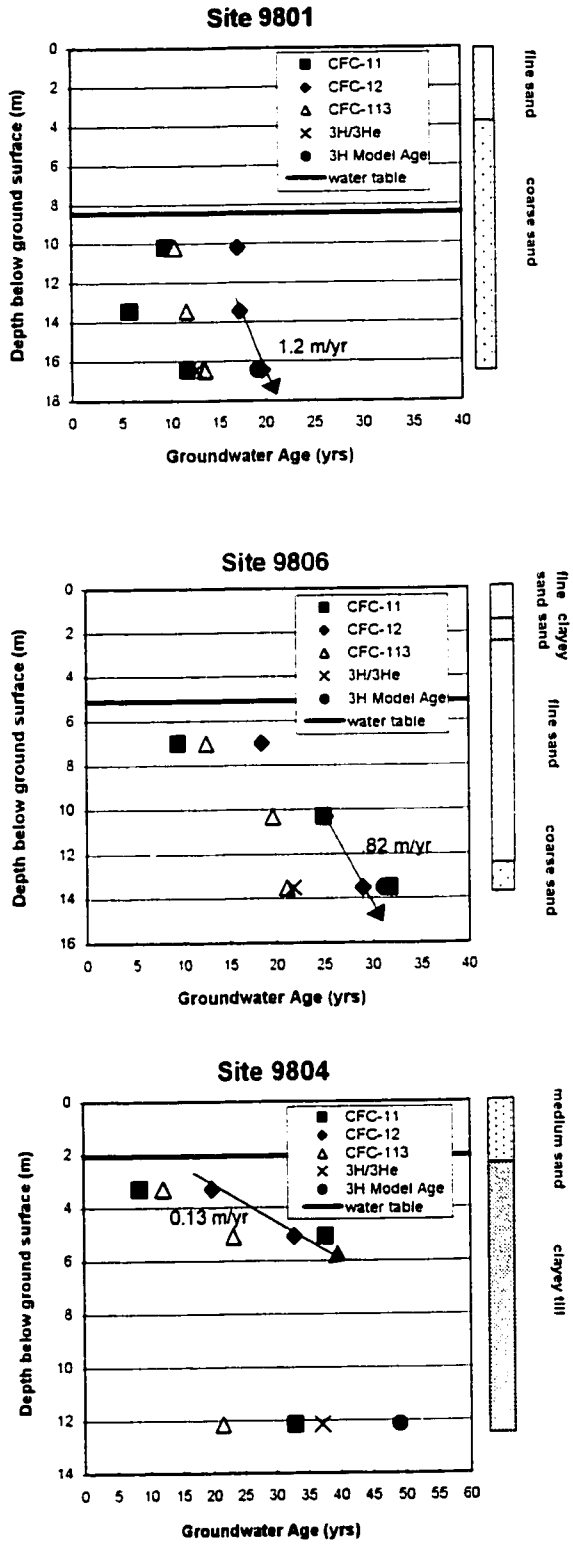

Figure 21. Groundwater age depth profiles at three piezometer nests CFC-12 ages were used to illustrate groundwater velocities at each site. Stratigraphic columns illustrate the different sediment types present at each location.

While groundwater ages at sites 9801 and 9804 also increase with depth, there are a couple of observations worth noting. CFC groundwater ages increase by only 3 years with depth at site 9801. This small age gradient is within the limitations of the age dating method and results in greater uncertainty in the vertical velocity. The presence of coarse grained sediments at this site may have resulted in rapid groundwater infiltration and subsequently a small age gradient. Vertical groundwater velocities could nonetheless be calculated and are on the order of 1.2 m/yr. Hydraulic gradients could not be measured at this sight but given the permeability of the sediments ($K= 9.34*10^{-5}$ m/s) this value does not seem unreasonable.

The presence of clayey till below a thin sand unit at site 9804 provides a valuable opportunity to assess groundwater age profiles in the lower permeability sediments of the region. Groundwater ages increase by over 29 years from the shallow piezometer in the sand to the first piezometer in the till resulting in a groundwater velocity of 0.13 m/yr. This value is over 9 times lower than the groundwater velocity calculated for the sand indicating that groundwater flow rates through the till are much slower than in the sand. However, groundwater ages in the deepest piezometer which is over 7 meters deeper in the till do not increase. The CFC age dating method is generally not applied in low permeability aquifer materials. It is possible that CFC concentrations in groundwater from these piezometers were affected by contamination due to the sampling method. In particular, samples were collected after the piezometers were bailed and allowed to recover for several days. Trace contamination as a result of contact between infiltrating well water and the atmosphere may have caused underestimation of groundwater ages in the deeper piezometer. CFC concentrations in the middle piezometer may have been affected to a lesser extent by

atmospheric contamination as recovery times were on the order of a day in contrast to the deeper piezometer where recovery was on the order of weeks. This hypothesis is supported by ^{3}H and ^{3}He concentrations which suggest that groundwater may in fact be much older than 50 years. This is more than 18 years greater than the groundwater ages estimated by the CFC dating method in the deeper piezometer. In addition, the groundwater velocity through the till estimated using a Darcy's Flux of 35 mm/yr (using a gradient of 0.135 and K = 8.31 $*10^{-9}$ m/s) is on the order of 117 mm/yr which suggests that groundwater is approximately 59 years old in the deeper piezometer.

Comparison of groundwater age profiles at the sites discussed above indicates that vertical groundwater velocities vary considerably between sites. Consider the CFC-12 groundwater velocity, which is quite high at site 9801 and much lower at sites 9806 and 9804. This trend is attributed to different sediment types found at each site. A much lower groundwater velocity at site 9804 is likely due to the presence of lower permeability clayey till. While hydraulic conductivity values do not differ between sites 9801 and 9806, the more sensitive tracer methods support the fact that textural differences can have an important effect on groundwater flow rates.

Piezometer nests where groundwater velocities could not be determined were useful in providing insight into the groundwater flow system and in assessing factors that limit the application of the CFC groundwater dating method in the study area. Piezometer nests located close to the Bedford Ridge (Figure 22) could not be used to estimate groundwater velocities due do an inverted age gradient (site 9803). Inverted groundwater age profiles have been found in unconfined aquifers downgradient of a shallow water table where the

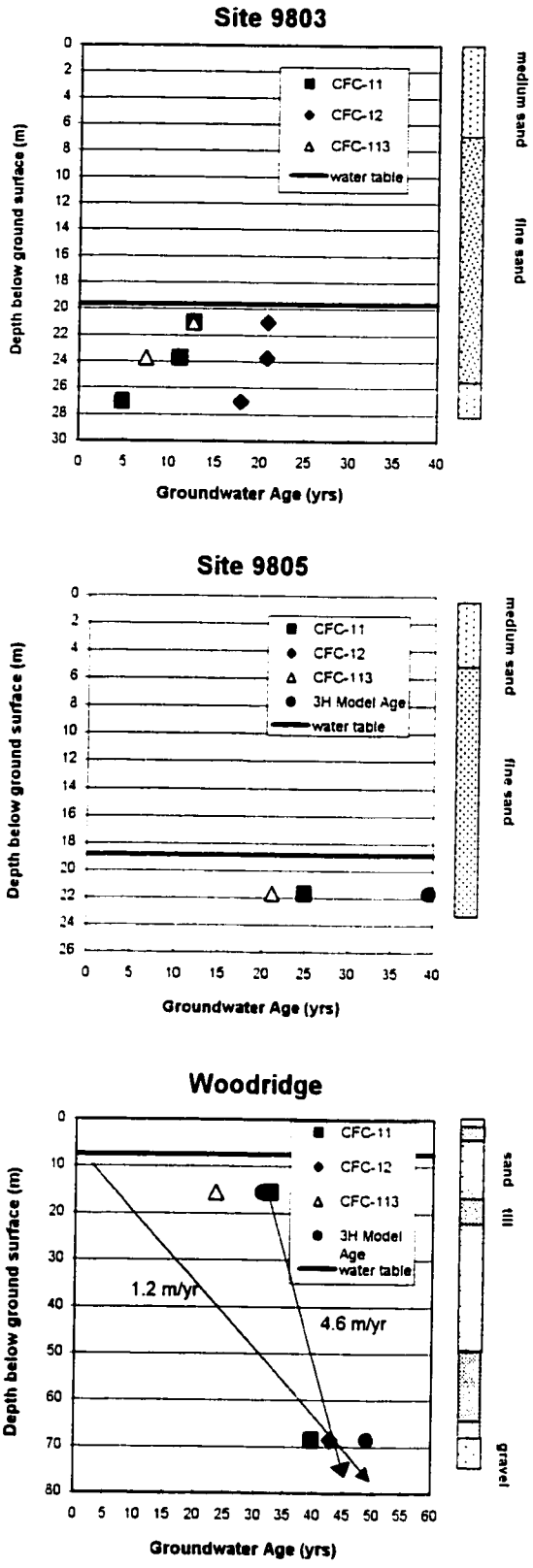

Figure 22. Groundwater age profiles at sites located near the Bedford Ridge and at a deeper piezometer nest (Woodridge)

unsaturated zone is thick and there is a substantial horizontal flow component (Cook and Solomon, 1995).

Site 9805 may be representative of groundwater ages affected by diffusional time lags through a thick unsaturated zone (18.8 meters). Diffusional time lags, the time it takes CFC gases in the atmosphere to diffuse through the unsaturated zone to the water table, through thick unsaturated zones have been extensively documented in previous studies (Cook and Solomon, 1995; Johnston et al., 1998). However, site 9805 is a good indicator that it is occurring in the Sandilands. CFC groundwater ages 2.5 meters below the water table are between 21 and 25 years. CFC groundwater ages from sites 9806 and 9801 with thin unsaturated zones, are on the order of 10 years at a comparable depth, suggesting that the CFC gas time lag may be on the order of 10 years at site 9805. A ^{3}H model age of 40 years suggests groundwater flow times through the unsaturated zone are large and as a result it is difficult to compare the CFC and ^{3}H groundwater ages.

Groundwater samples for CFC analyses were collected from the Woodridge provincial well nest as it was originally thought that groundwater in the deeper piezometer would be CFC free and would provide a check on the sampling method. The deep piezometer at this site is completed in a coarse sand and gravel at a depth of 60 meters below the water table. Although, clayey till overlies the sand and gravel, detectable concentrations of CFC were measured (Table 13). It is possible that the sand and gravel is part of a preferential flow path for groundwater and CFC concentrations are indicating that groundwater flow is not vertical down through the till. The CFC and ^{3}H groundwater ages in the shallower piezometer are between 31 and 32.4 years. A vertical groundwater velocity based on the 11

year age difference over 52 meters between the shallow and deep piezometers is 4.6 m/yr and does not seem reasonable given the thickness of lower permeability sediments between the piezometers. Groundwater ages on the order of 43 years in the deep piezometer would only be possible if there is a preferential flow path through coarse sediments from the surface near the piezometer nest down to the deep piezometer. If this were the case and the travel distance was not much larger than 60 meters, the groundwater velocity would be on the order of 1.4 m/yr which is more comparable to velocities estimated at other locations in the study area. Hydraulic head data shows there is not a downward gradient between the two piezometers at this site and it is possible they are part of two different local flow systems (Table 13). ^{3}H model ages on the order of 49 years provide some evidence that CFC groundwater ages may be overestimations in the deeper piezometer and point towards trace CFC contamination as another possible explanation for the observed groundwater age distribution.

Table 13
Groundwater Ages at the Woodridge Well Nest

Piezometer #	Depth below water table (m)	CFC-11 conc. (pg/kg)	CFC-11 Age (yrs)	CFC-12 conc. (pg/kg)	CFC-12 Age (yrs)	^{3}H conc. (TU)	^{3}H Age (yrs)	Hydraulic Head (m.a.s.l.)	Hydraulic Gradient
Woodridge # 2	7.54	129.74	32.4	76.34	31.4	52.5	31	371.4	
Woodridge #1	60.2	43.18	39.7	15.3	42.8	<0.8	>49	371.5	0.001899 upward

5.4 Groundwater Recharge

5.4.1 Tracer Recharge Rates

As discussed in the previous section, vertical groundwater velocities could not be calculated at all of the piezometer nests due to the distribution of groundwater ages with depth and as a result only three sites could be used to estimate groundwater recharge rates.

Tracer recharge rates were estimated using two methods; a slope method and a water table method. The slope method involves calculating the vertical groundwater velocity by taking the difference between the groundwater ages in two piezometers in the nest and dividing it by the vertical distance between them. The water table method uses the groundwater age in a single piezometer and its distance below the water table to calculate the groundwater velocity. An empirical estimate of 0.3 for the effective porosity (Domenico and Schwartz, 1998) of unconsolidated sediments was used to calculate the recharge rates.

Comparison of the two calculation methods for determining recharge rates indicates that the water table method is the most consistent (Table 14). Coefficients of variation for the slope method vary between 44 % and 49 % and are much larger than the variations in the water table method (with the exception of site 9804). The vertical spacing of the piezometers may be too close to produce large enough groundwater age differences from adjacent piezometers due to the limitations of the CFC dating method. This appears to be the case at site 9801 where the recharge rates calculated using CFC-12 and CFC-113 are well above those that would generally be observed under the given climate. The groundwater ages in the deepest piezometers used for the water table method may be resulting in more reasonable recharge rates as they are averaged over a greater vertical distance and are influenced to a

Table 14
Recharge Rates Calculated using each Tracer Method at Three Locations in the Study Area

Site	Dating Method	Recharge Rate (mm/yr) [g] effective porosity = 0.3 Calculation: Water Table[b]	Slope[c]
9801[a]	CFC-12	122	373
	CFC-11	206	153
	CFC-113	178	465
	$^3H/^3He$	190	----
	Average[a]	174 +/- 36	330 +/- 160
	coeff of variation	21%	49%
9806[e]	CFC-12	87	248
	CFC-11	79	87
	CFC-113	46	225
	$^3H/^3He$	115	----
	Average	82 +/- 28	187 +/- 87
	coeff of variation	35%	47%
9804[f]	CFC-12	28	40
	CFC-11	24	18
	CFC-113	39	48
	$^3H/^3He$*	81	----
	Average	43 +/- 26	35 +/- 16
	coeff of variation	61%	44%

[a] Average of the four methods +/- one standard deviation

[b] Calculation based on the groundwater age in the deepest piezometer and depth below the water table.

[c] Calculation based on difference between groundwater ages at two piezometers and the vertical distance between them

[d] slope method calculations using the middle and deepest piezometers

[e] slope method calculation done using the shallowest and deepest piezometers for CFC-11 and CFC-113 and the middle and deepest piezometers for CFC-12

[f] slope method calculations done between the shallowest and middle piezometer.

[g] an uncertainty in the effective porosity of +/- 0.05 results in a 10 % difference in the calculated recharge rate.

* maximum recharge rate as groundwater age is a minimum

lesser extent by uncertainties in the groundwater ages. In addition, CFC groundwater ages in the deeper piezometers are less sensitive to uncertainties in the recharge temperature. While there are uncertainties associated with dating older groundwater due to trace CFC contamination, the uncertainties in the younger groundwater caused by a poorly constrained recharge temperature are likely much larger. As a result, using the age in the deeper piezometer to estimate groundwater velocities minimizes the uncertainty in the recharge rate. For these reasons the remainder of the discussion of recharge rates will be based on ages in the deepest peizometer and the depth below the water table. In the case of site 9804, where the $^{3}H/^{3}He$ recharge rate is significantly higher than the CFC recharge rates it should be noted that this is a maximum recharge rate as the $^{3}H/^{3}He$ groundwater age is a minimum.

Average recharge rates at each site are discussed with respect to precipitation in the Sandilands and compared with physical estimates. The average annual precipitation in the study area is approximately 574 mm/yr based on five years of precipitation data collected in the Sandilands Provincial Forest by the Forestry Branch of the Manitoba Ministry of Natural Resources. Data were collected from 1981-1985 in the vicinity of the Marchand Forestry station, 6 kilometers to the northwest of the piezometer nests. Longer term precipitation records from the towns of Marchand and St.Labre indicate that precipitation ranges from 574 mm/yr in the west across the study area to 612 mm/yr in the east.

The average recharge rates calculated at each of the three sites are within a reasonable range compared with the total annual precipitation (Table 15). Groundwater recharge in the study area ranges from 8 % to 30 % of the total precipitation. Site 9801 shows the highest percentage of recharge at 30 % of the average annual precipitation. Previous studies have

found that in temperate climates where there is greater than 500 mm/yr of precipitation groundwater recharge can exceed 24 % of the total precipitation (Lerner, 1990).

Table 15
Average Recharge Rates as a Percentage of Spring/Fall Precipitation

Site	Average Recharge Rate[a] (mm/yr)	% of spring/fall precipitation[b]	% of annual precipitation[c]
9801	174 +/- 36	73 %	30 %
9806	82 +/- 28	35 %	14 %
9804	43 +/- 26	18 %	8 %

[a] average recharge rates based on water table calculations
[b] 5 yr average of March-June and Sept-Nov precipitation (238 mm/yr)
[c] 5 yr average of total annual precipitation (574 mm/yr)

Comparison of the average $\delta^{18}O$ value of groundwater in the study area (−14.2 ‰) (Table 9) with the weighted average $\delta^{18}O$ in precipitation (−12.4 ‰) suggests that groundwater recharge is seasonal and occurs predominantly when evapotranspiration is at a minimum in the spring and fall. The total precipitation during this time period is 238 mm/yr and as indicated by site 9801, large percentages of this precipitation may be recharging groundwater in the Sandilands (Figure 23). Much of the precipitation that falls in the late spring and early fall occurs as showers and intense thunderstorms (Betcher et al., 1995). Site 9801 suggests that where there are coarse sands at the surface this precipitation may infiltrate rapidly into the unsaturated zone and contribute substantially to groundwater recharge. In a similar CFC and $^{3}H/^{3}He$ groundwater recharge study, Ekwurzel et al. (1995) found that

similar CFC and $^{3}H/^{3}He$ groundwater recharge study, Ekwurzel et al. (1995) found that groundwater recharge through unconsolidated sandy sediments ranged from 30 – 83 % of the non-growing season precipitation.

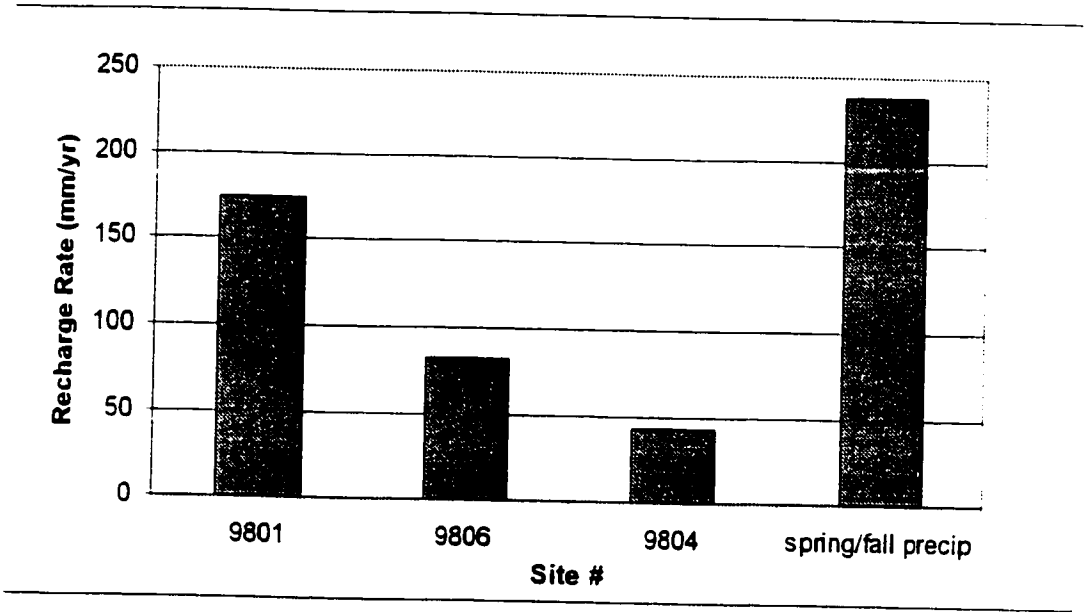

Figure 23. Variations in average recharge rates at each site compared with annual spring/fall precipitation.

Groundwater recharge rates vary between the three locations from a high of 174 ± 36 mm/yr to a low of 43 ± 26 mm/yr. The lowest recharge rate, 43 ± 26 mm/yr, is actually a maximum value for recharge at site 9804 as the $^{3}H/^{3}He$ recharge rate is a maximum (due to detection limit ^{3}H). If this value was not used in the calculation of the average recharge rate the value would be closer to 30 +/- 8 mm/yr with a coefficient of variation of 25 %. The local recharge rates estimated at each site indicate that there is significant spatial variation in groundwater recharge throughout the study area. The three sites are all located in the plateau region of the Bedford Ridge and ground surface elevations do not vary noticeably between

the sites. Site 9804 is located almost directly on the groundwater divide with sites 9806 and 9801 in close proximity to the divide suggesting that differences in the water table elevations are not responsible for the differences observed in the recharge rates.

The variation seen in the recharge rates is best explained with respect to different sediment types. Table 16 indicates that each site is characterized by a different dominant sediment type, ranging from predominantly coarse sand at site 9801 to clayey till at site 9804. The coarser sand at site 9801 coincides with a recharge rate over four times greater than the recharge rate at site 9804 where the sediments are mainly clayey till. Similarly, the net vertical hydraulic conductivity at site 9804 (Table 16) is four orders of magnitude less

Table 16
Average Recharge Rates Compared with Hydraulic Conductivities and Sediment Type

Site	Average Recharge Rate (mm/yr)	Net Vertical Hydraulic Conductivity[a] K_z (m/s)	Dominant Sediment Type
9801	174 +/- 36	8.74E-05	coarse sand
9806	82 +/- 28	1.35E-04	fine sand
9804	43 +/- 26	1.12E-08	clayey till

[a] weighted harmonic mean of the hydraulic conductvities measured at each piezometer in the nest using bail tests and the Hvorslev method.
$K_z = d / \text{sum}(d_i/K_i)$; where d is the total vertical distance of the piezometer nest; d_i is the thickness of the unit the ith piezometer is screended in; K_i is the hydraulic conductivity of the ith piezometer in the nest.

than at sites 9801 and 9806. While the hydraulic conductivities between sites 9801 and 9806 are not substantially different, the dominant sediment types are not the same. The average recharge rate is much lower at site 9806 and may be a more accurate measurement of the variations between the hydraulic conductivities of the different sediments. Based on observations made in the field during drilling and sediment sample collection variations between recharge rates at sites 9801, 9806 and 9804, due to textural differences in the sands and different sediment types, seem to be quite reasonable.

5.4.2 Physical Recharge Rates

A comparison of recharge rates estimated using tracer techniques versus physical methods was only possible at site 9804 where there was a measurable vertical hydraulic gradient. The Darcy flux calculated using the net vertical hydraulic conductivity and a gradient of 0.136 is on the order of 48 mm/yr, although this is a rough estimate as it is difficult to measure the hydraulic conductivity with a high degree of accuracy. This value is comparable to the average recharge rate of 43 ± 26 mm/yr calculated using the CFC and $^{3}H/^{3}He$ methods and provides further evidence that the tracer techniques are reliable estimates of groundwater recharge in the Sandilands.

5.4.3 Water Balance Recharge Rates

Groundwater recharge in the study area was estimated using a water balance method and compared with the recharge estimates obtained using the tracer methods. Using the water balance method, recharge is defined as the sum of evapotranspiration, runoff and storage

changes subtracted from the total precipitation in the area (Equation 6). Generally over an annual cycle, changes in the storage term will be negligible compared to the other water balance components and efforts can be focused on estimating evapotranspiration (Dunne and Leopold, 1978).

Evapotranspiration can be estimated based on precipitation and temperature data from the study area using the methods described by Thornthwaite and Mather (1957). Evapotranspiration encompasses two processes, which affect water in the subsurface and include free water evaporation and transpiration of water by vegetation. Evapotranspiration is often discussed with respect to two terms; 1) potential evapotranspiration which is the amount of water that would transpire and evaporate if the input of water were unlimited and 2) actual evapotranspiration which is limited by the available water. In this context, actual evapotranspiration may be lower than potential evapotranspiration and depends largely on the soil moisture content.

In this study both potential and actual evapotranspiration were estimated based on precipitation data from the Marchand Forestry Station and temperature data from the Winnipeg International airport (Table 17). For a detailed discussion of the Thornthwaite calculations used for estimating evapotranspiration refer to Appendix IV. Potential evapotranspiration that exceeds available precipitation in the summer months in the Sandilands results in actual evapotranspiration rates on the order of 503 mm/yr. Based on the definition of groundwater recharge discussed above, precipitation in excess to evapotranspiration that is available for groundwater recharge and runoff and is approximately 71 mm/yr or 12 % of the annual precipitation. This value falls within the range of recharge

rates estimated using the tracer methods and is similar to the recharge rate at site 9806. Comparison of the recharge rates calculated using the tracer methods and the water budget method indicates that groundwater recharge may be higher than predicted using the water budget method where shallow sediments are dominated by coarse sands. In contrast, the presence of near surface lower permeability clayey tills may reduce groundwater recharge and increase the runoff component of the water balance.

Table 17
Yearly Potential and Actual Evapotranspiration Estimates

Annual Precipitation P (mm/yr)	Potential Evapotranspiration PET (mm/yr)	Actual Evapotranspiration AET (mm/yr)	P - AET	% of P available for recharge & runoff
574	557	503	71	12%

5.4.4 Spatial Variations in Recharge

Based on the spatial variability of the recharge rates and the high correlation with sediment type, groundwater recharge rates will be strongly influenced by the distribution of sediment types within the Sandilands. In the surficial aquifer recharge is probably highest in the central, western and northern portions of the study area where the surface sediments are predominantly sand (Figure 4) and extend to depths of over 40 meters (Figure 6). In contrast, the eastern and southern portions of the study area are characterized by near surface tills that

may decrease the rate of groundwater infiltration and therefore increase the amount of precipitation that is lost to groundwater recharge as runoff.

Previously documented $\delta^{18}O$ values for groundwater in southeastern Manitoba from the freshwater portion of the regional bedrock aquifer near the Sandilands are generally between −13 and −14 ‰ (Fritz et al., 1974). Fritz and others found that the bedrock values were comparable to values collected from a few wells in the surficial deposits in the southeast and suggested that the region may be an area of groundwater recharge. Comparison of their $\delta^{18}O$ data with values obtained as part of this study (-14.17 ‰) provides further evidence that groundwater recharge through the surficial sediments in the Sandilands is an important component of modern groundwater recharge to the bedrock aquifer. Based on the relationship between recharge rates and sediment type established above it is proposed that groundwater recharge rates through the surficial deposits to the bedrock will likely be substantially affected by the distribution of thick clayey tills that overlie portions of the bedrock (Figure 6).

6.0 Conclusions

6.1 Groundwater Flow

A compilation of piezometric data obtained from the piezometer nests and provincial wells in the Sandilands indicate that peak groundwater table elevations are located in the center of the study area and are offset to the east of the topographic high. Water table elevations are regionally the highest in the Bedford Ridge area and decrease outwards to the north, south, east and west. The steepest water table gradients are found where there is a

steep decrease in the topography, most notably at the Bedford Ridge. Shallow groundwater flow was shown to be predominantly vertical at sites 9804 and 9806, which are located on or in close proximity to the groundwater divide. Piezometeric data at piezometer nest 9804 indicate that there is a substantial downward vertical gradient of 0.135. A comparison of horizontal gradients between sites to the vertical gradient at site 9803 suggests that there are larger components of lateral flow at sites located closest to the ridge (9803, 9805) and to the north of the groundwater divide (9802).

Installation of deeper piezometers at the nests would improve the understanding of vertical versus horizontal flow components in the study area and may improve the interpretation of groundwater age estimates and recharge rates. On a regional scale, constraining groundwater flow directions would provide insight into the extent of recharging conditions within the Sandilands.

6.2 Groundwater Geochemistry

Shallow groundwater in the Sandilands is dominated by a Ca-Mg-HCO_3 facies saturated with respect to calcite with pHs between 7.8 and 8.2. $\delta^{13}C_{DIC}$ values range from -9.4 to -12.9 ‰. Values in the range of -9.4 ‰ suggest that the dissolution of carbonates in the sand, with an average $\delta^{13}C$ of -0.7 ‰, is enriching the $\delta^{13}C_{DIC}$ component of groundwater. Groundwater geochemistry in the till is characterized by higher Na^+ and SO_4^{2-} concentrations, which may be associated with the weathering of feldspars and pyrite oxidation, respectively. The rapid decline in SO_4^{2-} concentrations in groundwater 7 meters deep in the till suggest that redox conditions in the till may evolve rapidly with depth from

aerobic groundwater saturated with dissolved oxygen through to sulphate reducing conditions.

Regional groundwater sampling of domestic and provincial wells indicates that groundwater evolves towards a Ca-Mg-Na-HCO_3 facies as most groundwater with longer flow paths will have encountered till. Similarly, redox conditions evolve with depth in the groundwater flow system from groundwater saturated with dissolved oxygen to anaerobic groundwater with high dissolved Fe concentrations (up to 1.4 mg/l). At depths greater than 40 meters SO_4^{2-} concentrations decrease from over 10 mg/l to less than .05 mg/l suggesting that sulphate reduction is the dominant redox buffer of deeper groundwater. The groundwater geochemistry in both the surficial deposits and two bedrock wells located on the periphery of the Sandilands has a unique geochemical signature with higher concentrations of Na^+ and Cl^-, which is attributed to the influence of shale bedrock units in the region.

In the future, application of the CFC groundwater age dating methods to groundwater deeper in the regional aquifer as well as in shallow till may need to be assessed with respect to redox conditions. CFC degradation associated with anaerobic groundwater conditions may make it difficult to estimate CFC groundwater ages at depths of 40 meters or greater in the Sandilands.

6.3 Groundwater Ages

Groundwater ages estimated using the CFC dating technique range from 4 to 40 years with the youngest groundwater found in the shallow water table piezometers and the oldest groundwater found at a depth of 7 meters in the till and in the sand at a depth of 60 meters

below the water table. Comparison of groundwater ages estimated using CFC-11, CFC-12, and CFC-113 indicate that sampling methods in the shallow piezometers and in the till and trace CFC-113 contamination were the limiting factors on the CFC age dating technique in the Sandilands. Typical non-conservative processes such as anaerobic degradation did not appear to affect the CFC age estimates.

Dissolved neon analyses performed in conjunction with dissolved ^{3}He analyses indicate that dissolved gases were lost to varying degrees in all of the ^{3}He samples. This was attributed to gas stripping due to partial vacuum pumping during the sampling of shallow piezometers. In addition, early closure of the check valve during sampling may have resulted in non-equilibrium dissolved gas conditions in the copper tubes. As a result, $^{3}H/^{3}He$ groundwater ages could only be calculated at three of the deeper piezometers. Ages range from 12.6 years to 37.1 with the oldest groundwater found at depth in the till.

^{3}H concentrations range from 0.8 TU (detection limit) to 56.3 TU with most of the intermediate concentrations between 8 and 16 TU. This range of concentrations suggests that qualitatively groundwater ages range from pre-bomb through to modern groundwater. Mathematical plug flow modeling of the tritium concentrations indicates that deep groundwater in the sand (60 meters) and groundwater in the till is a minimum of 49 years old. Modeling of groundwater with 56 TU showed that groundwater recharged predominantly in the late 1960s can be found in the sand between 13.5 and 15 meters below ground surface.

$^{3}H/^{3}He$, ^{3}H and CFC groundwater ages were comparable to within 22 % indicating that the groundwater age estimates are reasonably reliable and may have been affected only slightly by subsurface processes, such as dispersion.

One of the largest limitations on estimating groundwater ages in the Sandilands was associated with the sampling procedures of both the CFC and ^{3}He dating techniques. Insight was gained into conditions that adversely affected the sampling methods, such as sampling under partial vacuum and early check valve closure. Application of this information to refine the sampling methods would improve the reliability of the groundwater ages and hence the recharge rates. In addition, constraining the CFC recharge temperature by measuring dissolved noble gases (Argon, Xenon) in conjunction with CFC concentrations would decrease the uncertainties in the groundwater age estimates, particularly for younger groundwater. Given the uncertainties associated with the CFC age dating method (contamination, recharge temperature, etc) it is difficult to apply this method to a study area where little is known about the groundwater flow system. In areas such as these, it appears to be quite important to combine the CFC dating method with other methods in order to estimate the reliability of the CFC groundwater age estimates.

6.4 Groundwater Age Profiles

Groundwater ages with depth were assessed at six locations in the study area. Where groundwater ages could not be used to estimate groundwater velocities due to complicated age distributions they, nonetheless, provided valuable insight into groundwater flow conditions. Groundwater ages suggest long unsaturated zone travel times and preferential

groundwater flow paths may be important components of the groundwater flow system. In addition, on the Bedford Ridge where unsaturated zone thicknesses exceed 18 meters, CFC age inversions and diffusional time lags were observed which complicated the use of groundwater ages to estimate vertical velocities at these locations.

At sites where groundwater age profiles could be used to calculate vertical velocities the age gradients ranged between sites from 3 to 24.5 years over a vertical distance of approximately 6 meters resulting in vertical groundwater velocities between 0.13 and 1.2 m/yr.

6.5 Groundwater Recharge Rates

Recharge rates were estimated at three locations in the Sandilands. The average recharge rates determined using CFC-11, CFC-12, CFC-113 and $^{3}H/^{3}He$ dating methods at each site were found to range between 43 ± 26 mm/yr to 174 ± 36 mm/yr and are comparable to water balance and Darcian estimates. Comparison of recharge rates with precipitation in the area indicates that these rates comprise between 8 and 30 % of the average annual precipitation and appear to be reasonable estimates of groundwater recharge.

Recharge rates were found to vary spatially in the study area and are highly coincident with variations in sediment type. Groundwater recharge is highest (174 ± 36 mm/yr) where sediments are dominated by coarse sands and lowest (43 ± 26 mm/yr) through clayey till sediments. This is consistent with variations in the hydraulic conductivities of the different sediments.

Groundwater recharge rates in the surficial aquifer will likely be strongly influenced by the distribution of sediment types and may be highest in the western and northern portions of the study area (Figure 4) where the surface sediments are sandy and extend to depths of up to 40 meters. In addition, groundwater recharge to the bedrock may be significantly affected by the presence of thick clayey tills overlying the bedrock (Figure 5). In the future, constraining the distribution of the sediments and more specifically, assessing the degree of hydraulic continuity between the coarser sediments will be an important aspect of quantifying the contribution of groundwater recharge in the Sandilands region to the bedrock aquifers.

The understanding of groundwater recharge in the surficial aquifer in the Sandilands was improved by recharge rate estimates obtained using a multi-tracer groundwater age dating technique. The advantage of using the tracer recharge rate estimates in the Sandilands, over water balance and Darcian estimates, was that spatial variations of recharge in shallow groundwater could be evaluated. The sensitivity of the tracer method to identify the control of textural differences of the sand, not seen in the hydraulic conductivities, on recharge rates may improve the constraints on locating areas of high recharge within the Sandilands. Application of the recharge estimates to regional groundwater flow models and to direct future research in the Sandilands region will allow for better groundwater resource management in southeastern Manitoba.

References

Allison, G.B. and Hughes, M.W., 1975. The use of environmental tritium to estimate recharge to a south-Australian aquifer. J. Hydrol., 26: 245-254.

Andrews, J.N. and Lee, D.J., 1979. Inert gases in groundwater from the Bunter Sandstone of England as indicators of age and paleoclimatic trends. J. Hydrol., 41: 233-252.

Betcher, R., Grove, G., and Pupp, C., 1995. Groundwater in Manitoba: hydrogeology, quality concerns, management. Environment Canada, NHRI contribution no. CS-93017.

Böhlke, J.K. and Denver, J.M., 1995. Combined use of groundwater dating, chemical, and isotopic analyses to resolve the history and fate of nitrate contamination in two agricultural watersheds, Atlantic coastal plain, Maryland. Water Resour. Res., 13(9) 2319-2339.

Bottomley, D.J., Ross, J.D. and Clarke, W.B., 1984. Helium and neon isotopes geochemistry of some groundwaters from the Canadian Precambrian Shield. Geochimica et Cosmochimica Acta, 54:933-1008.

Brown, R.M., 1961. Hydrology of tritium in the Ottawa Valley. Geochim. Cosmochim. Acta, 21: 199-204.

Bu, X. and Warner, M.J., 1995. Solubility of chlorofluorocarbon 113 in water and seawater Deep-Sea Research I, 42(7): 1151-1161.

Bullister, J.L. and Weiss, R.F., 1983. Anthropogenic chlorofluoromethanes in the Greenland and Norwegian seas. Science, 221: 265-268

Busenberg, E., and Plummer, L.N., 1991. Chlorofluorocarbons CCl_3F and CCl_2F_2: Use as an age dating tool and hydrologic tracer in shallow groundwater systems. U S Geol Surv. Water Resour. Invest., 91-4034:542-547.

Busenberg, E. and Plummer, L.N., 1992. Use of chlorofluorocarbons (CCl_3F and CCl_2F_2) as hydrologic tracers and age-dating tools: The alluvium and terrace system of central Oklahoma. Water Resour. Res., 28(9): 2257-2283.

Cerling, T.E., Poreda, R.J., and Solomon, D.K., 1987. Use of tritium and helium isotopes in the study of a shallow unconfined aquifer. EOS, 68: 300.

Clark, I.D. and Fritz, P., 1997. Environmental Isotopes in Hydrogeology. CRC Lewis Publishers, New York, 328 pp.

Clarke, W.B., Jenkins, W.J. and Top, Z., 1976. Determination of tritium by mass spectrometric measurement of ^{3}He. Int. Journal of Applied Radiation Isotopes., 27: 515-522.

Cook, P.G. and Solomon, D.K., 1995. Transport of atmospheric trace gases to the water table: Implications for groundwater dating with chlorofluorocarbons and krypton 85 Water Resour. Res., 31(2): 263-270.

Cook, P.G. and Solomon, D.K., 1997. Recent advances in dating young groundwater: chlorofluorocarbons $^{3}H/^{3}He$, and ^{85}Kr. J. of Hydrol., 191: 245-265.

Cook, P.G., Solomon, D.K., Plummer, L.N., Busenberg, E. and Schiff, S.L., 1995 Chlorofluorocarbons as tracers of groundwater transport processes in a shallow, silty sand aquifer. Water Resour. Res., 31(3): 425-434.

Cook, P.G. et al., 1996. Inferring shallow groundwater flow in saprolite and fractured rock using environmental tracers. Water Resour. Res., 32(6): 1501-1509.

Cunnold, D.M. et al., 1994. Global Trends and Annual Releases of CCl_3F and CCl_2F_2 Estimated from ALE/GAGE and Other Measurements from July 1978 to June 1991. Geophysical Research, 99: 1107-1126.

Domenico, P.A. and Schwartz, F.W., 1990. Physical and Chemical Hydrogeology. John Wiley and Sons, Inc., New York, 506 pp.

Dunkle, S.A., Plummer, L.N., Busenberg, E., Phillips, P.J., Denver, J.M., Hamilton, P.A., Michel, R.L. and Coplen, T.B., 1993. Chlorofluorocarbons (CCl_3F and CCl_2F_2) as dating tools and hydrologic tracers in shallow groundwater of the Delmarva peninsula, Atlantic coastal plain, United States. Water Resour. Res., 29(12): 3837-3860.

Dunne, T and Leopold, L.B., 1978. Water in Environmental Planning.W.H. Freeman and Company, New York, 818 pp.

Egboka, B.C.E, Cherry, J.A., Farvolden, R.N., and Frind, E.O., 1983. Migration of contaminants in groundwaters at a landfill: A case study, 3. Tritium as an indicator of dispersion and recharge. J. Hydrol., 63: 51-80.

Ekwurzel, B., Schlosser, P., Smethie, Jr. W.M., Plummer, L.N., Busenberg, E., Michel, R.L., Weppernig, R. and Stute, M., 1994. Dating of shallow groundwater: comparisons of the transient tracers, $^{3}H/^{3}He$, chlorofluorocarbons, and ^{85}Kr. Water Resour. Res., 30(6): 1693-1708.

Environment Canada, (1999). Canadian climate normals for Winnipeg, Manitoba., www.cmc.ec.gc.ca.

Fritz, P., Drimmie, R.J. and Render, F.W., 1974. Stable isotope contents of a major prairie aquifer in central Manitoba, Canada. International Atomic Agency, IAEA-SM-182/22.

Gammon, R.H., Cline, J., and Wisegarver, D., 1982. Chlorofluoromethanes in the North Pacific Ocean: measured vertical distribution and application as transient tracers of upper ocean mixing. J. Geophys. Res., 87: 9441-9454.

Gascoyne, M. and Kotzer, T., 1995. Isotopic Methods in hydrogeology and their application to the underground research laboratory, Manitoba. Atomic Energy Canada report 11370.

Hammer, P.M., Hayes, J. M., Jenkins, W.L., and Gagosian, R.B., 1978. Exploratory analyses of trichlorofluoromethane (F-11) in North Atlantic water columns, Geophys. Res. Lett., 5:645-648.

Heaton, T.H.E. and Vogel, J.C., 1981. "Excess air" in groundwater. J. of Hydrol., 50: 201-216.

Herzberg, O. and Mazor, E., 1979. Hydrological applications of noble gases and temperature measurements in underground water systems: Examples from Israel. J. of Hydrol., 41: 217-231.

IAEA, International Atomic Energy Agency, 1999.www.iaea.or.at:80/programs/ri/gnip/gnipmain.htm

Johnston, C.T., Cook, P.G., Frape, S.K., Plummer, L.N., Busenberg, E., Blackport, R.J., 1998. Ground water age and nitrate distribution within a glacial aquifer beneath a thick unsaturated zone. Ground Water, 36(1): 171-180.

Kotzer, T., 1998. Atomic Energy Canada Limited, Chalk River, Ontario. personal communication.

Khalil, M.A.K. and Rasmussen, R.A., 1989. The potential of soils as a sink of chlorofluorocarbons and other man-made chlorocarbons. Geophys. Res. Lett., 16(7): 679-682.

Lerner, D.N., Issar, A.S. and Simmers, I., 1990. Groundwater recharge: A guide to understanding and estimating natural recharge. International Association of Hydrogeologists, 8: 99-107.

Little, J., 1980. Groundwater availibility map series: Winnipeg area (62-H). Manitoba Natural Resources, Water Resources Branch.

Lovely, D.R. and Woodward, J.C., 1992. Consumption of freons CFC-11 and CFC-12 by anaerobic sediments and soils. Envir. Science Tech., 26: 925-929.

Maloszewski, P. and Zuber,A., 1996. Lumped parameter models for the interpretation of environmental isotope tracer data. International Atomic Energy Agency., IAEA-TECDOC-910.

McCarthy, R.L., Bower, F.A. and Wade, R.J., 1977. The fluorocarbon-ozone theory, I, production and release: World production and release of CCl_3F and CCl_2F2 (fluorocarbons 11 and 12) through 1975. Atmos. Environ., 11:491-497.

Nir, A., 1964. On the interpretation of tritium 'age' measurements in groundwater J. Geophys. Res., 69: 2589-2595.

NOAA, National Oceanic and Atmospheric Administration, Climate Monitoring and Diagnostics Laboratory (CMDL)., 1999. Boulder, Colorado. www. cmdl.noa.gov

Noack, M., 1995. Estimating groundwater velocityfor a shallow unconfined aquifer using 3H/3He dating technique: a comparison of other hydrogeologic methods. Unpublished MSc. thesis, Trent University: 138 pp.

Oster, H., Sonntag, C. and Munnich, K.O., 1996. Groundwater Age Dating With Chlorofluorocarbons. Water Resour. Res., 32(10): 2989-3001.

Poreda, R.J., Cerling, T.E. and Solomon, D.K., 1988. Tritium and helium isotopes as hydrologic tracers in a shallow unconfined aquifer. J. Hydrol., 103: 1-9.

Plummer, L.N., Michel, R.L., Thurman, E.M. and Glynn, P.D., 1993. Environmental Tracers for Age Dating Young Ground Water. In: W.M. Alley (Editor), Regional ground-water quality. Van Nostrand Reinhold, New York, pp. 255-294.

Rasmussen, R.A. and Kahil, M.A.K., 1986. Atmospheric trace gases: Trends and distributions over the last decade. Science, 232: 1623-1624.

Reilly, T.E., Plummer, I.N., Phillips, P.J. and Busenberg, E., 1994. The use of simulation and multiple environmental tracers to quantify groundwater flow in a shallow aquifer. Water Resour. Res., 30(2): 421-433.

Render, F.W., 1970. Geohydrology of the metropolitoan Winnipeg area as related to groundwater supply and construction. Canadian Geotechnical Journal ., 7: 243-274.

Render, F.W., 1971. Electric analog and digital modelling of the upper carbonate aquifer in the metropolitan Winnipeg area. The Geological Association of Canada, special paper number 9.

Render, F.W. and Betcher, R., 1998. Manitoba Water Resources Branch, Winnipeg, Manitoba, personal communication.

Robertson, W.D. and Cherry, J.A., 1989. Tritium as an indicator of recharge and dispersion in a groundwater system in central Ontario. Water Resour. Res., 25(6): 1097-1109.

Russell, A.D. and Thompson, G.M., 1983. Mechanisms leading to enrichment of the atmospheric fluorocarbons CCL3F and CCl2F2 in groundwater. Water Resour. Res., 19(1): 57-60.

Schlosser, P., Stute, M., Dörr, H., Sonntag, C. and Münnich, K.O., 1988. Tritium/^{3}He dating of shallow groundwater. Earth and Planetary Sciences Letters, 89: 353-362.

Schlosser, P., Stute, M., Sonntag, C. and Münnich, K.O., 1989. Tritiogenic ^{3}He in shallow groundwater. Earth and Planetary Science Letters, 94: 245-256.

Semprini, L., Hopkins, G.D., Roberts, P.V. and McCarty, P.L., 1991. In situ biotransformation of carbon tetrachloride, freon-113, freon-11 and 1,1,1-TCA under anoxic conditions. In On-Site Bioreclamation Processes for Xenobiotic and Hydrocarbon Treatment, Reed Publishers: 41-58.

Smethie, W. (1998). Lamont-Doherty Earth Observatory Of Columbia University, Palisades, New York, personal communication (CFC-113 data obtained via the University of Waterloo CFC Laboratory, Waterloo, Ontario from W. Smethie).

Solomon, D.K. and Sudicky, E.A., 1991. Tritium and helium 3 isotope ratios for direct estimation of spatial variations in groundwater recharge. Water Resour. Res., 27(9): 2309-2319.

Solomon, D.K., Poreda, R.J., Schiff, S.L. and Cherry, J.A., 1992. Tritium and helium 3 as groundwater age tracers in the Borden aquifer. Water Resour. Res., 28(3): 741-755.

Solomon, D.K., Schiff, S.L., Poreda, R.J. and Clarke, W.B., 1993. A validation of the $^{3}H/^{3}He$ method for determining groundwater recharge. Water Resour. Res., 29(9): 2951-2962.

Solomon, D.K., Poreda, R.J., Cook, P.G. and Hunt, A., 1995. Site characterization using 3H/3He ground water ages, Cape Cod, Massachusetts. Ground Water, 33(6): 998-996.

Szabo, Z., Rice, D.E., Plummer, L.N., Busenberg, E., Drenkard, S., and Schlosser, P., 1996 Age dating of shallow groundwater with chlorofluorcarbons, tritium/helium-3, and flow path analysis, Southern New Jersey Coastal Plain. Water Resour. Res., 32(4): 1032-1038.

Teller, J.T. and Fenton, M.M., 1980. Late Wisconsinan glacial stratigraphy and history of southeastern Manitoba. Can. J. Earth Sci., 17 : 19-35.

Thompson, G.M. and Hayes, J.M., 1979. Trichlorofluoromethane in groundwater a possible tracer and indicator of groundwater age. Water Resour. Res., 15(3): 546-554.

Thornthwaite, C.W. and Mather, J.R., 1957. Instructions and tables for computing potential evapotranspiration and the water balance. Publications in Climatology: Vol X, No 3 Drexel Institute of Technology, Laboratory of Climatology.

von Buttlar, H., 1959. Groundwater studies in New Mexico using tritium as a tracer. II J Geophys. Res. 64: 1031-1038.

Warner, M.J. and Weiss, R.F., 1985. Solubilities of chlorofluorocarbons 11 and 12 in water and seawater. Deep-Sea Research, 32(12): 1485-1497.

Weeks, E.P., Earp, D.E., and Thompson, G.M., 1982. Use of atmospheric fluorocarbons F-11 and F-12 to determine the diffusion parameters of the unsaturated zone in the southern high plains of Texas. Water Resour. Res., 18: 1365-1378.

Weiss, R.F., 1970. Helium isotope effect in solution in water and seawater. Science, 168 247-248.

Weiss, R.F., 1971. Solubility of helium and neon in solution in water and seawater. J Chem. Eng. Data, 16(2): 247-248.

Appendix I: Site Instrumentation

I.1 Piezometer Nest Installation

The Geological Survey of Canada in collaboration with the Manitoba Water Resources Branch installed the piezometer nests used in this study. The piezometers are constructed of 5 cm (2 inch) nominal polyvinyl chloride (PVC) tubing in 6 meter sections with a 24 cm screen at the base. The piezometers were installed using a solid stem auger and PVC drive points. The hole was drilled, the auger was removed and as the aquifer material collapsed into the hole the PVC tubing was driven into the hole to the required depth. The hole was then backfilled with aquifer material, sealed with 1 meter of bentonite at the water table, and backfilled again with aquifer material to within 0.5 meters of the surface. Protective steel casing was installed around each piezometer and cemented in at the surface. At each piezometer nest three piezometers were installed approximately 3, 6 and 9 meters below the water table.

Three previously installed provincial wells were also used in this study. These wells are all constructed of 12 to 20 cm diameter black iron tubes with the exception of a 1.5 meter stainless steel screening at the base of the well.

I.2 Drilling Logs from Piezometer Nest Installation

Drilling logs from the instrumentation of the 5 piezometer nests and one single piezometer in July, 1998.

Piezometer Nest # **9801**

Depth b.g.s. (m)		Sediment type
start	finish	
0.00	1.83	fine-medium sand
1.83	3.81	fine sand
3.81	4.57	coarse to medium sand
4.57	6.10	coarse to medium sand
6.10	7.62	medium to coarse sand
7.62	8.38	coarse sand
8.38	9.14	coarse sand
9.14	16.76	coarse sand

Piezometer Nest # **9802**

Depth b.g.s. (m)		Sediment type
start	finish	
0.00	1.52	medium sand
1.52	3.96	medium to fine sand
3.96	5.33	silty sandy till
5.33	6.10	silty sand
6.10	9.45	fine sand
9.45	10.67	medium sand

Piezometer Nest # **9803**

Depth b.g.s. (m)		Sediment type
start	finish	
0.00	3.05	medium to coarse sand
3.05	4.57	medium to coarse sand, some gravel
4.57	6.10	medium sand
6.10	22.86	very fine sand
22.86	25.15	fine sand
25.15	27.43	medium sand

Piezometer Nest # **9804**

Depth b.g.s. (m)		Sediment type
start	finish	
0.00	1.52	medium sand
1.52	3.51	medium sand, some gravel
3.51	6.86	sandy, clayey till
6.86	9.91	clayey till
9.91	12.19	silty sandy till

Piezometer Nest # **9805**

Depth b.g.s. (m)		Sediment type
start	finish	
0.00	4.57	medium sand
4.57	21.64	fine sand

Piezometer Nest # **9806**

Depth b.g.s. (m)		Sediment type
start	finish	
0.00	0.76	fine to medium sand
0.76	1.52	fine sand
1.52	2.29	clayey silty sand
2.29	2.90	silty sand
2.90	5.33	fine to medium sand
5.33	6.10	fine sand
6.10	12.19	fine to medium sand
12.19	13.72	medium coarse sand, some gravel

Appendix II: Physical Hydrogeology Data

II.1 Piezometric Data

Table 1. Piezometric data collected during the two periods of field work in July and September, 1998.

Piezometer #	Elevation of Piezometer Screen m.a.s.l.	Hydraulic Head m.a.s.l	
		July 1998 Measurement	September 1998 Measurement
9801-1	369.8	371.509	371.642
9801-2	366.5	371.509	371.645
9801-3	363.5	371.510	371.642
9802-1	359.5	360.900	360.627
9802-2	356.5	Dry, perched water table	Dry , perched water table
9802-3	353.4	353.877	353.975
9803-1	365.5	366.805	366.808
9803-2	362.9	366.815	366.861
9803-3	359.4	366.796	366.822
9803-4	317.18	----------	366.110
9804-1	380.4	381.605	381.897
9804-2	378.6	381.610	381.906
9804-3	371.5	380.659	NA
9805-1	366.0	367.786	367.884
9806-1	374.8	376.652	376.633
9806-2	371.6	376.649	376.631
9806-3	368.4	376.655	376.639

II.2 Hydraulic Conductivity

The range of hydraulic conductivities of the sediments present at the piezometer nests is presented in Table 2. Hydraulic conductivities were determined using the Hvorslev method on groundwater bail tests performed at each piezometer.

Table 2. Hydraulic conductivities determined for each piezometer.

Piezometer #	Depth b.g.s (m)	Geologic Unit	# of bail tests	*$K_{average}$ (m/s)
9801-1	10.16	Coarse sand	2	$8.37 * 10^{-5}$
9801-2	13.41	Coarse sand	3	$9.34 * 10^{-5}$
9801-3	16.15	Coarse sand	2	$5.47 * 10^{-5}$
9802-1	4.23	Silty, sandy till	1	$6.83 * 10^{-6}$
9802-3	10.42	Medium sand	2	$2.44 * 10^{-5}$
9803-1	21.03	Very fine sand	1	$8.15 * 10^{-6}$
9803-2	23.71	Fine sand with pebbles	2	$2.67 * 10^{-5}$
9803-3	27.03	Medium sand	2	$9.27 * 10^{-5}$
9804-1	3.32	Medium sand	3	$1.08 * 10^{-4}$
9804-2	5.10	Sandy,clayey till	1	$3.47 * 10^{-8}$
9804-3	12.16	Clayey till	1	$8.31 * 10^{-7}$
9805-1	21.70	Fine sand	2	$5.54 * 10^{-5}$
9806-1	7.01	Medium sand	3	$1.25 * 10^{-4}$
9806-2	10.31	Medium sand	2	$9.73 * 10^{-5}$
9806-3	13.51	Coarse sand & gravel	3	$2.43 * 10^{-4}$

*Hydraulic conductivity value is an average of the number of bail tests performed at each piezometer.

II.3 Grain Size Analysis

Grain size analyses were performed on selected sediment samples obtained at the piezometer nests during site instrumentation. Analyses were performed by undergraduate students in the Department of Earth Sciences at the University of Ottawa.

Table 3. Grain Size Analysis of Selected Sediment Samples from Piezometer Nests

Site	Depth b.g.s.(m)	Geologic Unit	Grain Size		
			% Sand	% Silt	% Clay
9805	0 - .76	Medium sand	98	2	0
9805	.76 – 1.52	Medium sand	98	2	0
9805	3.05 – 3.81	Medium to fine sand	54	45	0
9805	3.81 – 4.57	Medium to fine sand	85	15	0
9805	6.10 – 6.86	Fine sand	85	15	0
9805	6.86 – 7.62	Fine sand	96	4	0
9805	7.62 – 8.38	Fine sand	84	16	0
9802	3.05 – 3.81	Medium sand	93	7	0
9802	3.81 – 4.57	Sandy, silty till	37	46	17
9802	5.33 – 6.10	Sandy,silty till	68	28	4

Appendix III: CFC and ^{3}He Sampling and CFC Data

III.1 CFC Atmospheric Curves

Concentrations of CFC-11, CFC-12, and CFC-113 in the atmosphere have been increasing steadily from 1945 through to the mid-1990s. Prior to 1975, measurements of atmospheric CFC concentrations were not made on a regular basis and the atmospheric curves were reconstructed based on the methods of McCarthy et al (1977). The method used to estimate atmospheric CFC concentrations from CFC manufacturing data, estimates of CFC releases to the atmosphere, rates of photolysis in the stratosphere, and CFC removal by soils and the hydrosphere is described in detail (McCarthy et al., 1977). Groundwater ages determined in this time period are less accurate due to the limitations on the reconstruction method.

Measured atmospheric CFC data was obtained from the National Oceanic and Atmospheric Administration's monitoring station at Niwot Ridge, Colorado. CFC monitoring stations located in Canada are limited to the Alert, NWT station where CFC data was only collected from 1988-1993 and therefore the more comprehensive data set from Niwot Ridge was used for this study. Studies have indicated that spatial variations in global atmospheric CFC concentrations are less than 10% and as a result it is generally not necessary to apply a latitudinal correction to data obtained from monitoring stations (Kahil and Rasmussen, 1989). Atmospheric CFC data from Alert, NWT was compared to the Niwot Ridge, Colorado data and did not vary significantly. CFC groundwater studies in Canada have been limited however a study by Cook et al. (1995) in Sturgeon Falls, Ontario (at similar latitude to the

Sandilands Provincial Forest) indicated that local atmospheric values did not differ significantly from Niwot Ridge data.

III.3 CFC Groundwater Age Sensitivity Analysis: Atmospheric Pressure

Assumptions made in the calculation of the equivalent CFC atmospheric concentration from dissolved CFC concentrations in groundwater using Henry's Law may have resulted in some error in the groundwater ages. The extended form of Henry's Law is:

$$C = K * x * (P - p_{H2O}) \quad (1)$$

Where C is the dissolved concentration of the *i*th CFC in groundwater in pmoles/kg, K is the Henry's Law constant, x is the concentration of the *i*th CFC in air in pptv, P is the total atmospheric pressure and p_{H2O} is the water vapour pressure. If the total atmospheric pressure minus the water vapour pressure is equal to the barometric pressure in the Sandilands then the assumption that the P- p_{H2O} term may cause errors in the calculated equivalent CFC concentration in the atmosphere. Barometric data from the Sandilands was not available. It was possible, however, to use an estimate of 0.9659 atm based on the relationship between atmospheric pressure and altitude (maximum of 296 meters above sea level in the Sandilands).

Below is a series of calculations examining the validity of the 1 atm assumption. Overall, the calculated CFC concentrations using the atmospheric pressure in the Sandilands (0.9659) increase by 3.5 % over the CFC concentrations calculated using 1 atm, resulting in younger groundwater age estimates.

CFC-12

Young Groundwater in Piezometer 9801-1:

Using a pressure of 1 atm

Calculated CFC (pptv)	Estimated Groundwater Age (yrs)
339.98	17.0

Using a pressure of 0.9659 atm

Calculated CFC (pptv)	Estimated Groundwater Age (yrs)
351.98	16.4

Age Difference: 0.65 yrs or of approximately 3.8 %

Old Groundwater in Woodridge # 1:

Using a pressure of 1 atm

Calculated CFC (pptv)	Estimated Groundwater Age (yrs)
15.8	42.8

Using a pressure of 0.9659 atm

Calculated CFC (pptv)	Estimated Groundwater Age (yrs)
16.4	42.7

Age Difference: 0.3 yrs or of approximately 0.7 %

CFC-11

Young Groundwater in Piezometer 9802-1:

Using a pressure of 1 atm

Calculated CFC (pptv)	Estimated Groundwater Age (yrs)
254.5	10.7

Using a pressure of 0.9659 atm

Calculated CFC (pptv)	Estimated Groundwater Age (yrs)
263.4	9.6

Age Difference: 1.1 yrs or of approximately 10 %

Old Groundwater in Woodridge # 1:

Using a pressure of 1 atm

Calculated CFC (pptv)	Estimated Groundwater Age (yrs)
9.8	39.7

Using a pressure of 0.9659 atm

Calculated CFC (pptv)	Estimated Groundwater Age (yrs)
10.1	39.3

Age Difference: 0.4 yrs or of approximately 1 %

CFC-113

Young Groundwater in Piezometer 9803-2:

Using a pressure of 1 atm

Calculated CFC (pptv)	Estimated Groundwater Age (yrs)
82.0	7.5

Using a pressure of 0.9659 atm

Calculated CFC (pptv)	Estimated Groundwater Age (yrs)
84.85	5.2

Age Difference: 2.3 yrs or of approximately 30 %

Old Groundwater in Woodridge # 1:

Using a pressure of 1 atm

Calculated CFC (pptv)	Estimated Groundwater Age (yrs)
11.7	23.3

Using a pressure of 0.9659 atm

Calculated CFC (pptv)	Estimated Groundwater Age (yrs)
12.4	23.2

Age Difference: 0.1 yrs or of approximately 0.4%

Results of this sensitivity analysis indicate that uncertainty in the atmospheric pressure at the study site results in a 10 % or less difference in groundwater ages with the exception of young CFC-11 groundwater. In general, older groundwater was used to calculate groundwater recharge rates in this study and the error associated with this groundwater is on the order of 0.5 years, or less than 1 %, and would result in very minimal changes in the values determined in section 5.4

III.4 CFC and ^{3}He Sampling Methods

CFC samples were collected using a down hole stainless steel and copper tube sampling apparatus adapted from a design used by Dr. K. Solomon of the Department of Geology and Geophysics at the University of Utah (Figure 1). The equipment consists of two 1 p.s.i *Swagelock* stainless steel check valves placed in series to reduce leaking and atmospheric contamination of the sample. One sample was collected in each section of 55 cm 3/8 inch diameter copper tubing. The copper tubes were connected to 1 inch diameter stainless steel tubing to increase the amount of "clean flushing" through the system and to eliminate any plastics from coming into contact with the well water. Above this polyethylene tubing was used in order to lower the metal sampling equipment down to the water table. All connections were made with stainless steel *Swagelock* adapters and connectors.

CFC samples were collected by pressurizing the entire apparatus to 20 p.s.i and lowering it down the piezometer to within 50 cm of the bottom. The pressure was then slowly released to allow the check valves to open and the water to rise statically (for approximately 6 to 7 minutes) into the copper and stainless steel tubing. The system was then repressurized to 20 p.s.i. and brought to the surface where the pressure was released. Each

copper tube was sealed off from the atmosphere by cold welding it at the ends using a *Team Co.* 3/8 inch copper tube crimper. Samples collected from shallow piezometers were lowered to within 25 cm of the bottom of the well and pumped under low vacuum for 8 minutes to increase the volume of water flushed through the system. Quadruplicate samples were collected at each piezometer by repeating the sampling procedure twice.

^{3}He samples were collected as above with the exception that the pressure was not released after sample collection at the surface prior to sealing the copper tubes. In addition, the copper tubes were sealed using stainless steel refrigeration clamps.

Dissolved CFC and ^{3}He concentrations indicated that the sampling method described above had its limitations. Pumping on the shallow samples may have stripped the dissolved gases in the copper tubes and is not recommended. In addition, the 1 p.s.i check valves may have closed before hydraulic equilibrium was achieved in the copper tubes. This may have resulted in incomplete dissolved gas sampling and was observed in the ^{3}He samples. It is uncertain how this may have affected the dissolved CFC concentrations however it is recommended that the sampling apparatus be modified to eliminate this concern.

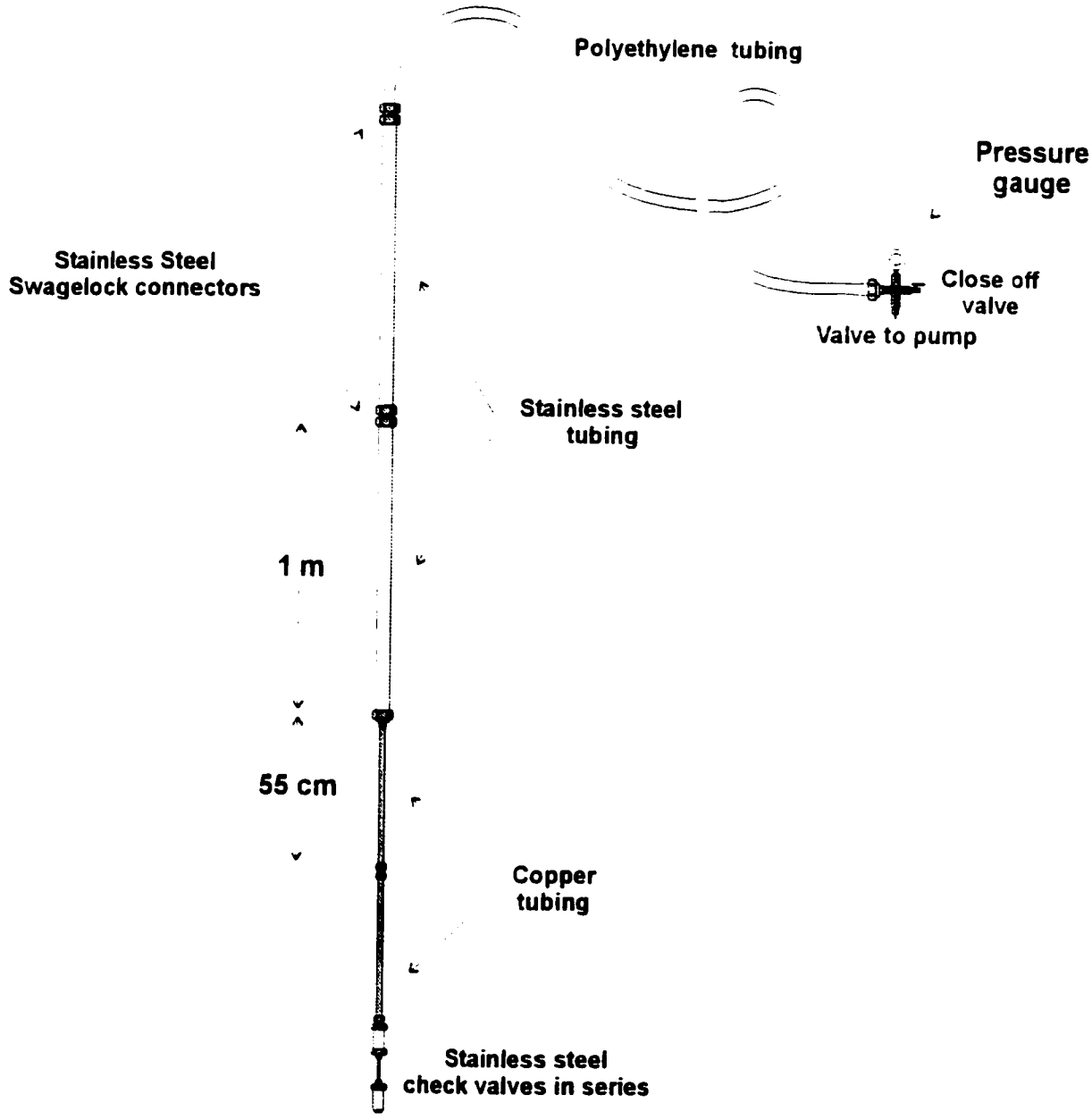

Figure 1. Schematic of CFC and ^{3}He sampling apparatus

III.5 CFC Quadruplicate Data

Analytical results for each CFC sample submitted. Tables contain the measured dissolved CFC concentrations in pg/kg, the constants used to calculate the equilibrium CFC partial pressure, and the calculated partial pressures in pptv. Data that was not used to calculate the average CFC concentrations present in the body of the thesis are indicated. In general, data was not removed from the sample set unless the calculated partial pressure in pptv was above the highest atmospheric concentration.

Table 1

Quadruplicate CFC-11 Data

Sample i.d. (piezometer #, sample #)	Weight (g)	Sample Weight (g)	CFC-11 10^{-3} pmole	Recharge Temp (°C)	Solubility Constants a1	a2	a3	Henry's Law Constant K_{11} (moles/(kg*atm))	Dissolved CFC-11 Concentration (pmoles/kg)	Dissolved CFC-11 Concentration (pg/kg)	CFC-11 Partial Pressure (pptv)	Sample Used to Calculate Avg. CFC conc
9801-1 U	48.92	19.39	167.46	3	-136.2685	206.115	57.2805	0.032	8.64	1187.51	268.33	yes
V	49.04	19.51	168.15	3	-136.2685	206.115	57.2805	0.032	8.62	1185.07	267.78	yes
S	49.13	19.60	164.87	3	-136.2685	206.115	57.2805	0.032	8.41	1156.61	261.35	yes
W	48.91	19.38	162.19	3	-136.2685	206.115	57.2805	0.032	8.37	1150.73	260.02	yes
9801-2 M	49.07	19.54	176.86	3	-136.2685	206.115	57.2805	0.032	9.05	1244.54	281.22	yes
N	49.41	19.88	180.95	3	-136.2685	206.115	57.2805	0.032	9.10	1251.54	282.80	yes
O	49.23	19.70	176.41	3	-136.2685	206.115	57.2805	0.032	8.95	1231.29	278.22	yes
P	49.30	19.77	173.52	3	-136.2685	206.115	57.2805	0.032	8.78	1206.83	272.70	yes
9801-3 M	48.46	18.93	193.6	3	-136.2685	206.115	57.2805	0.032	10.23	1406.23	317.75	no
N	48.76	19.23	151.74	3	-136.2685	206.115	57.2805	0.032	7.89	1084.98	245.16	yes
O	49.23	19.70	153.11	3	-136.2685	206.115	57.2805	0.032	7.77	1068.66	241.48	yes
P	49.30	19.77	154.12	3	-136.2685	206.115	57.2805	0.032	7.80	1071.90	242.21	yes
9802-1 C	50.71	21.18	171.95	3	-136.2685	206.115	57.2805	0.032	8.12	1116.29	252.24	yes
D	50.65	21.12	170.24	3	-136.2685	206.115	57.2805	0.032	8.06	1108.33	250.44	yes
E	50.89	21.36	178.97	3	-136.2685	206.115	57.2805	0.032	8.38	1152.08	260.32	yes
F	50.77	21.24	174.21	3	-136.2685	206.115	57.2805	0.032	8.20	1127.77	254.83	yes
9802-3 C	50.38	20.85	131.82	3	-136.2685	206.115	57.2805	0.032	6.32	869.32	196.43	yes
D	50.63	21.10	133.06	3	-136.2685	206.115	57.2805	0.032	6.31	867.10	195.93	yes
E	50.78	21.25	134.37	3	-136.2685	206.115	57.2805	0.032	6.32	869.45	196.46	yes
9803-1 A	50.39	20.86	154.72	3	-136.2685	206.115	57.2805	0.032	7.42	1019.85	230.45	yes
B	49.18	19.65	143.22	3	-136.2685	206.115	57.2805	0.032	7.29	1002.18	226.45	yes
C	49.67	20.14	150.31	3	-136.2685	206.115	57.2805	0.032	7.46	1026.20	231.88	yes
D	49.52	19.99	147.02	3	-136.2685	206.115	57.2805	0.032	7.35	1011.27	228.51	yes
9803-2 A	49.15	19.62	157.19	3	-136.2685	206.115	57.2805	0.032	8.01	1101.61	248.92	yes
B	49.21	19.68	161.11	3	-136.2685	206.115	57.2805	0.032	8.19	1125.64	254.35	yes
C	49.46	19.93	160.87	3	-136.2685	206.115	57.2805	0.032	8.07	1109.87	250.79	yes
D	49.34	19.81	153.72	3	-136.2685	206.115	57.2805	0.032	7.76	1066.96	241.09	yes
9803-3 A	49.81	20.28	194.68	3	-136.2685	206.115	57.2805	0.032	9.60	1319.95	298.26	no
C	49.37	19.84	177.25	3	-136.2685	206.115	57.2805	0.032	8.93	1228.42	277.58	
E	49.26	19.73	176.02	3	-136.2685	206.115	57.2805	0.032	8.92	1226.70	277.19	yes
G	49.38	19.85	171.45	3	-136.2685	206.115	57.2805	0.032	8.64	1187.63	268.36	yes

Table 1 (cont.)
Quadruplicate CFC-11 Data

Sample i.d. (piezometer #, sample #)	Weight (g)	Sample Weight (g)	CFC-11 10^{-3} pmoles	Recharge Temp (°C)	Solubility Constants a1	a2	a3	Henry's Law Constant K_{11} (moles/(kg*atm))	Dissolved CFC-11 Concentration (pmoles/kg)	Dissolved CFC-11 Concentration (pg/kg)	CFC-11 Partial Pressure (pptv)	Sample Used to Calculate Avg. CFC conc
9804-1 A	49.80	20.27	169.7	3	-136.2685	206.115	57.2805	0.032	8.37	1151.15	260.11	yes
B	49.58	20.05	173.48	3	-136.2685	206.115	57.2805	0.032	8.65	1189.70	268.83	yes
C	52.86	23.33	217.98	3	-136.2685	206.115	57.2805	0.032	9.34	1284.71	290.29	yes
D	49.43	19.90	168.05	3	-136.2685	206.115	57.2805	0.032	8.44	1161.15	262.37	yes
9804-2 A	49.40	19.87	8.32	3	-136.2685	206.115	57.2805	0.032	0.42	57.57	13.01	yes
B	49.47	19.94	7.8	3	-136.2685	206.115	57.2805	0.032	0.39	53.79	12.15	yes
C	50.95	21.42	8.4	3	-136.2685	206.115	57.2805	0.032	0.39	53.92	12.18	yes
D	49.20	19.67	6.58	3	-136.2685	206.115	57.2805	0.032	0.33	46.00	10.39	yes
9804-3 A	49.69	20.16	19.56	3	-136.2685	206.115	57.2805	0.032	0.97	133.41	30.14	yes
B	49.60	20.07	19.19	3	-136.2685	206.115	57.2805	0.032	0.96	131.47	29.71	yes
C	49.82	20.29	18.17	3	-136.2685	206.115	57.2805	0.032	0.90	123.13	27.82	yes
D	49.92	20.39	20.46	3	-136.2685	206.115	57.2805	0.032	1.00	137.97	31.18	yes
9805-1 A	49.88	20.35	64.58	3	-136.2685	206.115	57.2805	0.032	3.17	436.35	98.60	yes
B	49.09	19.56	63.38	3	-136.2685	206.115	57.2805	0.032	3.24	445.54	100.67	yes
C	49.84	20.31	64.64	3	-136.2685	206.115	57.2805	0.032	3.18	437.62	98.88	yes
D	49.13	19.60	67.78	3	-136.2685	206.115	57.2805	0.032	3.46	475.50	107.44	yes
9806-1 A	49.95	20.42	191.67	3	-136.2685	206.115	57.2805	0.032	9.39	1290.63	291.63	yes
B	50.39	20.86	172.86	3	-136.2685	206.115	57.2805	0.032	8.29	1139.42	257.46	yes
C	50.34	20.81	174.28	3	-136.2685	206.115	57.2805	0.032	8.37	1151.54	260.20	yes
D	50.29	20.76	175.04	3	-136.2685	206.115	57.2805	0.032	8.43	1159.34	261.97	yes
9806-2 A	50.36	20.83	68.94	3	-136.2685	206.115	57.2805	0.032	3.31	455.08	102.83	yes
B	49.47	19.94	63.97	3	-136.2685	206.115	57.2805	0.032	3.21	441.12	99.68	yes
C	50.30	20.77	68.14	3	-136.2685	206.115	57.2805	0.032	3.28	451.10	101.93	yes
D	50.64	21.11	70.36	3	-136.2685	206.115	57.2805	0.032	3.33	458.29	103.56	yes
9806-3 A	50.67	21.14	25.53	3	-136.2685	206.115	57.2805	0.032	1.21	166.05	37.52	yes
B	50.55	21.02	25.5	3	-136.2685	206.115	57.2805	0.032	1.21	166.81	37.69	yes
E	50.75	21.22	23.95	3	-136.2685	206.115	57.2805	0.032	1.13	155.19	35.07	yes
F	51.14	21.61	24.31	3	-136.2685	206.115	57.2805	0.032	1.12	154.68	34.95	yes
Woodridge #1 A	45.17	15.64	5.17	3	-136.2685	206.115	57.2805	0.032	0.33	45.45	10.27	yes
C	48.92	19.39	5.99	3	-136.2685	206.115	57.2805	0.032	0.31	42.48	9.60	yes
G	49.02	19.49	6.6	3	-136.2685	206.115	57.2805	0.032	0.34	46.56	10.52	yes
E	49.17	19.64	5.46	3	-136.2685	206.115	57.2805	0.032	0.28	38.23	8.64	yes
Woodridge #2 A	49.26	19.73	17.51	3	-136.2685	206.115	57.2805	0.032	0.89	122.03	27.57	yes
B	49.25	19.72	18.5	3	-136.2685	206.115	57.2805	0.032	0.94	128.99	29.15	yes
C					Sample Lost During Analysis							
D	48.88	19.35	19.45	3	-136.2685	206.115	57.2805	0.032	1.01	138.21	31.23	yes
Sandilands #1 A	49.44	19.91	83.27	3	-136.2685	206.115	57.2805	0.032	4.18	575.07	129.94	yes
B	49.99	20.46	88.48	3	-136.2685	206.115	57.2805	0.032	4.32	594.62	134.36	yes
C					Sample Lost During Analysis							
D	49.17	19.64	172.22	3	-136.2685	206.115	57.2805	0.032	8.77	1205.72	272.44	no

Table 2

Quadruplicate CFC-12 Data

Sample I.d (piezometer #, sample #)	Weight (g)	Sample Weight (g)	CFC-12 10^{-3} pmoles	Recharge Temp (°C)	Solubility Constants a1	a2	a3	Henry's Law Constant K_{12} moles/(kg*atm)	Dissolved CFC-12 (pmoles/kg)	Dissolved CFC-12 (pg/kg)	Partial Pressure CFC-12 (pptv)	Sample Used to calculate Avg CFC conc.
9801-1 U	48.92	19.39	53.67	3	-124.4395	185.4299	51.6383	0.008	2.77	334.92	346.56	yes
V	49.04	19.51	54.32	3	-124.4395	185.4299	51.6383	0.008	2.78	336.89	348.60	yes
S	49.13	19.60	52.92	3	-124.4395	185.4299	51.6383	0.008	2.70	326.70	338.06	yes
W	48.91	19.38	50.57	3	-124.4395	185.4299	51.6383	0.008	2.61	315.74	326.71	yes
9801-2 M	49.07	19.54	53.01	3	-124.4395	185.4299	51.6383	0.008	2.71	328.26	339.67	yes
N	49.41	19.88	53.89	3	-124.4395	185.4299	51.6383	0.008	2.71	328.00	339.41	yes
O	49.23	19.70	53.09	3	-124.4395	185.4299	51.6383	0.008	2.69	326.09	337.42	yes
P	49.30	19.77	52.53	3	-124.4395	185.4299	51.6383	0.008	2.66	321.50	332.68	yes
9801-3 M	48.46	18.93	43.71	3	-124.4395	185.4299	51.6383	0.008	2.31	279.39	289.11	yes
N	48.76	19.23	46.50	3	-124.4395	185.4299	51.6383	0.008	2.42	292.59	302.76	yes
O	49.23	19.70	45.43	3	-124.4395	185.4299	51.6383	0.008	2.31	279.04	288.74	yes
P	49.30	19.77	47.45	3	-124.4395	185.4299	51.6383	0.008	2.40	290.41	300.51	yes
9802-1 C	50.71	21.18	56.13	3	-124.4395	185.4299	51.6383	0.008	2.65	320.67	331.82	yes
D	50.65	21.12	56.08	3	-124.4395	185.4299	51.6383	0.008	2.66	321.29	332.46	yes
E	50.89	21.36	56.32	3	-124.4395	185.4299	51.6383	0.008	2.64	319.04	330.13	yes
F	50.77	21.24	55.81	3	-124.4395	185.4299	51.6383	0.008	2.63	317.94	328.99	yes
9802-3 C	50.38	20.85	41.57	3	-124.4395	185.4299	51.6383	0.008	1.99	241.25	249.63	yes
D	50.63	21.10	42.45	3	-124.4395	185.4299	51.6383	0.008	2.01	243.43	251.90	yes
E	50.78	21.25	43.10	3	-124.4395	185.4299	51.6383	0.008	2.03	245.42	253.95	yes
9803-1 A	50.39	20.86	46.91	3	-124.4395	185.4299	51.6383	0.008	2.25	272.10	281.57	yes
B	49.18	19.65	44.39	3	-124.4395	185.4299	51.6383	0.008	2.26	273.34	282.85	yes
C	49.67	20.14	45.85	3	-124.4395	185.4299	51.6383	0.008	2.28	275.46	285.04	yes
D	49.52	19.99	45.38	3	-124.4395	185.4299	51.6383	0.008	2.27	274.69	284.24	yes
9803-2 A	49.15	19.62	46.77	3	-124.4395	185.4299	51.6383	0.008	2.38	288.44	298.47	yes
B	49.21	19.68	44.39	3	-124.4395	185.4299	51.6383	0.008	2.26	272.93	282.42	yes
C	49.46	19.93	44.27	3	-124.4395	185.4299	51.6383	0.008	2.22	268.77	278.12	yes
D	49.34	19.81	45.20	3	-124.4395	185.4299	51.6383	0.008	2.28	276.08	285.68	yes
9803-3 A	49.81	20.28	53.75	3	-124.4395	185.4299	51.6383	0.008	2.65	320.70	331.85	yes
C	49.37	19.84	51.58	3	-124.4395	185.4299	51.6383	0.008	2.60	314.58	325.51	yes
E	49.26	19.73	52.31	3	-124.4395	185.4299	51.6383	0.008	2.65	320.81	331.96	yes
G	49.38	19.85	48.94	3	-124.4395	185.4299	51.6383	0.008	2.47	298.32	308.70	yes

Sample i.d (piezometer #,	Weight (g)	Sample Weight	CFC-12 10^{-3}	Recharge Temp	Solubility Constants a1	a2	a3	Henry's Law Constant K_{12}	Dissolved CFC-12	Dissolved CFC-12	Partial Pressure CFC-12	Sample Used to calculate

Table 2 (cont.)
Quadruplicate CFC-12 Data

Sample i.d (piezometer #, sample #)	Weight (g)	Sample Weight (g)	CFC-12 10^{-3} pmoles	Recharge Temp (°C)	Solubility Constants a1	a2	a3	Henry's Law Constant K_{12} moles/(kg*atm)	Dissolved CFC-12 (pmoles/kg)	Dissolved CFC-12 (pg/kg)	Partial Pressure CFC-12 (pptv)	Sample Used to calculate Avg CFC conc.
9804-1 A	49.80	20.27	46.76	3	-124.4395	185.4299	51.6383	0.008	2.31	279.13	288.83	yes
B	49.58	20.05	47.43	3	-124.4395	185.4299	51.6383	0.008	2.37	286.24	296.19	yes
C	52.86	23.33	55.03	3	-124.4395	185.4299	51.6383	0.008	2.36	285.41	295.33	yes
D	49.43	19.90	46.57	3	-124.4395	185.4299	51.6383	0.008	2.34	283.16	293.01	yes
9804-2 A	49.40	19.87	10.58	3	-124.4395	185.4299	51.6383	0.008	0.53	64.43	66.67	yes
B	49.47	19.94	10.27	3	-124.4395	185.4299	51.6383	0.008	0.52	62.32	64.49	yes
C	50.95	21.42	10.75	3	-124.4395	185.4299	51.6383	0.008	0.50	60.73	62.84	yes
D	49.20	19.67	9.70	3	-124.4395	185.4299	51.6383	0.008	0.49	59.67	61.74	yes
9804-3 A	49.69	20.16	11.13	3	-124.4395	185.4299	51.6383	0.008	0.55	66.80	69.12	yes
B	49.60	20.07	9.81	3	-124.4395	185.4299	51.6383	0.008	0.49	59.14	61.20	yes
C	49.82	20.29	10.38	3	-124.4395	185.4299	51.6383	0.008	0.51	61.90	64.05	yes
D	49.92	20.39	10.48	3	-124.4395	185.4299	51.6383	0.008	0.51	62.19	64.35	yes
9805-1 A	49.88	20.35	28.57	3	-124.4395	185.4299	51.6383	0.008	1.40	169.88	175.78	yes
B	49.09	19.56	28.34	3	-124.4395	185.4299	51.6383	0.008	1.45	175.31	181.41	yes
C	49.84	20.31	27.50	3	-124.4395	185.4299	51.6383	0.008	1.35	163.84	169.53	yes
D	49.13	19.60	27.77	3	-124.4395	185.4299	51.6383	0.008	1.42	171.44	177.40	yes
9806-1 A	49.95	20.42	57.16	3	-124.4395	185.4299	51.6383	0.008	2.80	338.71	350.48	yes
B	50.39	20.86	50.56	3	-124.4395	185.4299	51.6383	0.008	2.42	293.28	303.47	yes
C	50.34	20.81	51.62	3	-124.4395	185.4299	51.6383	0.008	2.48	300.15	310.58	yes
D	50.29	20.76	49.27	3	-124.4395	185.4299	51.6383	0.008	2.37	287.17	297.16	yes
9806-2 A	50.36	20.83	29.41	3	-124.4395	185.4299	51.6383	0.008	1.41	170.84	176.78	yes
B	49.47	19.94	25.46	3	-124.4395	185.4299	51.6383	0.008	1.28	154.50	159.87	yes
C	50.30	20.77	29.35	3	-124.4395	185.4299	51.6383	0.008	1.41	170.98	176.93	yes
D	50.64	21.11	29.46	3	-124.4395	185.4299	51.6383	0.008	1.40	168.86	174.73	yes
9806-3 A	50.67	21.14	19.21	3	-124.4395	185.4299	51.6383	0.008	0.91	109.95	113.78	yes
B	50.55	21.02	16.70	3	-124.4395	185.4299	51.6383	0.008	0.79	96.13	99.47	yes
E	50.75	21.22	19.00	3	-124.4395	185.4299	51.6383	0.008	0.90	108.34	112.11	yes
F	51.14	21.61	19.09	3	-124.4395	185.4299	51.6383	0.008	0.88	106.89	110.61	yes
Woodridge #1 A	45.17	15.64	2.37	3	-124.4395	185.4299	51.6383	0.008	0.15	18.34	18.97	yes
C	48.92	19.39	2.31	3	-124.4395	185.4299	51.6383	0.008	0.12	14.42	14.92	yes
G	49.02	19.49	2.40	3	-124.4395	185.4299	51.6383	0.008	0.12	14.90	15.42	yes
E	49.17	19.64	2.20	3	-124.4395	185.4299	51.6383	0.008	0.11	13.55	14.03	yes
Woodridge #2 A	49.26	19.73	11.83	3	-124.4395	185.4299	51.6383	0.008	0.60	72.55	75.07	yes
B	49.25	19.72	12.19	3	-124.4395	185.4299	51.6383	0.008	0.62	74.80	77.40	yes
C												
D	48.88	19.35	13.06	3	-124.4395	185.4299	51.6383	0.008	0.67	81.67	84.51	yes
Sandilands #1 A	49.44	19.91	35.62	3	-124.4395	185.4299	51.6383	0.008	1.79	216.48	224.00	yes
B	49.99	20.46	36.00	3	-124.4395	185.4299	51.6383	0.008	1.76	212.90	220.31	yes
C												
D	49.17	19.64	35.43	3	-124.4395	185.4299	51.6383	0.008	1.80	218.28	225.87	yes

Table 3

Quadrupilicate CFC-113 Data

Sample i.d (piezometer #, sample #)	Weight (g)	Sample Weight (g)	CFC-113 10^{-3} pmoles	Recharge Temp (°C)	Solubility Constants a1	a2	a3	Henry's Law Constant K_{12} moles/(kg*atm)	Dissolved CFC-113 (pmoles/kg)	Dissolved CFC-113 (pg/kg)	Partial Pressure CFC-113 (pptv)	Sample Used to calculate Avg CFC conc
9801-1 U	48.92	19.39	14.06	3	-136.129	206.475	55.8957	0.010	0.73	135.96	70.16	yes
V	49.04	19.51	13.93	3	-136.129	206.475	55.8957	0.010	0.71	133.87	69.08	yes
S	49.13	19.60	11.75	3	-136.129	206.475	55.8957	0.010	0.60	112.40	58.00	yes
W	48.91	19.38	10.71	3	-136.129	206.475	55.8957	0.010	0.55	103.62	53.47	yes
9801-2 M	49.07	19.54	10.79	3	-136.129	206.475	55.8957	0.010	0.55	103.54	53.43	yes
N	49.41	19.88	10.69	3	-136.129	206.475	55.8957	0.010	0.54	100.82	52.03	yes
O	49.23	19.70	11.07	3	-136.129	206.475	55.8957	0.010	0.56	105.36	54.37	yes
P	49.30	19.77	11.50	3	-136.129	206.475	55.8957	0.010	0.58	109.07	56.28	yes
9801-3 M	48.46	18.93	8.29	3	-136.129	206.475	55.8957	0.010	0.44	82.11	42.37	yes
N	48.76	19.23	8.79	3	-136.129	206.475	55.8957	0.010	0.46	85.71	44.23	yes
O	49.23	19.70	7.33	3	-136.129	206.475	55.8957	0.010	0.37	69.77	36.00	yes
P	49.30	19.77	9.43	3	-136.129	206.475	55.8957	0.010	0.48	89.43	46.15	yes
9802-1 C	50.71	21.18	19.84	3	-136.129	206.475	55.8957	0.010	0.94	175.64	90.63	no
D	50.65	21.12	14.65	3	-136.129	206.475	55.8957	0.010	0.69	130.06	67.12	yes
E	50.89	21.36	19.75	3	-136.129	206.475	55.8957	0.010	0.92	173.37	89.46	no
F	50.77	21.24	23.83	3	-136.129	206.475	55.8957	0.010	1.12	210.36	108.55	no
9802-3 C	50.38	20.85	8.39	3	-136.129	206.475	55.8957	0.010	0.40	75.45	38.93	yes
D	50.63	21.10	11.28	3	-136.129	206.475	55.8957	0.010	0.53	100.24	51.73	yes
E	50.78	21.25	9.80	3	-136.129	206.475	55.8957	0.010	0.46	86.47	44.62	yes
9803-1 A	50.39	20.86	10.44	3	-136.129	206.475	55.8957	0.010	0.50	93.84	48.42	yes
B	49.18	19.65	9.56	3	-136.129	206.475	55.8957	0.010	0.49	91.22	47.07	yes
C	49.67	20.14	10.07	3	-136.129	206.475	55.8957	0.010	0.50	93.75	48.38	yes
D	49.52	19.99	9.22	3	-136.129	206.475	55.8957	0.010	0.46	86.48	44.63	yes
9803-2 A	49.15	19.62	17.09	3	-136.129	206.475	55.8957	0.010	0.87	163.32	84.28	yes
B	49.21	19.68	16.69	3	-136.129	206.475	55.8957	0.010	0.85	159.01	82.06	yes
C	49.46	19.93	16.97	3	-136.129	206.475	55.8957	0.010	0.85	159.65	82.39	yes
D	49.34	19.81	16.20	3	-136.129	206.475	55.8957	0.010	0.82	153.33	79.12	yes
9803-3 A	49.81	20.28	96.66	3	-136.129	206.475	55.8957	0.010	4.77	893.68	461.16	no
C	49.37	19.84	71.02	3	-136.129	206.475	55.8957	0.010	3.58	671.18	346.35	no
E	49.26	19.73	68.76	3	-136.129	206.475	55.8957	0.010	3.49	653.45	337.20	no
G	49.38	19.85	58.17	3	-136.129	206.475	55.8957	0.010	2.93	549.46	283.54	no

Table 3 (cont.)
Quadruplicate CFC-113 Data

Sample I.d (piezometer #, sample #)	Weight (g)	Sample Weight (g)	CFC-113 10^{-3} pmoles	Recharge Temp (°C)	Solubility Constants a1	a2	a3	Henry's Law Constant K_{12} moles/(kg*atm)	Dissolved CFC-113 (pmoles/kg)	Dissolved CFC-113 (pg/kg)	Partial Pressure CFC-113 (pptv)	Sample Used to calculate Avg CFC conc
9804-1 A	49.80	20.27	11.06	3	-136.129	206.475	55.8957	0.010	0.55	102.31	52.79	
B	49.58	20.05	9.92	3	-136.129	206.475	55.8957	0.010	0.49	92.77	47.87	no
C	52.86	23.33	13.27	3	-136.129	206.475	55.8957	0.010	0.57	106.65	55.03	yes
D	49.43	19.90	10.05	3	-136.129	206.475	55.8957	0.010	0.51	94.69	48.86	yes
9804-2 A	49.40	19.87	1.83	3	-136.129	206.475	55.8957	0.010	0.09	17.27	8.91	yes
B	49.47	19.94	3.01	3	-136.129	206.475	55.8957	0.010	0.15	28.30	14.61	yes
C	50.95	21.42	2.76	3	-136.129	206.475	55.8957	0.010	0.13	24.16	12.47	yes
D	49.20	19.67	2.49	3	-136.129	206.475	55.8957	0.010	0.13	23.74	12.25	yes
9804-3 A	49.69	20.16	3.48	3	-136.129	206.475	55.8957	0.010	0.17	32.37	16.70	yes
B	49.60	20.07	3.46	3	-136.129	206.475	55.8957	0.010	0.17	32.32	16.68	yes
C	49.82	20.29	3.89	3	-136.129	206.475	55.8957	0.010	0.19	35.95	18.55	yes
D	49.92	20.39	2.08	3	-136.129	206.475	55.8957	0.010	0.10	19.13	9.87	yes
9805-1 A	49.88	20.35	3.97	3	-136.129	206.475	55.8957	0.010	0.20	36.58	18.88	yes
B	49.09	19.56	2.92	3	-136.129	206.475	55.8957	0.010	0.15	27.99	14.44	yes
C	49.84	20.31	2.50	3	-136.129	206.475	55.8957	0.010	0.12	23.08	11.91	yes
D	49.13	19.60	3.61	3	-136.129	206.475	55.8957	0.010	0.18	34.53	17.82	yes
9806-1 A	49.95	20.42	11.32	3	-136.129	206.475	55.8957	0.010	0.55	103.94	53.64	yes
B	50.39	20.86	10.22	3	-136.129	206.475	55.8957	0.010	0.49	91.86	47.40	yes
C	50.34	20.81	9.58	3	-136.129	206.475	55.8957	0.010	0.46	86.32	44.54	yes
D	50.29	20.76	10.54	3	-136.129	206.475	55.8957	0.010	0.51	95.20	49.12	yes
9806-2 A	50.36	20.83	5.66	3	-136.129	206.475	55.8957	0.010	0.27	50.95	26.29	yes
B	49.47	19.94	3.51	3	-136.129	206.475	55.8957	0.010	0.18	33.01	17.03	yes
C	50.30	20.77	3.78	3	-136.129	206.475	55.8957	0.010	0.18	34.12	17.61	yes
D	50.64	21.11	3.81	3	-136.129	206.475	55.8957	0.010	0.18	33.84	17.46	yes
9806-3 A	50.67	21.14	3.52	3	-136.129	206.475	55.8957	0.010	0.17	31.22	16.11	yes
B	50.55	21.02	19.80	3	-136.129	206.475	55.8957	0.010	0.94	176.62	91.14	yes
E	50.75	21.22	25.99	3	-136.129	206.475	55.8957	0.010	1.22	229.65	118.51	no
F	51.14	21.61	27.52	3	-136.129	206.475	55.8957	0.010	1.27	238.78	123.22	no
Woodridge #1 A	45.17	15.64	34.96	3	-136.129	206.475	55.8957	0.010	2.24	419.12	216.28	no
C	48.92	19.39	28.54	3	-136.129	206.475	55.8957	0.010	1.47	275.98	142.41	no
G	49.02	19.49	28.99	3	-136.129	206.475	55.8957	0.010	1.49	278.89	143.92	no
E	49.17	19.64	28.10	3	-136.129	206.475	55.8957	0.010	1.43	268.27	138.43	no
Woodridge #2 A	49.26	19.73	1.82	3	-136.129	206.475	55.8957	0.010	0.09	17.30	8.93	yes
B	49.25	19.72	2.96	3	-136.129	206.475	55.8957	0.010	0.15	28.14	14.52	yes
C												
D	48.88	19.35	25.84	3	-136.129	206.475	55.8957	0.010	1.34	250.39	129.21	yes
Sandilands #1 A	49.44	19.91	4.07	3	-136.129	206.475	55.8957	0.010	0.20	38.33	19.78	yes
B	49.99	20.46	3.20	3	-136.129	206.475	55.8957	0.010	0.16	29.33	15.13	yes
C												
D	49.17	19.64	3.85	3	-136.129	206.475	55.8957	0.010	0.20	36.76	18.97	yes

Appendix IV: Thornthwaite Evapotranspiration Estimate

IV.1 Thornthwaite Evapotranspiration Estimates

Variables used to calculate evapotranspiration using Thornthwaite's methods are reported in Table 1. For details on how the variables were calculated refer to (Thornthwaite and Mather, 1957). Below is a list of definitions of the variables used in Table 1.

Thornthwaite Variables:

T °C = Average monthly temperature from Winnipeg International Airport.

P = Average monthly precipitation from the Marchand Forestry station in the Sandilands reported in mm/month.

I = Monthly heat index, calculated using the average monthly temperature.

PE = Potential monthly evapotranspiration (mm/month)

Correction Factor = Correction factor for PE based on latitude (49° 20').

ACC Pot WL = Accumulated potential water losses based on negative values of P-PE

ST = Soil moisture storage (maximum capacity for a mature forest and sandy soil = 250 mm).

AET = Actual evapotranspiration based on soil moisture capacity and precipitation

D = Moisture Deficit

S = Moisture Surplus

SMRO = Snow Melt Runoff

Table 1
Monthly Thornthwaite Variables Used to Calculate Evapotranspiration

	T °C	P mm/mo	I	PE mm/mo	Correction Factor	$PE_{corrected}$ mm/mo	P-PE mm/mo	ACC Pot WL mm/mo	ST mm/mo	ΔST mm/mo	AET mm/mo	D mm/mo	S mm/mo	SMRO mm/mo	RO mm/mo
Jan	-18.30	25.16	0.00	0.00	0.71	0.00	25.16	25.16	255.44	25.16	0.00	0.00	0.00	0.00	0.00
Feb	-15.10	17.48	0.00	0.00	0.84	0.00	17.48	17.48	272.92	17.48	0.00	0.00	0.00	0.00	0.00
March	-7.00	22.30	0.00	0.00	0.98	0.00	22.30	22.30	295.22	22.30	0.00	0.00	0.00	0.00	0.00
April	3.80	22.54	0.66	19.91	1.14	22.70	-0.16	-0.16	248.00	-47.22	22.70	0.00	0.00	10.03	10.03
May	11.60	47.42	3.53	59.58	1.28	76.26	-28.84	-29.00	222.00	-26.00	73.42	2.84	0.00	45.00	45.00
June	16.90	113.98	6.21	86.22	1.36	117.25	-3.27	-32.27	220.00	-2.00	115.98	1.27	0.00	22.50	22.50
July	19.80	83.04	7.88	100.72	1.33	133.96	-50.92	-83.19	178.00	-42.00	125.04	8.92	0.00	11.25	11.25
Aug	18.30	70.66	7.00	93.22	1.21	112.80	-42.14	-125.33	151.00	-27.00	97.66	15.14	0.00	5.63	5.63
Sept	12.40	60.54	3.91	63.61	1.06	67.43	-6.89	-132.22	146.00	-5.00	65.54	1.89	0.00	2.81	2.81
Oct	5.70	59.62	1.22	29.65	0.90	26.68	32.94	32.94	178.94	32.94	2.67	24.02	0.00	1.41	1.41
Nov	-4.70	27.10	0.00	0.00	0.76	0.00	27.10	27.10	206.04	27.10	0.00	0.00	0.00	0.00	0.00
Dec	-14.60	24.24	0.00	0.00	0.68	0.00	24.24	24.24	230.28	24.24	0.00	0.00	0.00	0.00	0.00
Yearly			30.42			557.08					503.01			98.62	